

MOLECULAR TARGETING OF TRANSLESION SYNTHESIS DNA
POLYMERASES FOR NOVEL COMBINATION CHEMOTHERAPY

By

Kinrin Yamanaka

A DISSERTATION

Presented to the Department of Physiology & Pharmacology

and the Oregon Health & Science University

School of Medicine

in partial fulfillment of

the requirements for the degree of

Doctor of Philosophy

May 2012

School of Medicine
Oregon Health & Science University

CERTIFICATE OF APPROVAL

This is to certify that the Ph.D. dissertation of

Kinrin Yamanaka

has been approved

R. Stephen Lloyd

Maureen Hoatlin

Xiangshu Xiao

Mitchell Turker

Jeffrey Karpen

TABLE OF CONTENTS

LIST OF TABLES	v
LIST OF ILLUSTRATIONS	vi
LIST OF ABBREVIATIONS	viii
ACKNOWLEDGEMENTS	x
ABSTRACT	xii
1. CHAPTER 1: LITERATURE REVIEW	1
1.1. PREFACE	2
1.2. INTRODUCTION	3
1.3. OVERVIEW OF THE TLS POLYMERASES	7
1.3.1. Y family polymerases	7
1.3.1.1. DNA polymerase eta	7
1.3.1.1.1. General and biochemical properties	7
1.3.1.1.2. <i>In vivo</i> functions and implications in tumorigenesis/chemotherapy resistance	10
1.3.1.1.3. Phenotype of pol η knockout mice	15
1.3.1.2. DNA polymerase kappa	16
1.3.1.2.1. General and biochemical properties	16
1.3.1.2.2. <i>In vivo</i> functions and implications in tumorigenesis/chemotherapy resistance	19
1.3.1.2.3. Phenotype of pol κ knockout mice	23
1.3.1.3. DNA polymerase iota	23

1.3.1.3.1. General and biochemical properties	23
1.3.1.3.2. <i>In vivo</i> functions and implications in tumorigenesis/chemotherapy resistance	25
1.3.1.3.3. Phenotype of pol ι knockout mice	27
1.3.1.4. Rev1	27
1.3.1.4.1. General and biochemical properties	27
1.3.1.4.2. <i>In vivo</i> functions and implications in tumorigenesis/chemotherapy resistance	28
1.3.1.4.3. Phenotype of Rev1 knockout mice	30
1.3.2. B family polymerase	30
1.3.2.1. DNA polymerase zeta	30
1.3.2.1.1. General and biochemical properties	30
1.3.2.1.2. <i>In vivo</i> functions and implications in tumorigenesis/chemotherapy resistance	32
1.3.2.1.3. Phenotype of pol ζ knockout mice	36
1.3.3. A family polymerases	38
1.3.3.1. DNA polymerase nu	38
1.3.3.1.1. General and biochemical properties	38
1.3.3.1.2. <i>In vivo</i> functions and implications in tumorigenesis/chemotherapy resistance	39
1.3.3.2. DNA polymerase theta	41
1.3.3.2.1. General and biochemical properties	41
1.3.3.2.2. <i>In vivo</i> functions and implications in tumorigenesis/chemotherapy resistance	42
1.3.3.2.3. Phenotype of pol θ knockout mice	44

1.4. COOPERATIVE ACTIONS OF MULTIPLE TLS POLYMERASES IN LESION BYPASS	45
1.5. TLS POLYMERASE INHIBITORS FOR CANCER PREVENTION AND THERAPY	47
2. CHAPTER 2: NOVEL ENZYMATIC FUNCTION OF DNA POLYMERASE ν IN TRANSLATION DNA SYNTHESIS PAST MAJOR GROOVE DNA-PEPTIDE AND DNA-DNA CROSS-LINKS	55
2.1. PREFACE	56
2.2. INTRODUCTION	58
2.3. MATERIALS AND METHODS	59
2.4. RESULTS	70
2.5. DISCUSSION	78
3. CHAPTER 3: ROLE OF HIGH-FIDELITY <i>ESCHERICHIA COLI</i> DNA POLYMERASE I IN REPLICATION BYPASS OF A DEOXYADENOSINE DNA-PEPTIDE CROSS-LINK	85
3.1. PREFACE	86
3.2. INTRODUCTION	87
3.3. MATERIALS AND METHODS	88
3.4. RESULTS	93
3.5. DISCUSSION	103
4. CHAPTER 4: REPLICATION BYPASS OF THE ACROLEIN-MEDIATED DEOXYGUANINE DNA-PEPTIDE CROSS-LINKS BY DNA POLYMERASES OF THE DINB FAMILY	108
4.1. PREFACE	109
4.2. INTRODUCTION	111
4.3. MATERIALS AND METHODS	114
4.4. RESULTS	117

4.5. DISCUSSION	128
5. CHAPTER 5: A COMPREHENSIVE STRATEGY TO DISCOVER INHIBITORS OF THE TRANSLESION SYNTHESIS DNA POLYMERASE κ	132
5.1. PREFACE	133
5.2. INTRODUCTION	134
5.3. MATERIALS AND METHODS	136
5.4. RESULTS	140
5.5. DISCUSSION	152
6. SUMMARY AND CONCLUSION	157
7. FUTURE DIRECTIONS	160
8. REFERENCES	163

LIST OF TABLES

1.5. Summary of inhibitors of TLS polymerases	52
2.3. Sequences of DNA primers and lesion-containing templates	62
4.4. Efficiency of <i>E. coli</i> transformation using vector DNAs containing DNA–peptide cross-links	126
5.4. Summary of IC ₅₀ s of top 60 hits obtained from qHTS and radioactive gel-based primer extension assays using ND oligodeoxynucleotides	145
5.4. Summary of IC ₅₀ s of candesartan cilexetil, manoalide, and MK-886 obtained from qHTS and radioactive gel-based primer extension assays using oligodeoxynucleotides unadducted or adducted with acrolein-derived ring-opened reduced form of γ -HOPdG	147

LIST OF ILLUSTRATIONS

1.2. Two models of TLS	6
1.5. Model of new combination chemotherapy	49
1.5. Structures of small molecule inhibitors of various TLS polymerases	51
2.3. Structures of DNA adducts	61
2.3. Scheme 1	63
2.4. Replication bypass of N^6 -dA peptide cross-links by human pol ν	72
2.4. Replication bypass of N^6 -dA- N^6 -dA ICLs by human pol ν	74
2.4. Replication bypass of N^2 -dG peptide and interstrand cross-links by human pol ν	75
2.4. Replication bypass of ϵ dA and (+)-BPDE-dA by human pol ν	77
2.5. Replication bypass of N^6 -dA peptide cross-link by yeast pol δ	82
2.5. Replication bypass of N^6 -dA peptide cross-link by yeast pol ζ	83
2.5. Replication bypass of N^6 -dA peptide cross-links by human pol η	83
3.2. Structure of a γ -HOPdA-derived peptide cross-link	87
3.4. Replication blockage of pol III* by N^6 -dA PCL12	94
3.4. Replication bypass of N^6 -dA PCL12 by pol I and KFexo ⁻	96
3.4. Replication blockage of pol IV by N^6 -dA PCL12	97
3.4. Replication bypass of N^6 -dA PCL12 by pol V	99
3.4. Replication bypass of N^6 -dA PCL12 by pol II	100
3.4. Ability of <i>E. coli</i> strains to replicate DNA containing N^6 -dA PCL12	102
3.5. Replication blockage of human pol κ by N^6 -dA PCL12	105

4.2. Structure of DNA adducts used in the current study	113
4.4. Replication bypass of DNA–peptide cross-links by human pol κ	119
4.4. Replication bypass of γ -HOPdG, reduced γ -HOPdG, and DNA–peptide cross-links by <i>E. coli</i> pol III	120
4.4. Replication bypass of γ -HOPdG, reduced γ -HOPdG, and DNA–peptide cross-links by <i>E. coli</i> pol IV	122
4.4. Replication bypass of γ -HOPdG, reduced γ -HOPdG, and DNA–peptide cross-links by <i>E. coli</i> pol II	124
4.4. Replication bypass of γ -HOPdG, reduced γ -HOPdG, and DNA–peptide cross-links by <i>E. coli</i> pol V	124
5.4. Principle of the fluorescence-based polymerase-catalyzed strand displacement assay	141
5.4. Miniaturized HTS assay	141
5.4. Reagent stability (A) and quality (B) of strand displacement assay	143
5.4. Summary of results from qHTS	144
5.4. Dose-response activities of (A) candesartan cilexetil, (B) manoalide, and (C) MK-886 on pol κ -catalyzed primer extension reactions on ND DNAs	147
5.4. Dose-response activities of (A) candesartan cilexetil, (B) manoalide, and (C) MK-886 on pol κ -catalyzed primer extension reactions on DNAs adducted with acrolein-derived ring-opened reduced form of γ -HOPdG	148
5.4. The effect of candesartan cilexetil on cytotoxicity of UV-treated XP30RO cells using crystal violet staining assay	149
5.4. The effect of candesartan cilexetil on cytotoxicity of UV-treated XP30RO cells using CellTiter Glo Luminescent Cell Viability Assay	150
5.4. Candesartan cilexetil did not interfere with the activity of topoisomerase I to relax plasmid DNA	151
5.4. The non-DNA-intercalating property of candesartan cilexetil	151

LIST OF ABBREVIATIONS

In order of appearance

HNE: *trans*-4-hydroxy-2-nonenal
εdA: 1,*N*⁶-ethenodeoxyadenosine
UV: ultraviolet
B[*a*]P: benzo[*a*]pyrene
NER: nucleotide excision repair
MMR: mismatch repair
BER: base excision repair
NHEJ: non-homologous end joining
HR: homologous recombination
TLS: translesion DNA synthesis
ICLs: DNA–DNA interstrand cross-links
ND: non-damaged
CPDs: cyclobutane pyrimidine dimers
γ-HOPdG: γ-hydroxypropano-deoxyguanosine
8-oxo-dG: 7,8-dihydro-8-oxo-guanine
m6G: *O*⁶-methyl-dG
AAF: *N*-(deoxyguanosin-8-yl)-2-acetylaminofluorene
AP site: abasic site
4-OHEN: 4-hydroxyequilenin
4-OHEQ: 4-hydroxyequilin
PdG: 1,*N*²-propano-deoxyguanosine
DSBs: double-strand breaks
XP-V: xeroderma pigmentosum variant
E. coli: *Escherichia coli*
NSCLC: non-small cell lung cancer
AF: *N*-(deoxyguanosin-8-yl)-2-aminofluorene
MEFs: mouse embryonic fibroblasts
CTX: cyclophosphamide
(+)-BPDE-dA: (+)-*trans-anti*-BPDE-dA
NaCNBH₃: sodium cyanoborohydride
γ-HOPdA: γ-hydroxypropano-deoxyadenosine
PAGE: polyacrylamide gel electrophoresis
CGE: capillary gel electrophoresis
BSA: bovine serum albumin
DTT: dithiothreitol
COS7 cells: African green monkey kidney cells
KFlexo⁻: exonuclease-deficient Klenow fragment
Pol III*: Pol III replicase

qHTS: quantitative high-throughput screening
DMSO: dimethyl sulfoxide
NPC: NCGC Pharmaceutical Collection
FRD: Flying Reagent Dispenser™

ACKNOWLEDGMENTS

Throughout my time as a graduate student at Oregon Health & Science University, I was fortunate enough to encounter a number of people whose guidance, support, patience, and love make the completion of this dissertation possible. It is to them that I owe my deepest gratitude.

First and foremost, I would like to express my sincere gratitude to my advisor, Dr. R. Stephen Lloyd. Under his supervision, I have learned to take initiatives to tackle challenging research questions and have developed good communication skills. I also greatly appreciate him for giving me an opportunity to initiate drug discovery project and travel around the country to gain training in several experimental techniques to advance the project. I am very privileged to learn under his guidance.

I would like to extend my gratitude to Dr. Irina G. Minko for her willingness and patience to guide me through the laboratory techniques and critique my writings.

Furthermore, I am very grateful that I have benefited from the outstretched and guiding hands of several exceptional scientists who invested professional resources into my training; I would like to thank Dr. Anton Simeonov, Dr. Martin Egli, and Dr. Robert L. Eoff for giving me a very valuable opportunity to visit their laboratories as part of my graduate training to learn several laboratory techniques.

I would like to thank members of my thesis advisory committee, Dr. Maureen Hoatlin, Dr. Xiangshu Xiao, and Dr. Mitchell Turker, for helping me make progress towards completion of this dissertation.

I also would like to thank scientists who have generously provided me reagents; Dr. Nicholas E. Geacintov, Dr. Peter M. J. Burgers, Dr. Masaaki Moriya, Dr. Michael E. O'Donnell, Dr. Roger Woodgate, Dr. James E. Cleaver, Dr. Carmelo J. Rizzo, and Dr. Steven E. Finkel.

Many thanks go to my best friend, Myat-Hsu Mon, who have truly made my life outside laboratory very enjoyable.

My deepest appreciation goes to my family members, especially my grandparents and my mother, for their unconditional love and complete support of my pursuit of a dream to become a scientist. They have helped me develop strong mental tenacity to overcome difficulties to reach my goals and have taught me to always have confidence and faith in myself.

I also would like to acknowledge funding sources that have supported all these works: P01ES05355 (R.S.L, C.J.R), R01CA106858 (R.S.L), 2R01CA099194 (Geacintov Laboratory), M.D. Anderson Research Trust (R.D.W, K.T), ES012259 (M.F.G), GM21422 (M.F.G), NSF Career Award (#MCB0237975), R03MH 094179, GM38839 (M.O.D.), R37GM21244 (M.F.G), ES012259 (M.F.G.), P30ES000267 (C.J.R), R00GM 084460 (R.L.E.), Tartar Trust Fellowship, and Oregon Health & Science University School of Medicine Graduate Research Scholarship.

ABSTRACT

Genomic DNAs are continuously exposed to a wide variety of DNA-damaging agents generated from both endogenous and exogenous sources. As a consequence, various DNA lesions can be formed. Cells have evolved multiple mechanisms to either repair or tolerate DNA lesions. One of the DNA damage tolerance mechanisms is translesion DNA synthesis (TLS), a process carried out by specialized DNA polymerases (TLS polymerases). TLS polymerases can prevent cancer formation by catalyzing accurate replication bypass of specific DNA lesions and performing DNA repair synthesis, but on different DNA substrates, they may also promote carcinogenesis and chemotherapeutic resistance by introducing mutations in crucial genes during error-prone replication bypass of DNA lesions or performing TLS past DNA lesions induced by chemotherapeutic agents. Research leading to the understanding of the cellular functions of individual TLS polymerase and the development of small molecule inhibitors targeting TLS polymerases that are implicated in carcinogenesis and chemotherapeutic resistance is thus critically important to gain insight into how cancer and chemotherapeutic resistance arise and to discover novel adjunct cancer therapeutics (the functions of each TLS polymerase and its implications for cancer risk and opportunities as therapeutic targets are extensively reviewed in Chapter 1).

In this regard, the aim of the first part of the dissertation (Chapter 2) was to discover biochemical functions of the newly discovered DNA polymerase ν in order to elucidate the biological functions of this enzyme.

The size, stereochemistry, and location of DNA lesions significantly dictate the identity of DNA polymerases involved in the bypass. Therefore, in order to understand the functions of DNA polymerases, it is essential to investigate the identity of DNA polymerases that cells utilize to process different types of lesions. Given the significance of this research, the aim of the second part of the dissertation (Chapter 3 and Chapter 4) was to identify DNA polymerases involved in the replication bypass of DNA–peptide cross-links. As DNA–peptide cross-links can be formed by linkage through N^6 position of deoxyadenosine or N^2 position of deoxyguanosine, resulting in major groove or minor groove lesions, respectively, studies were conducted to investigate DNA polymerases involved in the processing of these two different types of peptide cross-links.

One of the TLS polymerases, polymerase κ , is implicated in carcinogenesis and chemotherapy resistance, since it is overexpressed in gliomas and can catalyze TLS past DNA–DNA interstrand cross-links induced by the chemotherapeutic agent, mitomycin C. Thus, this enzyme can serve as an important target for cancer therapy. With this regard, the aim of the third part of the dissertation (Chapter 5) was to identify small molecule inhibitors of pol κ .

Collectively, the results presented in this dissertation will significantly move research toward the understanding of the contributions of TLS polymerases to carcinogenesis and chemotherapeutic resistance, as well as the development of novel combination cancer therapeutics to combat cancers.

CHAPTER 1: LITERATURE REVIEW

Kinrin Yamanaka^{1,2} and R. Stephen Lloyd^{1,3}

Functions of Translesion DNA Polymerases: Implications for Cancer Risk and Opportunities as Therapeutic Targets, in *DNA Repair and Cancer: Bench to Clinic* (Madhusudan, S. and Wilson, D. M. III., Eds.) Science Publishers, Enfield, NH. *In press*.

¹Center for Research on Occupational and Environmental Toxicology, ²Department of Physiology and Pharmacology, and ³Department of Molecular and Medical Genetics, Oregon Health & Science University, Portland, OR 97239

1.1. PREFACE

This work is currently in press.

My contribution to this work was the writing of the manuscript.

R. Stephen Lloyd contributed to the editing and critical reading of the manuscript.

Adapted and modified with permission from Science Publishers.

1.2. INTRODUCTION

Genomic DNA is continuously damaged by both endogenously produced species and exogenous agents. Examples of endogenous species include byproducts of lipid peroxidation such as acrolein, *trans*-4-hydroxy-2-nonenal (HNE), and 1,*N*⁶-ethenodeoxyadenosine (ϵ dA). Some of these species can induce secondary lesions such as DNA–protein, DNA–peptide, and DNA–DNA cross-links (1,2). Exogenous agents may include environmental agents such as ultraviolet (UV) and γ irradiation, chemical carcinogens such as benzo[*a*]pyrene (B[*a*]P), and therapeutic agents such as mitomycin C, platinum drugs, temozolomide, fotemustine, nucleoside analogues, nitrogen mustards, equine estrogens, and psoralen.

Multiple biochemical pathways exist to either remove or tolerate DNA lesions, including direct DNA damage reversal, nucleotide excision repair (NER), mismatch repair (MMR), base excision repair (BER), non-homologous end joining (NHEJ), replication fork reversal, and homologous recombination (HR). Because of differential cellular responses relative to the location of the damage, the magnitude of the helical distortion, and the degree of chromatin compaction, some lesions can escape the repair machineries or the timing of the repair processes can be sufficiently delayed. As a consequence, blockage to replication fork progression can occur. This interference is due to the limited ability of replicative polymerases, pol α , pol δ , and pol ϵ in eukaryotes, to synthesize DNA past damaged sites. Translesion DNA synthesis (TLS) is a DNA damage tolerance mechanism that helps cells to tolerate unrepaired DNA lesions and is carried out by specialized DNA polymerases (TLS polymerases). To date, at least 11 polymerases have been identified

that may potentially be involved in TLS and these polymerases are classified into different families based on sequence homology: pol ν and pol θ from the A family, pol ζ from the B family, pol β , pol λ , pol μ , and terminal deoxynucleotidyl transferase from the X family, and pol η , pol κ , pol ι , and Rev1 from the Y family (3-6).

Currently two models of TLS have been proposed: the polymerase-switching mechanism and the gap-filling mechanism (3-5). In the polymerase-switching mode, TLS takes place during active DNA replication in which fork progression could be terminated when the movement of the replicative helicase is disrupted by a DNA lesion (7). Blockage of a replicative polymerase by a DNA lesion is hypothesized to trigger polymerase switching, potentially recruiting multiple TLS polymerases to the site of replication. Subsequently, a TLS polymerase incorporates a nucleotide opposite the lesion and it either dissociates or extends the primer from opposite the lesion. In the former case, the extension step can be performed by another TLS polymerase. The identity of the polymerases that catalyze this two-step reaction is likely influenced by the substrate structure and catalytic efficiency of the polymerase, its relative abundance in the cell, and its affinity for the primer/template. The number of nucleotides incorporated by a polymerase prior to its dissociation depends on the intrinsic processivity of the polymerase, the ability of polymerase to extend the primer opposite the lesion, and the interactions of the specific polymerase with other components of the replication machinery. The re-recruitment of a replicative polymerase to the primer terminus follows, thus resuming normal DNA replication (Figure 1A) (3-5,8-12). In the gap-filling mode, following replication blockage, reinitiation of DNA synthesis occurs downstream of the DNA lesion, generating a single-stranded DNA gap,

and a TLS polymerase is recruited to fill in the resulting gap (Figure 1B). In this mode, TLS polymerases function outside the replication fork and this process may occur both during the later stages of S phase or following DNA replication in the G₁ or G₂/M phase of the cell cycle (3-5,13-16). Both models are supported by strong evidence and are not necessarily exclusive. As an example, gap-filling mode is hypothesized to be utilized during the processing of DNA–DNA interstrand cross-links (ICLs) (4).

Several lines of evidence show that the recruitment of TLS polymerases to their site of action, either the site of stalled replication or a single-stranded DNA gap, is governed by multiple protein-protein interactions. Current models propose that PCNA monoubiquitination by Rad6/Rad18 ubiquitin conjugase/ligase complex signals TLS polymerases to enter their site of action (Figure 1A, steps 2-4). Once TLS is completed, PCNA deubiquitination may occur and normal replication by replicative polymerases resumes (Figure 1A, steps 5 and 6). In addition to PCNA, 9-1-1 complex, an alternative processivity clamp, may also be important for recruiting TLS polymerases (Figure 1B, steps 1-3). Additionally, certain TLS polymerases, for example Rev1, can also function as scaffolds for TLS machinery and recruit other TLS polymerases to the site of the DNA lesion (3,4,17).

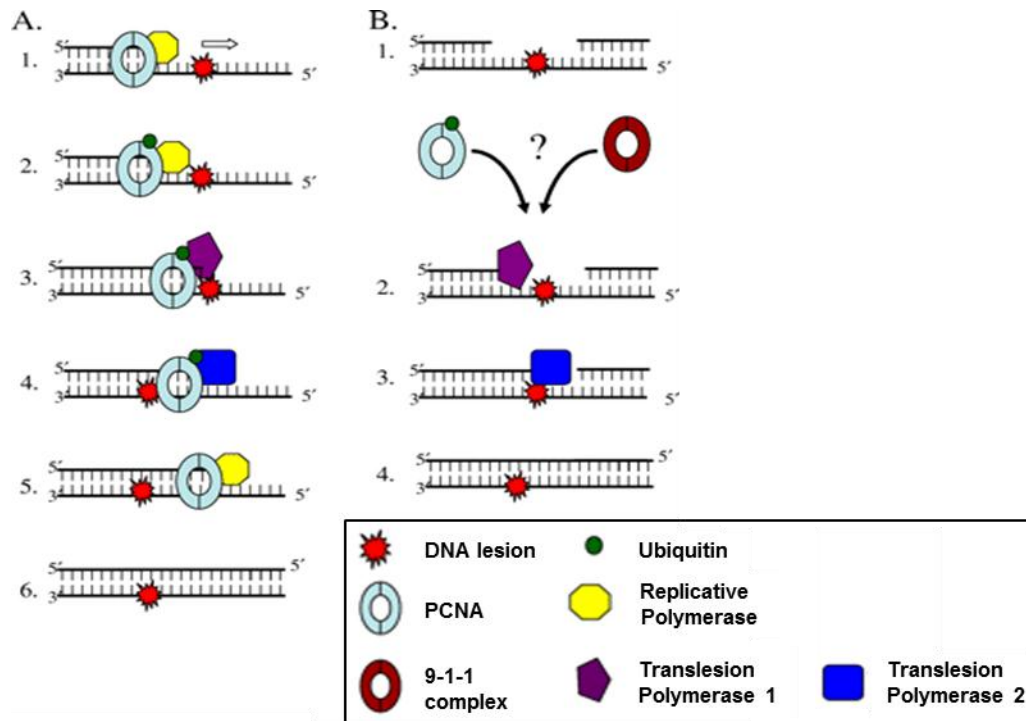


Figure 1. Two models of TLS. (A) In the polymerase-switching mode, TLS polymerases restart a blocked replication fork. (B) In the gap-filling mode, TLS polymerases fill the single-stranded gap opposite the DNA lesion. (Adapted and modified from (4) with permission from American Society for Microbiology).

The efficiency and accuracy of lesion bypass is both polymerase and lesion specific. Each TLS polymerase is hypothesized to be particularly proficient in the bypass of specific DNA lesions (cognate lesions), and the outcome of TLS past these lesions is generally non-mutagenic. In this case, a TLS polymerase can serve as a tumor suppressor. However, the fidelity of DNA synthesis is often compromised when TLS polymerases act on non-cognate lesions. Furthermore, these enzymes generally exhibit low-fidelity when copying non-damaged (ND) DNA, in contrast to replicative polymerases that faithfully duplicate chromosomal DNA (18). Multiple factors can account for the low fidelity replication of TLS polymerases, including the lack of 3'-5' proofreading exonuclease activity, a spacious active site, and the limited number of contacts made with the template base and incoming nucleotide (4,18,19). Thus, TLS polymerases have dual-functions, serving as

tumor-suppressors during the bypass of their cognate lesions, while promoting mutagenesis during the bypass of non-cognate lesions and the replication of ND DNA. As a consequence, the dysregulation of TLS polymerases can result in carcinogenesis.

In this Chapter, the functions of each TLS polymerase and its roles in tumorigenesis and chemotherapy resistance will be discussed. This introduction highlights the significance of the studies to investigate the roles of TLS polymerases. The importance of the development of inhibitors targeting TLS polymerases for new combination cancer therapy and existing TLS polymerase inhibitors will be discussed at the end of the Chapter. Although polymerases belonging to X family also have known TLS activities, their primary physiological functions appear to be non-TLS activity such as in BER and NHEJ. Therefore, our discussion focuses on polymerases belonging to A, B, and Y family. For comprehensive analyses of inhibitor studies of viral replicative polymerases, readers are referred to the following recent review (20).

1.3. OVERVIEW OF THE TLS POLYMERASES

1.3.1. Y family polymerases

1.3.1.1. DNA polymerase eta

1.3.1.1.1. *General and biochemical properties*

Pol η is a 78 kDa protein whose gene is located on chromosome 6p21.1 (21,22). Pol η lacks 3'-5' proofreading exonuclease activity (23) and has a low processivity, generally elongating 1-8 nucleotides (24,25). Pol η is a low fidelity polymerase, with the frequency

of nucleotide misincorporation opposite ND nucleotides being $\sim 10^{-2}$ to 10^{-3} (26). Additionally, studies using gapped M13mp2 plasmids demonstrate that during synthesis of the target *lacZ α* gene, the frequency of *lacZ* mutants generated by pol η was 34% (23) versus $\leq 1\%$ measured for the high fidelity exonuclease-proficient replicative polymerases (27,28). Additionally, pol η primarily introduces base substitutions (29).

In vitro, human pol η functions to bypass a variety of DNA lesions. It is particularly well-known for its ability to catalyze efficient and accurate TLS past UV-induced T-T cyclobutane pyrimidine dimers (CPDs) (30,31). It has also been shown that dG-dG intrastrand cross-links induced by cisplatin or oxaliplatin are efficiently bypassed by pol η ; it preferentially incorporates the correct dC opposite both the 3' and 5' adducted dG, but other nucleotides were also incorporated (32).

Additionally, pol η can bypass acrolein-derived γ -hydroxypropano-deoxyguanosine (γ -HOPdG) adducts and its ring-opened reduced form; the bypass of the former lesion is error-prone with high misincorporation of dA and dG, while the bypass of the latter lesion is accurate (33). Another lesion that pol η can bypass is 7,8-dihydro-8-oxo-guanine (8-oxo-dG), a common oxidative base lesion. Although this bypass was mostly accurate, pol η also incorporated incorrect nucleotides (31,34-36). Thymine glycols, another common oxidative base lesion, *O*⁶-methyl-dG (m6G), a lesion induced by alkylating chemotherapeutic agents, and *N*-(deoxyguanosin-8-yl)-2-acetylaminofluorene (AAF)-dG adducts can all be bypassed by pol η (25,37-40). During the bypass of thymine glycols, not only correct dA, but also other nucleotides were incorporated opposite the lesion.

However, the efficient extension past the lesion occurred when the correct dA was inserted opposite the lesion. Pol η inserted dC or dT opposite m6G, and dC was preferentially incorporated opposite AAF-dG. ϵ dA, a lesion that can be produced by exposure to vinyl chloride (41), is another lesion that pol η can bypass in an error-prone manner. In addition, pol η can replicate past an abasic site (AP site). dA was preferentially incorporated opposite either ϵ dA or an AP site (31,42). Interestingly the bypass of an AP site resulted in -1 deletion when the template base 5' to the lesion was a dT (31). With regard to ϵ dA, another group, using steady-state kinetic analyses, has shown that pol η preferentially incorporated a correct dT opposite the lesion and typically extended from the correct dT primer terminus. In contrast, when analyses of TLS products included frameshift mutations, it was found that although pol η preferentially incorporated dT, incorporation of other nucleotides and a one-base deletion were also observed. Collectively, these results show that pol η catalyzes both error-free and error-prone TLS past ϵ dA (42,43). Finally, pol η catalyzes very inefficient and error-prone bypass of B[a]P-induced (+)- and (-)-*trans*-BPDE- N^2 -dG (BPDE is a metabolically active form of B[a]P), mostly incorporating dA opposite the lesions. However, it was capable to fully bypass (+)-*trans*-BPDE- N^6 -dA adducts with preferential incorporation of correct dT (31,44,45).

Studies have shown that women treated with hormone replacement therapy consisting of the equine estrogens (equilin and equilenin) exhibit increased risk of developing cancers, including breast and endometrial cancers (46,47). One of the major metabolites associated with such treatment is 4-hydroxyequilenin (4-OHEN), which can react with

nucleobases to form lesions such as 4-OHEN-dA (48-52). A study has shown that pol η can bypass 4-OHEN-dA. Although it frequently incorporated the correct dT opposite the lesion, dA was also incorporated (53). Thus, pol η could potentially induce A to T transversions. These data correlate well with a previous study showing that A to T transversions are common at AT pairs of the *supF* reporter gene following replication of a DNA vector exposed to 4-hydroxyequilin (4-OHEQ), another metabolite that induces 4-OHEN-dA adducts (52). Thus, pol η may be responsible for inducing these types of mutation in the cells during the bypass of the 4-OHEN-dA adduct. Pol η can also catalyze TLS past nucleoside analogues commonly used in chemotherapy, such as cytarabine and gemcitabine (54). Despite its proficiency in the bypass of T-T CPDs, pol η is blocked by UV-induced (6-4) photoproducts (30,31) and cannot bypass a psoralen-induced ICL that models the intermediate structure during ICL repair (55). In addition, Pol η is inhibited by HNE-induced N^2 -dG adducts (56), and catalyzes limited TLS past an 1, N^2 -propano-deoxyguanosine (PdG) adduct when excess enzyme was used in the reactions (33).

1.3.1.1.2. *In vivo functions and implications in tumorigenesis/chemotherapy resistance*

The role of pol η in the processing of naturally occurring non-B-DNA structures to maintain genomic stability has been studied. When pol η was depleted from HeLa cells and the cells were transfected with plasmids containing G-rich sequences from the human c-MYC promoter region, there was an increase in the induction of DNA double-strand breaks (DSBs). Additionally, it was demonstrated that pol η may be involved in the processing of G-quadruplex DNA structures, since U2OS cells depleted of pol η showed

decreased survival in response to telomestatin, a G-quadruplex ligand that stabilizes G-quadruplex structures (57).

The importance of pol η in catalyzing replication bypass of UV-induced lesions to protect cells from UV-induced carcinogenesis is evident from an autosomal recessive disease xeroderma pigmentosum variant (XP-V). Individuals with XP-V have normal function in NER, but lack high fidelity bypass of T-T CPD lesions due to defects in pol η . Thus, these individuals are at high risk of developing sunlight-induced skin cancers (30,58-60). Multiple mutations exist in XP-V, and many of these mutations lead to truncated pol η proteins (30,61,62).

A number of studies highlight the essential role of pol η in the replication bypass of T-T CPDs. XP-V cells are sensitive to the cytotoxic and mutagenic effect of UV irradiation (54,63). UV irradiation causes a prolonged delay in S phase, and pol η functions to prevent this event. In the presence of caffeine, an inhibitor of the cell cycle checkpoint protein ATM, the sensitivity of XP-V cells to UV irradiation was enhanced. When UV-irradiated SV40-based shuttle vector pR2 was replicated in these mutant cells, notable increases in mutant frequencies were observed, and mutations occurred at both CG and TA base pairs. When UV-damaged plasmids were replicated in UV-irradiated cells, XP-V cells exhibited high mutation rates, and large increases in transversions were observed (64). Several studies have examined the TLS activity of pol η using a gapped plasmid-based assay. In this assay, a mixture of gapped plasmids carrying unadducted or a site-specific lesion were transfected into mammalian cells, and following gap-filling DNA

synthesis, plasmids were extracted and used to transform *Escherichia coli* (*E. coli*). These transformants were grown on plates containing kanamycin or chloramphenicol to select for progenies of damaged or unadducted plasmids, respectively. The efficiency of TLS was determined from the ratio of kanamycin resistant to chloramphenicol resistant transformants. In order to exclude plasmids that had been repaired by non-TLS events, such as those involving DSB formation as an intermediate, the precise efficiency of TLS was determined to be the extent of plasmid repair multiplied by the fraction of TLS events out of all plasmid repair events. The accuracy of TLS was measured by assessing the mutations in the vector DNAs isolated from the kanamycin resistant transformants. Using this assay, pol η has been shown to carry out efficient and accurate TLS past a T-T CPD (65). The accurate bypass of UV-induced lesions was also demonstrated by a study showing that the type I Burkitt's lymphoma BL2 cell lines deficient in pol η exhibited a 1.5-fold increase in UV-induced mutagenesis (66).

Consistent with data in human cells, a study using primary mouse fibroblasts deficient in pol η found that these cells were moderately sensitive to UV irradiation, and UV-induced mutagenesis at the *Hprt* locus was increased, with the majority of substitutions occurring at the dipyrimidine sites. Additionally, the bias of mutations on the nontranscribed strand was reduced to 2.9-fold in these cells, relative to 4.5-fold in the wild-type cells (67). Furthermore, an important role of pol η in protecting cells from the cytotoxic effect of UV irradiation in the repair-deficient background has been revealed by a study showing an up to 2-fold decrease in UV sensitivity in XPA cells depleted of pol η (68).

With regard to the ability of pol η to bypass lesions induced by chemotherapeutic agents, the function of pol η in the bypass of cisplatin-induced DNA lesions has been well-studied. Cisplatin induced elevated level of mutations at *Hprt* locus in XP-V cells, indicating the role of pol η in the accurate TLS past cisplatin-induced DNA lesions (63). Additionally, XP-V cells were hypersensitive to a number of platinum-based drugs, not only cisplatin, but also carboplatin and oxaliplatin. These cells manifested prolonged cisplatin-induced S phase arrest (69). XP-V cells were also sensitive to cytarabine, gemcitabine, cisplatin, and the combination of gemcitabine and cisplatin (54).

In addition to cisplatin, pol η bypasses mitomycin C-induced ICLs. By using plasmids containing both a site-specific mitomycin C-induced ICL and a firefly luciferase reporter gene, it was shown that reactivation of the luciferase activity was dramatically reduced when these plasmids were introduced into XP-V cells. These data suggest the involvement of pol η in recombination-independent repair of the lesion. However, in this study, since the mutation frequency was only reduced from 22% to 15% relative to repair proficient cells, it was not possible to conclude that pol η catalyzed the mutagenic bypass of this lesion (70).

Germane to the correlation between pol η expression and cellular response to chemotherapeutic agents, the use of pol η expression levels as a marker to predict the efficacy of cisplatin has been evaluated and the need of alternative non-platinum chemotherapy regimens has been addressed, specifically for the treatment of non-small cell lung cancer (NSCLC) patients with high pol η levels (71). In patients with advanced

NSCLC who receive platinum-based chemotherapy, the expression of pol η predicted their survival, in which high expression correlated with poor survival. Pol η was also found to be an independent factor associated with survival of these patients. Additionally, pol η transcript levels were up-regulated in cisplatin-treated NSCLC cell lines, and NSCLC cell lines expressing a low level of pol η exhibited sensitivity to cisplatin, while cells expressing high level of pol η were refractory to cisplatin. These data indicated that high level of pol η can confer cellular resistance to cisplatin (71).

The expression of pol η also correlated with sensitivity of gastric cancer cell lines to oxaliplatin; cells with lower pol η expression were more sensitive to oxaliplatin (72). Additionally, pol η expression has been found to predict the response of patients with metastatic gastric cancer receiving FOLFOX (fluorouracil, leucovorin, and oxaliplatin) or XELOX (capecitabine and oxaliplatin). These data indicate that higher pol η levels correlate with a poor treatment response and shorter survival in patients treated with platinum-based drugs (72). Moreover, a cell-based study has shown that when XP-V cells were complemented with pol η , they were more refractory to gemcitabine, cisplatin, and the combination of gemcitabine and cisplatin than non-complemented XP-V cells (54). Similarly, fibroblasts depleted of pol η were more sensitive to cisplatin or gemcitabine alone, as well as the combination of cisplatin and gemcitabine, than pol η -proficient cells.

Furthermore, pol η expression is frequently dysregulated in tumors. Analyses of individual patients with NSCLC showed that pol η transcripts were highly elevated in

tumor tissue compared to normal tissue (71). It has also been shown that pol η transcripts were downregulated in human lung, colorectal, and stomach cancers (57,73).

Pol η may be involved in TLS past other DNA lesions, such as AAF-dG adducts, since XP-V cell extracts showed defects in replication bypass of such modifications (61,74). The role of pol η in protecting cells from both spontaneous and damage-induced mutagenesis has been studied, with emphasis on 8-oxo-dG-induced mutagenesis. In both XP-V cells and human fibroblasts depleted of pol η , the background mutant frequencies on both normal plasmids and plasmids treated with a 8-oxo-dG inducer, photoactivated methylene blue, were increased by approximately 2-fold (75).

Another function of pol η , in addition to lesion bypass, is to carry out somatic hypermutation of immunoglobulin genes. This programmed cellular process of directed mutagenesis is necessary to generate antibody diversity in the face of a foreign antigen challenge. In XP-V patients, a reduction in the mutations at A/T base pairs was observed and over 80% of mutations were G/C transversion at both J_H4 intron and pre-switch sequences at immunoglobulin gene locus (76).

1.3.1.1.3. Phenotype of pol η knockout mice

Pol η knockout mice are viable and fertile. However, they are susceptible to chronic sunlight-induced skin cancer, reflective of the XP-V patient clinical phenotype. These mice are particularly susceptible to epithelial skin tumor development (77). Additionally, pol $\eta^{-/-}$ mice have a dramatic reduction in mutations at A/T in the intronic sequence of the

J_H4 region in germinal center B cells, and a complete lack of A/T mutations was observed in mice deficient in both the MMR protein MSH2 and pol η (78,79). Furthermore, in pol $\eta^{-/-}$ mice, a reduction in the mutations at A/T base pairs was observed and over 80% of mutations were at G/C base pairs at both J_H4 intron and pre-switch sequences at immunoglobulin gene locus (76). These data confirm that pol η plays an important role in not only TLS, but also in somatic hypermutation of immunoglobulin genes.

1.3.1.2. DNA polymerase kappa

1.3.1.2.1. General and biochemical properties

Pol κ is a 99 kDa protein whose gene is located on chromosome 5q13.1 (80-82). Pol κ lacks a 3'-5' proofreading exonuclease activity and has a moderate processivity by elongating 1 to more than 25 nucleotides (29,81-84). Pol κ is a low fidelity enzyme, with the frequency of nucleotide misincorporation opposite ND nucleotides being $\sim 10^{-2}$ to 10^{-4} (29,85). Additionally, studies using gapped M13mp2 plasmids demonstrated that during synthesis of the target *lacZ α* gene, the frequency of *lacZ* mutants generated by pol κ was 25-34% (83). With regard to the types of mutations generated, base substitutions were the most prevalent, with the most frequent mutation being T to G transversions (29). Although pol κ exhibits low fidelity opposite all ND bases, it most frequently misincorporates opposite a template dT (29,86). Moreover, it can extend primers from several mismatched base pairs such as G-G, G-T and T-C, though it catalyzes the most efficient extension from canonical Watson-Crick base pairs (29). Furthermore, during DNA synthesis, it often generates DNA products that are one or two nucleotides shorter than what would be predicted based on the length of the template DNA (29,44,86-88).

Pol κ has been shown to catalyze replication bypass of a wide variety of DNA lesions. It can catalyze high fidelity bypass of (+)- and (-)-*trans-anti*-BPDE- N^2 -dG, with the correct dC being incorporated predominantly (44,45,87,89). It is intriguing that although pol κ can efficiently bypass the minor groove (+)- and (-)-*trans*-BPDE- N^2 -dG DNA adducts, it is completely blocked by major groove (+)- and (-)-*trans*-BPDE- N^6 -dA adducts (44). Germane to these observations, other studies have shown that pol κ could efficiently and accurately bypass acrolein-derived N^2 -dG peptide cross-links, while the polymerase was strongly blocked by N^6 -dA peptide cross-links; these lesions are chemically identical to N^2 -dG peptide cross-links, except that they are positioned in the major, not the minor groove of DNA (90,91). Additional N^2 -dG lesions that pol κ can efficiently and accurately bypass are acrolein-derived N^2 -dG ICLs (92) and the ring-opened reduced form of γ -HOPdG adducts (93). Pol κ also carries out accurate TLS past HNE-induced N^2 -dG adducts, though with reduced efficiency (56). Although pol κ was inhibited by γ -HOPdG at the nucleotide insertion step, the polymerase efficiently extended the primer from dC opposite the lesion (94). A variety of N^2 -alkyl dG lesions varying in size can also be bypassed by pol κ (95). Collectively, these data suggest that the cognate lesions of pol κ may be minor groove N^2 -dG lesions. Furthermore, the polymerase catalyzes bypass of 8-oxo-dG, an AP site, and AAF-dG or *N*-(deoxyguanosin-8-yl)-2-aminofluorene (AF)-adducted dG (AF-dG) adducts. When replicating DNAs containing 8-oxo-dG, pol κ predominantly incorporates dA opposite this lesion. Interestingly, the efficiency and specificity of nucleotides incorporated opposite an AP site were affected by the template base 5' to the lesion. Specifically, nucleotide incorporation occurred most efficiently and further extension was enhanced when the template base 5' to the AP site

was a dT. When DNAs containing site-specific AAF-dG were replicated, dC and dT were the most frequently incorporated nucleotides (44,82,86-88,96). Similar to the replication of ND DNA, pol κ can extend a mismatched primer termini past AAF-dG (86). When replicating DNAs containing AF-dG, pol κ predominantly incorporated dC and dA opposite the lesion (88).

The DNA lesions that block pol κ are T-T CPDs and (6-4) photoproducts, and dG-dG intrastrand cross-links induced by cisplatin (82,86,87). Although pol κ cannot incorporate a nucleotide opposite a T-T CPD, it can efficiently extend from mismatched primer termini past this lesion. In particular, the polymerase catalyzes the most efficient extension when dG is opposite the 3' T of the lesion, with the efficiency 3-fold higher than extension from a G-T mispair on ND DNA. These data suggest that pol κ may play a role in mutagenic bypass of T-T CPDs (97).

A study has shown that pol κ can bypass 4-OHEN-dA. It preferentially incorporated the correct dT opposite the lesion, but also incorporated dC, inducing A to G transitions (53). These data correlate well with a previous study showing that A to G transitions are one of the predominant base substitutions found at AT pairs of the *supF* reporter gene following replication of a DNA vector exposed to 4-OHEQ (52). Thus, pol κ may be responsible for inducing these types of mutations in cells during the bypass of the 4-OHEN-dA adduct. It is important to mention that these findings indicate that the miscoding property of 4-OHEN-dA due to error-prone TLS may contribute significantly to the development of cancers induced by equine estrogens.

Similarly, pol κ may contribute to the generation of mutations following replication past ϵ dA. Steady-state kinetic analyses revealed that pol κ preferentially incorporates the correct dT opposite the lesion, and also efficiently extends from a ϵ dA:A mispair. When TLS products were analyzed for both base substitutions and frameshift mutations, it was found that one nucleotide deletions were the predominant product of pol κ -catalyzed TLS, followed by dT, dA, and dC incorporation. Overall, these results show that pol κ catalyzes both error-free and error-prone TLS past ϵ dA (43). However, contradicting data have been presented by another group who reported that pol κ catalyzes only error-free TLS past this lesion (42).

1.3.1.2.2. *In vivo functions and implications in tumorigenesis/chemotherapy resistance*

The role of pol κ in the processing of naturally occurring non-B-DNA structures has been studied. When pol κ was depleted from HeLa cells and these cells were then transfected with plasmids containing G-rich sequences from the human c-MYC promoter region, an increase in the induction of DSBs was observed. Pol κ depletion also enhanced DSB formation in HeLa cells transfected with plasmids containing GA-rich sequences from the breakage hotspot region of the Kaposi sarcoma associated Herpes virus genome or the major break region of human *BCL-2* gene. Additionally, it was demonstrated that pol κ is involved in the processing of G-quadruplex DNA structures, since U2OS cells depleted of pol κ exhibit decreased survival in response to telomestatin. Collectively, these data show that pol κ plays an important role in genomic stability maintenance at naturally occurring unusual DNA sequences (57).

As observed *in vitro*, pol κ has been shown to be involved in TLS past various DNA lesions in cells. Using SV40-based pBS/pSB vectors, when pol κ was depleted from human fibroblasts, the efficiency of TLS past either the 5R,6S or 5S,6R thymine glycol lesion decreased to about 50%; additionally, replication of DNAs containing these lesions during pol κ depletion resulted in an increase in the mutagenic frequencies by more than 2-fold (98). These data predict a role of pol κ in efficient and accurate bypass of thymine glycols. Moreover, when gapped plasmids harboring a site-specific (+)-*trans*-BPDE- N^2 -dG adduct were replicated in U2OS cells depleted of pol κ , the efficiency of TLS decreased by 2.3-fold, and mutagenic TLS decreased by 1.9-fold, with increases in deletions and insertions from 14 to 25.9%, respectively (99).

Pol κ plays a role in the processing of cross-link lesions. The function of pol κ in the accurate and efficient TLS past N^2 -dG ICLs was proposed based on *in vitro* observations and is supported by cellular studies reported by Minko *et al.* They demonstrated that human fibroblasts depleted of pol κ are moderately sensitized to a N^2 -dG ICL-inducing agent mitomycin C. Furthermore, mitomycin C enhanced formation of aberrant chromosomal structures, in particular, radial structures, in these cells (92). Studies using gapped plasmids carrying site-specific cisplatin-induced dG-dG intrastrand cross-links showed that when these plasmids were replicated in U2OS cells that had been depleted for pol κ , there was a 34% decrease in the efficiency of TLS and 5.7-fold decrease in mutagenic TLS (99). This is an unexpected finding, as pol κ cannot bypass this type of cross-link *in vitro*.

Consistent with data derived from human cells, the role of pol κ in accurate TLS past B[a]P-induced dG adducts has been observed in mouse cells. Using a gapped plasmid containing a site-specific B[a]P-induced dG adduct, the efficiency of TLS was found to be reduced in pol $\kappa^{-/-}$ mouse embryonic fibroblasts (MEFs), and the incorporation of the incorrect nucleotides was increased in these cells (100). Another group has reported similar results that mouse embryonic stem cells knocked out for pol κ exhibit a 3-fold increase in killing following exposure to B[a]P and had an increase in mutation frequency by 10-fold, with G to T transversions predominating at the *Hprt* locus (101). Additionally, pol κ has been shown to be important for cells to recover from BPDE-induced S-phase checkpoint and to overcome replication fork blocks and prevent the formation of DSBs. This study also found that pol κ is required for cellular survival after BPDE exposure, and in response to BPDE, pol κ -deficient MEFs exhibit prolonged checkpoint activation and formation of DSBs, as observed by prolonged Chk1 phosphorylation and an increased level of histone γ -H2AX. The increase in phosphorylation of ATM and Chk2 were detected in these cells as well (102). In addition to B[a]P, pol κ may be involved in coping with lesions induced by other types of polycyclic aromatic hydrocarbons, since both the transcript and protein levels of pol κ are upregulated when mice are exposed to 3-methylcholanthrene (103).

Mouse embryonic stem cells and fibroblasts knocked out for pol κ exhibit elevated sensitivity to UV (101,102,104). Similar to the response to BPDE, pol κ was needed for cells to progress through S phase after being arrested by UV irradiation (102). The role of pol κ in the processing of DNA lesions is also evident in studies showing that pol

κ transcripts can be upregulated in mice in response to several DNA-damaging agents, including UV irradiation and doxorubicin (105).

In addition to its role in TLS, a role for pol κ in the repair synthesis step of NER has been investigated. Several lines of evidence support this model, including the greatly diminished capability of pol κ -deficient MEFs to remove (6-4) photoproducts. This unexpected function of pol κ may explain its sensitivity to UV damage despite of its inability to bypass UV-induced lesions *in vitro* (106).

In addition to studies suppressing or knocking out pol κ , the effects of overexpression of pol κ have been investigated. In both human cells and mice, the mutation rate at the *Hprt* locus was increased upon pol κ overexpression. In a separate study when pol κ was ectopically expressed, mutation rates, DNA breaks, genetic recombination, loss of heterozygosity, and aneuploidy were enhanced. All these data suggest that dysregulated pol κ expression may perturb normally accurate chromosome duplication and thus promote mutagenic replication (12,81).

With regard to the link between pol κ and specific types of tumors, pol κ activity may be germane to the etiology of gliomas. Recent studies have demonstrated that the expression of pol κ protein is upregulated in over 50% of glioma patients, and there was a significant association between pol κ expression and the advanced stage of the disease. Moreover, pol κ has been identified as an independent prognostic factor for glioma patients, where high expression indicates poor survival (107). Pol κ has also been shown to be

overexpressed in NSCLC. Since pol κ is involved in the replication bypass of adducts induced by B[a]P, a common constituent of cigarette smoke, pol κ expression may be dysregulated in smokers (108). However, data exist showing that the transcript level of pol κ is significantly down regulated in lung cancer tissues. The down regulation of pol κ transcripts was also observed in stomach and colorectal cancer tissues (73).

1.3.1.2.3. *Phenotype of pol κ knockout mice*

Mice deficient in pol κ are viable and fertile (104). However, they exhibit significantly elevated spontaneous mutations particularly in liver, kidney, and lung. Interestingly, there is a tissue-specific mutagenesis pattern observed in these mice. For instance, G:C to T:A mutations were predominant in the kidney and liver, while G:C to A:T mutations were moderately increased in the lung. Additionally, A:T to T:A mutations were moderately increased in lung and liver (109). Finally, these mice exhibit a mutator phenotype associated with ageing and the accumulation of endogenous DNA lesions, suggesting that pol κ is involved in the tolerance of oxidative damage (81).

1.3.1.3. DNA polymerase iota

1.3.1.3.1. *General and biochemical properties*

Pol ι is an 80 kDa protein, whose encoding gene resides on chromosome 18q21.1 (22,110,111). Pol ι lacks a 3'-5' proofreading exonuclease activity and has a low processivity, only elongating 1-3 nucleotides depending on the sequence context of the template (112). Pol ι is a low fidelity enzyme, with a tendency to preferentially misincorporate dG opposite a template dT and is capable of extending from some

mismatched bases. It also has an interesting property in preferentially utilizing dTTP (112). The frequency of nucleotide misincorporation opposite ND bases is $\sim 10^1$ to 10^{-6} (113-115). Additionally, studies using gapped M13mp2 plasmids demonstrated that during synthesis of the target *lacZ α* gene, the frequency of *lacZ* mutants generated by pol ι was 61% (116). This value is much higher than for other Y-family polymerases.

Several DNA lesions have been shown to be substrates for pol ι -catalyzed TLS. Generally, pol ι functions at the nucleotide insertion step. Pol ι can efficiently incorporate the correct dT opposite ϵ dA (42). Pol ι inserts dG and dC with similar efficiency opposite 8-oxo-dG (36). In addition, pol ι can incorporate the correct dC opposite AAF-dG (117). Although full bypass was not achieved, pol ι can incorporate nucleotides opposite (+)- and (-)-*trans*-BPDE- N^2 -dG adducts in an error-prone manner by preferential insertion of dG opposite (+)-*trans*-BPDE- N^2 -dG and both dA and dG opposite (-)-*trans*-BPDE- N^2 -dG. The bypass of (+)- and (-)-*trans*-BPDE- N^6 -dA adducts was similarly error-prone, though dT incorporation was preferred opposite (-)-*trans*-BPDE- N^6 -dA adducts (44). The polymerase also incorporated nucleotides opposite the 3' T and 5' T of (6-4) photoproducts and AP sites; in most sequence context, dA or dG and dT was preferentially inserted opposite the 3' T or 5' T of a (6-4) photoproduct, respectively, while opposite an AP site, the incorporation of either dG or dT was preferred (114,118). Pol ι can incorporate nucleotides opposite m6G as well, with dT incorporated most efficiently (119). In contrast, pol ι catalyzed limited or no TLS past a T-T CPD (114,117), and during the limited synthesis, either dT or dG was incorporated preferentially opposite the 3' dT (118). Although pol ι is generally more proficient at the nucleotide insertion

step than the primer extension step, the polymerase can extend primers past some lesions. For instance, pol ι has been shown to catalyze its most efficient primer extension when dT or dA is situated opposite m6G or 8-oxo-dG, respectively (119). Furthermore, pol ι can incorporate a nucleotide opposite acrolein-induced γ -HOPdG, or its ring-opened reduced form, PdG, as well as HNE-induced N^2 -dG adducts, by preferentially inserting dC or dT (56,93,94). dC incorporation opposite some N^2 -alkyl dG lesions could also be performed by pol ι (120).

1.3.1.3.2. *In vivo functions and implications in tumorigenesis/chemotherapy resistance*

An important role of pol ι in protecting cells from oxidative DNA damage has been investigated, where human fibroblasts stably down regulated for pol ι were found to be hypersensitive to agents that induce oxidative stress, including hydrogen peroxide and menadione (121). Moreover, these cells exhibited moderate sensitivity to low dose potassium bromate treatment, another oxidizing agent. From studies using human fibroblast cell extracts that had been depleted of pol ι , it was shown that the activity of BER was reduced (121).

Pol ι may play a mutagenic role in the processing of UV-induced DNA lesions. The replication of normal and UV-damaged plasmids in human 293T cells that were depleted of pol ι was significantly decreased (122). Fibroblasts from pol ι knockout mice were hypersensitive to UV irradiation (77). A 2-fold decrease in the frequencies of total mutants and base substitutions induced by UV was observed in primary fibroblasts derived from pol ι -deficient mice. The majority of these base substitutions were at dipyrimidines on the nontranscribed strand, resulting in a 2.4-fold bias toward the

nontranscribed strand. Since this strand bias was 4.5-fold in wild-type cells, pol ι is likely to contribute to the strand bias for UV-induced mutagenesis. The loss of pol ι resulted in a decrease in UV-induced mutagenesis, suggesting that mouse pol ι has a role in TLS past UV-induced lesions (67).

The potential role for pol ι in modulating carcinogenesis has received support in both an animal model system and human tumor data. Pol ι may play a role in breast cancer genomic instability by catalyzing error-prone bypass of UV-induced lesions, preferentially misincorporating dT or dG opposite the 3' T of T-T CPDs and 5' T of (6-4) photoproducts (118). These data are consistent with a large increase in the frequency of T to A transversions and T to C transitions in breast cancer cells, with UV-induced mutation frequencies reduced when pol ι is immunodepleted from nuclear extracts of breast cancer cells (123). Another study showed that the mouse 129XI locus harboring a mutated *pol ι* gene conferred susceptibility to lung tumors induced by urethane, suggesting a protective role of pol ι in the prevention of lung tumor development (124).

With regard to the correlation between pol ι expression and carcinogenesis, the dysregulation of pol ι expression was observed in several cancers. Pol ι is upregulated in breast cancer cells, both at the transcript and protein levels, and protein levels were rapidly increased after exposure to UV in both nonmalignant breast cells and breast cancer cells. Since breast cancer cells exhibit higher spontaneous and UV-induced mutant frequencies relative to normal breast cells in plasmid-based assays, pol ι activity may be germane to the development of breast cancers (123). Pol ι may also contribute to the

etiology of some gliomas, since protein expression of pol ι is upregulated in over 25% of glioma patients. Furthermore, glioma patients who were positive for elevated levels of pol ι had shorter survival prognoses (107). In contrast, down regulation of pol ι transcripts were observed in other types of tumors, such as colorectal, lung, and stomach cancers (73).

1.3.1.3.3. *Phenotype of pol ι knockout mice*

Pol ι knockout mice are viable and fertile. However, when exposed to chronic UV irradiation, these mice develop mesenchymal skin tumors, such as sarcomas and hemangiomas. Additionally, if there is a loss of a single allele of pol η in this genetic background, there is a concomitant increase in the incidence of epithelial skin tumor development following chronic UV exposure (77). Furthermore, the presence of pol ι significantly delayed the formation of UV-induced skin tumors, since the time to UV-induced tumor formation was earlier in mice deleted for both pol ι and pol η versus the pol η knockout alone (67).

1.3.1.4. Rev1

1.3.1.4.1. *General and biochemical properties*

Rev1 is a 138 kDa protein whose gene is located on chromosome 2q11.1-11.2 (125). Rev1 lacks a 3'-5' proofreading exonuclease activity (126). It is a template-dependent dCMP transferase, which catalyzes efficient insertion of dC opposite dG or dU. Rev1 is a low fidelity enzyme due to its unique ability to incorporate dC opposite bases, resulting in a frequency of nucleotide misincorporation opposite ND bases of

$\sim 10^0$ to 10^{-5} (126,127).

In vitro, Rev1 can catalyze replication bypass of a number of DNA lesions, and it primarily functions in the nucleotide incorporation step of TLS. Rev1 can insert a nucleotide dC opposite acrolein-derived γ -HOPdG (128), an AP site, 8-oxo-dG, (+)- and (-)-*trans-anti*-BPDE- N^2 -dG, ϵ dA, and some N^2 - and O^6 -alkyl dG adducts. Although it can incorporate dC opposite AAF-dG, the efficiency is low. The types of lesions that block Rev1 include T-T CPDs and (6-4) photoproducts (126,129,130).

1.3.1.4.2. *In vivo functions and implications in tumorigenesis/chemotherapy resistance*

The cellular function of Rev1 in TLS has been studied. Rev1 appears to play roles in both an early TLS pathway that allows for the progression of a stalled replication fork and late in the postreplicative gap-filling pathway for UV-induced lesions. Even though *in vitro* studies demonstrated that Rev1 was blocked at (6-4) photoproducts, it was found using gapped plasmids that TLS past a (6-4) photoproduct was reduced by more than 3-fold in Rev1-deficient MEFs. Additionally, Rev1 catalyzed mutagenic bypass of the (6-4) photoproduct resulted in transversions of GC to TA at a dG immediately 5' to the lesion. Furthermore, MEFs deficient in both Rev1 and the NER protein, XPC, underwent a G₂ phase arrest that was caused by accumulation of (6-4) photoproducts. Rev1 also protected cells from UV-induced lethality, since MEFs deficient for Rev1 are sensitive to UV irradiation (13). A study using SV40-based pMTEX4 vectors to replicate in Rev1-deficient MEFs has shown that Rev1 may be involved in TLS associated with the incorporation of dA opposite a heptanone-etheno-dC adduct (131).

Rev1 activity may be associated with carcinogenesis and chemotherapy resistance. Lymphoma cells deficient in Rev1 had reduced frequency of mutants induced by cyclophosphamide (CTX, a nitrogen mustard alkylating agent). Mice transplanted with mouse lymphoma cells during cancer relapse did not respond to CTX, while tumors with decreased Rev1 continued to exhibit sensitivity to CTX. Furthermore, the majority of these tumors still responded to CTX following a third round of CTX treatment (132). A role of Rev1 in the tolerance of both spontaneous and cisplatin-induced damages has also been demonstrated by studies using ovarian carcinoma cell lines stably depleted of Rev1. Down regulation of Rev1 rendered cells less mutagenic, with a 2.9-fold decrease in the spontaneous rate of mutations being observed. Additionally, these cells were 1.5-fold more sensitive to the cytotoxic effect of cisplatin, and the frequency of cisplatin-induced mutations was 2.6-fold lower when Rev1 was depleted. Furthermore, down regulation of Rev1 decreased the cisplatin-resistant variants, suggesting that drug resistance was mediated by a mutagenic function of Rev1. At the population level, the development of acquired resistance to cisplatin was dependent on the function of Rev1 (133). In addition, BPDE-induced mutant frequencies in primary mouse fibroblasts were reduced when Rev1 was down regulated by a ribozyme against Rev1. In these mice, a significant reduction in BPDE-induced lung tumor multiplicity was observed, and the formation of tumors was also prevented in 27% of these mice (134). The role of Rev1 in both the spontaneous and cisplatin-induced extrachromosomal HR has been suggested, since the frequency of spontaneous and cisplatin-induced HR events was decreased when Rev1 was down regulated (133).

Germane to the role of Rev1 in carcinogenesis, dysregulated expression of Rev1 may contribute to chemotherapy resistance. For example, ovarian carcinoma cell lines overexpressing Rev1 are resistant to the cytotoxic effect of cisplatin and exhibit an increased frequency of mutants induced by cisplatin. These cells also acquire resistance to cisplatin at a rate faster than the parental cells, indicating that Rev1 plays a role in controlling the rate of development of cisplatin resistance at the population level (135). Furthermore, Rev1 protein expression is increased in response to cisplatin in ovarian carcinoma cell lines (133).

1.3.1.4.3. *Phenotype of Rev1 knockout mice*

The viability of Rev1 knockout mice is strain-specific; in the C57BL/6 background, mice were not viable, whereas in the 129/OLA background, they were viable. These mice also lack the C to G transversions in the nontranscribed strand during somatic hypermutation of immunoglobulin genes, and this was accompanied by significant increases in the frequency of A to T and C to A transversions and T to C transitions (136).

1.3.2. B family polymerase

1.3.2.1. DNA polymerase zeta

1.3.2.1.1. *General and biochemical properties*

Human pol ζ is a 350 kDa protein composed of two subunits, the catalytic subunit Rev3L and the accessory subunit Rev7. The *Rev3L* and *Rev7* genes are located on chromosome 6q21 and 1p36, respectively (22,137,138). The human pol ζ has not been purified to date. Thus, the biochemical properties of human pol ζ are deduced based on studies using

yeast pol ζ . Pol ζ lacks a 3'-5' proofreading exonuclease activity and has a moderate processivity of elongating ≥ 3 nucleotides (139). Compared to other TLS polymerases, pol ζ is a relatively high fidelity enzyme. The frequency of nucleotide misincorporation opposite ND bases is $\sim 10^{-3}$ - 10^{-5} (114,129,140). Additionally, studies using gapped M13mp2 plasmids demonstrated that during synthesis of the target *lacZ α* gene, the frequency of *lacZ* mutants generated by pol ζ was 10 to 12%. This value is much lower than for Y-family polymerases (141).

Generally, pol ζ catalyzes inefficient nucleotide insertion opposite DNA lesions, but is proficient in extending a primer terminus positioned opposite a lesion. Although the ability of pol ζ to incorporate a nucleotide opposite 8-oxo-dG, the acrolein-mediated γ -HOPdG adduct, m6G, T-T CPD, (6-4) photoproduct, and an AP site was strongly inhibited, the polymerase can efficiently extend from the primers opposite these lesions. The extension was most efficient when dA was placed opposite 8-oxo-dG or an AP site, dC was placed opposite m6G or an acrolein-mediated γ -HOPdG adduct, or dG was placed opposite the 3' T of a T-T CPD or a (6-4) photoproduct (114,128,129,140). However, pol ζ can fully bypass thymine glycols, preferentially incorporating the correct dA opposite the lesion and efficiently extending from this correct base pair (40). A nitrogen mustard-like ICL is another lesion that pol ζ can accurately bypass. Additionally, it can insert dC opposite a cisplatin-induced ICL (142).

1.3.2.1.2. *In vivo functions and implications in tumorigenesis/chemotherapy resistance*

The function of pol ζ in TLS on a variety of DNA lesions has been demonstrated. Using gapped plasmids, depletion of Rev3L in U2OS cells was found to result in a decrease in the extent of TLS across a (+)-*trans*-BPDE- N^2 -dG adduct or a cisplatin-induced intrastrand dG-dG adduct by 5.5-fold. The TLS of a (6-4) photoproduct was also reduced by 10-fold (99). Moreover, it was demonstrated that the frequency of TLS past a thymine glycol lesion on an SV40-based pBS/pSB vector decreased about 50% in human fibroblasts depleted of either Rev3L or Rev7. TLS past these lesions was error-free, since knockdown of Rev3L or Rev7 increased the frequency of mutagenic TLS by more than 2-fold (98). The role of pol ζ in protecting cells from the cytotoxic effects of UV has been further addressed. In XP-V cells, depletion of Rev3L rendered these cells 33- to 39-fold more sensitive to UV, and in XPA cells, Rev3L knock down led to a 4 to 5-fold increase in UV sensitivity (68). Pol ζ may also play a role in mutagenic bypass of UV-induced DNA damage, since large decreases in mutations at the 3' nucleotide of a TT or CT dimer were observed (66). Furthermore, the type I Burkitt's lymphoma BL2 cell line deficient in Rev3L was 10-fold more sensitive to UV than wild-type cells (66), and there was a dramatic decrease in the UV-induced mutant rate in these cells (3.3 to 0.7%) (66). Double close mutations, a type of mutation that involves two point mutations spaced by one correct base, with thymidine predominantly being the correct nucleotide, were not detected in the Rev3L-deficient cells, indicating that Rev3L was responsible for introducing this type of mutation (66). The role of pol ζ in the processing of cisplatin-induced DNA lesions was also evident in studies using human fibroblasts (143). Cisplatin upregulated the transcripts of Rev3L, and Rev3L knockdown significantly reduced the

rate at which cells acquired resistance to cisplatin; the rate of development of cellular resistance to cisplatin was decreased by approximately 3-fold. These Rev3L depleted cells were also sensitive to cisplatin and the frequency of cisplatin-induced mutants was decreased (143). Finally, besides a role in TLS, pol ζ was shown to be important for both spontaneous and cisplatin-induced HR (143).

Consistent with data in human cells, studies in mice support the role of pol ζ in TLS past several DNA lesions. In MEFs deficient in Rev3L, the extent of TLS past a (+)-*trans*-BPDE- N^2 -dG adduct, cisplatin-induced intrastrand dG-dG adduct, an AP site, 4-hydroxyequilenin-C, a (6-4) photoproduct, or an artificial lesion with a chain of 12 methylenes inserted into the DNA backbone was significantly reduced. Additionally, mutagenic TLS across a (+)-*trans*-BPDE- N^2 -dG adduct, a cisplatin-induced intrastrand dG-dG adduct, a 4-hydroxyequilenin-C damage, or a (6-4) photoproduct was 6.3-fold, 7.2-fold, 3.5-fold, or 20-fold less, respectively (99). Furthermore, Rev3L knockout mouse cells were hypersensitive to the alkylating agents temozolomide and fotemustine, and these agents increased the levels of γ -H2AX foci in these cells. O^6 -benzylguanine, an agent that inactivates O^6 -methylguanine-DNA methyltransferase, had no effect on temozolomide-induced cell death in these cells, but it enhanced apoptosis when cells were treated with fotemustine. These studies suggest that pol ζ may be involved in the processing of fotemustine-induced O^6 -chloroethyl-dG adducts and temozolomide-induced damages other than m6G (144). Rev3L-deficient cells in a p53 null background are sensitive to several DNA-damaging agents, including UV, mitomycin C, γ -irradiation, and methyl methane sulfonate (145). Furthermore, a study using SV40-based pMTEX4

vectors in Rev3L-deficient MEFs has shown that pol ζ may be involved in TLS associated with the incorporation of dA opposite a heptanone-etheno-dC adduct (131).

The contribution of pol ζ to genomic stability has been illustrated in several studies. Multiple chromosomal abnormalities not seen in Rev3L-proficient MEFs were observed in Rev3L-deficient MEFs in a p53^{-/-} background. These included dicentrics, insertions, and compound isochromosome/translocation events; overall chromosomal aberrations were also increased in these cells. Among these aberrations, the largest increase was observed in the number of translocation events. Rev3L-deficient cells in a p53^{-/-} background exhibit spontaneous chromosomal instability; these cells had increased numbers of fused/translocated chromosomes, chromosomes with terminal deletions, micronuclei, and rearranged marker chromosomes (145). Additionally, in response to cisplatin and mitomycin C, cancer cell lines depleted of Rev3L or Rev7 had reduced survival and exhibit an increase in chromosomal aberrations (146).

Germane to the function of pol ζ in the maintenance of genomic stability, several lines of evidence suggest that pol ζ may participate in carcinogenesis. Depletion of Rev3L sensitized cisplatin-resistant lung adenocarcinoma cell lines and reduced mutations, suggesting that Rev3L protects cells from drug-induced cell death, but at the cost of introducing mutations in cisplatin-treated cells. These cells also exhibited increased cisplatin-induced γ -H2AX foci formation and senescence, indicating that Rev3L plays a role in the repair of cisplatin-induced DNA damage. Similar phenomena (decreased mitotic indices and increased apoptosis) were also observed in Rev3L-deficient lung

adenocarcinoma cell transplants in mice treated with cisplatin. In particular, these transplants exhibited tumor regression, or at a minimum, growth stasis, and these mice survived nearly twice as long as cisplatin-treated mice bearing control lung adenocarcinoma cell transplants. A rapid reduction in lymphomas was seen in mice harboring Rev3L-deficient tumors, and these tumors exhibited enhanced sensitivity to cisplatin (147). It is interesting to note that Rev3L heterozygous cells exhibit intermediate sensitivity to temozolomide and fotemustine (144). Such data indicate that Rev3L levels dictate the extent of cellular tolerance to alkylating drugs. Rev3L also plays a role in introducing mutations in gliomas, since the frequency of cisplatin-induced mutations at the *Hprt* locus was significantly reduced in Rev3L-depleted glioma cells (148). Thus, optimal chemotherapeutic protocols may require the determination of Rev3L expression levels in tumors of patients before and after they receive treatment with an alkylating agent.

Although Rev3L is important in both MMR-proficient and -deficient malignant colon carcinoma cells, cells depend more on pol ζ -catalyzed error-prone TLS past cisplatin-induced lesions for cell survival in the absence of MMR. This was made evident in a study demonstrating that Rev3L depletion in MMR-deficient cells results in decreased cisplatin-induced mutants by 58%, in contrast to the 38% reduction seen in MMR-proficient cells. Thus, targeting pol ζ to reduce the rate of drug resistance development may be more important in tumors that are defective in MMR (149).

The dysregulation of Rev3L may be germane to cancer etiology. Rev3L transcripts were slightly increased in lower grade gliomas (grade I and grade II), but significantly increased in higher grade gliomas (grade III and grade IV) compared with normal brain tissue, with highest expression in grade IV gliomas. As expected, glioma cells expressing high levels of Rev3L were refractory to cisplatin-induced apoptosis (148). Additionally, down regulation of Rev3L transcripts was observed in colorectal, lung, and stomach cancer tissues (73).

Pol ζ may function in protecting cells from carcinogenesis. Deletion of chromosome 6q21, including the *Rev3L* gene, has been observed in multiple cancers, such as acute lymphoblastic leukemia, T-cell lymphomas, and gastric high-grade large B-cell lymphoma (150-152). Additionally, the *Rev3L* gene is positioned within the fragile site of FRA6F, and there is an overlap between the 3' region of human *Rev3L* and one of the two breakage hotspots. A wide variety of cancers, including leukemia and melanoma, have deletion breakpoints at the FRA6F fragile site in a 1.2 Mbp region at 6q21. Thus, the loss of Rev3L may have a significant consequence in carcinogenesis (153).

1.3.2.1.3. Phenotype of *pol* ζ knockout mice

Even though pol ζ is not essential for cellular survival in yeast, several initial attempts to create viable mice disrupted in the *Rev3L* gene were not successful (154-156). Collectively, these investigations reported mid-gestation lethality, with retarded embryonic development, tissue disorganization, and reduced cell densities. Although these data demonstrate an essential role in embryonic genome stability, the non-

redundant, critical function of pol ζ in embryogenesis can only be speculated, and may include TLS past endogenously-induced DNA damage, replication of DNA with non-canonical structures, and/or participation in recombination.

Notably, MEFs derived from even early stage embryos were not viable long term. However, the laboratory of Dr. Rick Wood was ultimately successful in creating stable MEFs from a single E10.5 *Rev3L*^{-/-};*p53*^{-/-} embryo (145). As described above, these MEFs manifested marked chromosomal instability and displayed increased sensitivity to a variety of DNA-damaging agents (145).

More recently, the Wood laboratory has been successful in creating mice where the *Rev3L* gene can be conditionally inactivated from epithelial tissues (157). In mice deleted for *Rev3L* in a *Tp53*^{-/-} background, the latency of thymic lymphomas was shortened and the incidence was higher. In addition, conditional knockout animals developed significantly more mammary tumors in both *Tp53*^{+/+} and *Tp53*^{+/-} backgrounds, and deletion of *Rev3L* from *Tp53*^{+/-} mice resulted in an accelerated occurrence of these tumors. Finally, there was an increase in the number of both preneoplastic and neoplastic lesions in these mice. These data reveal that pol ζ functions to inhibit spontaneous tumor formation.

1.3.3. A family polymerases

1.3.3.1. DNA polymerase nu

1.3.3.1.1. *General and biochemical properties*

Pol ν is a 102 kDa protein whose gene is located on chromosome 4p16.3. Pol ν lacks a 3'-5' proofreading exonuclease activity and has a moderate processivity, elongating 1-100 nucleotides (158-160). It catalyzes efficient strand displacement on both ND and damage (psoralen-induced ICL)-containing substrates (55,158). *In vitro*, pol ν replicates ND DNA with low fidelity, primarily due to frequent misincorporation of dT opposite template dG, where the catalytic efficiency of incorporation of an incorrect dT opposite a template dG is approximately half that of the error-free reaction (158,159). The frequency of nucleotide misincorporation opposite ND nucleotides is $\sim 10^{-1}$ to 10^{-4} (158). Additionally, studies using gapped M13mp2 plasmids found that during synthesis of the target *lacZ α* gene, the frequency of *lacZ* mutants generated by pol ν was 2.3% when reactions were carried out at neutral pH, yet was 18% when reactions were carried out at alkaline pH (159,161). Furthermore, the polymerase can catalyze nontemplated nucleotide addition at a blunt end (158).

Initially, pol ν was shown to carry out efficient and high fidelity TLS of template DNAs containing a thymine glycol lesion, whereas the polymerase was completely blocked by a number of other DNA modifications, including a cisplatin-induced dG-dG intrastrand cross-link, an AP site, a T-T CPD, and a (6-4) photoproduct (158). Recently, it was discovered that pol ν is able to bypass very large DNA lesions that are positioned in the DNA major groove (162). Specifically, pol ν efficiently and accurately bypasses

acrolein-derived DNA–peptide cross-links in which peptides are linked to N^6 -dA. Additionally, pol ν bypasses an N^6 -dA ICL. However, when a chemically identical DNA–peptide or DNA interstrand cross-link was located in the minor groove via an N^2 -dG linkage, TLS by pol ν was completely inhibited. Thus, it is not the identity of the DNA lesion, but its location within the template that is critical for bypass by pol ν . Germane to the ability of pol ν to bypass ICLs, it was shown that pol ν can bypass an unhooked psoralen-induced ICL that models the intermediate structure generated during ICL repair in an error-free manner, albeit with low efficiency (55). Furthermore, it was shown that pol ν catalyzes inefficient, although accurate, bypass of ϵ dA, and predominantly incorporates an incorrect dA opposite (+)-*trans-anti*-BPDE-dA((+)-BPDE-dA), though full bypass of this latter lesion was not achieved (162).

1.3.3.1.2. *In vivo functions and implications in tumorigenesis/chemotherapy resistance*

Although cellular roles for pol ν have not been clearly identified, a function for pol ν in DNA cross-link repair via HR in human cells has been proposed (163). When pol ν is depleted, cells become sensitive to the cytotoxic effects of mitomycin C, cisplatin, and high doses of γ -irradiation. Indeed, the polymerase activity of pol ν is essential for conferring cellular resistance to mitomycin C (55,163). Pol ν -depleted cells also exhibit increased mitomycin C-induced chromosomal aberrations, particularly radial chromosomes, and the efficiency of HR in these cells is reduced by 50%. It is reasonable to hypothesize that the efficient strand displacement synthesis activity of pol ν plays an important role in HR associated with specific pathways of ICL repair. Pol ν -depleted cells are also mildly sensitive to the strand-break-inducers, camptothecin and bleomycin.

Finally, hydroxyurea or ionizing irradiation increased the accumulation of DSBs in cells stably depleted of pol ν .

The role of pol ν in HR is further supported by an observation that pol ν interacts with multiple proteins involved in HR, such as RAD51, as well as proteins in the Fanconi anemia pathway, including FANCD2, FANCI, FANCA, and FANCG. Pol ν also interacts with ubiquitinated FANCD2 following mitomycin C exposure, and some of the above interactions occur exclusively in S phase, correlating with the observation that the levels of pol ν decrease as cells exit S phase (163). Currently, a cellular role of pol ν in TLS has not been investigated. However, studies in chicken DT40 cells show that pol ν plays roles in both HR-dependent immunoglobulin V gene conversion and TLS-dependent immunoglobulin hypermutation by catalyzing TLS past AP sites to promote diversification of immunoglobulin V genes (164).

With regard to the link between pol ν and cancers, pol ν transcript levels were found to be significantly higher in breast carcinoma than in non-tumor breast tissue (165). It is of interest to note that deletion of chromosome 4p16.3, where the *pol \nu* gene is located, occurs in 50% of breast carcinomas (166). Since mutation frequencies generated during the replication of unadducted plasmids, UV-irradiated plasmids, or plasmids containing psoralen-induced lesions were also slightly increased when pol ν was knocked down, pol ν may function as a tumor suppressor under certain conditions (163). Pol ν may promote cancer progression in other situations, as suggested by the ubiquitous expression of pol ν in several cancer cell lines (160). Currently, the creation of pol ν knockout mice is in

progress. Future investigation using these mouse models will foster our understanding of the cellular functions of pol ν and its contribution to carcinogenesis.

1.3.3.2. DNA polymerase theta

1.3.3.2.1. *General and biochemical properties*

Pol θ is a >250 kDa protein whose gene is located on chromosome 3q13.33 (78,160). Pol θ lacks a 3'-5' proofreading exonuclease activity, and has a moderate processivity, elongating from 1 to greater than 75 nucleotides (161,167). Pol θ possesses single-stranded DNA-dependent ATPase activity (167). It is a low fidelity enzyme that is particularly inaccurate incorporating opposite dT, with the frequency of misincorporation measured at $\sim 10^{-2}$ to 10^{-3} (39). Additionally, studies using a gapped M13mp2 DNA found that during synthesis of the target *lacZ α* gene, the frequency of *lacZ* mutants generated by pol θ was 27% to 31%, similar to pol η and pol κ . It has also been shown that pol θ generates base insertion and deletion errors at a high rate, uniquely generating more addition than deletion errors. Furthermore, among the base substitutions generated by pol θ , the majority are introduced during replication of a template dA or dT (161). Pol θ potentially functions as a mismatch extender, since it is capable of extending all types of mispaired termini opposite dA or dT, and similar to pol ν , it can catalyze nontemplated addition at a blunt end (39,78). Pol θ also possesses 5' deoxyribose-phosphate lyase activity; it removes deoxyribose-phosphate from DNA and fills a 1 nucleotide gap, suggesting a role in single-nucleotide BER (168). Although this enzyme contains a helicase-like domain, responsible for its ATPase activity, a DNA unwinding activity has not been detected (167).

Pol θ can bypass several DNA lesions, including an AP site and a thymine glycol, but is blocked by a number of lesions, including a cisplatin-induced dG-dG intrastrand cross-link, a T-T CPD, and a (6-4) photoproduct (39,158). During the bypass of an AP site, pol θ preferentially inserts dA opposite the lesion and then extends the primer, potentially contributing to AP site-induced mutagenesis (39). Although pol θ can not insert nucleotides opposite a (6-4) photoproduct, it can extend the primer if positioned opposite the lesion (169). In addition, studies using a cell extract deficient in pol θ showed that the polymerase may have a role in both single-nucleotide and long-patch BER, and is important in BER of 8-oxo-dG (170).

1.3.3.2.2. *In vivo functions and implications in tumorigenesis/chemotherapy resistance*

The role of pol θ in the cellular tolerance of DSB-inducers has been shown. Specifically, it has been demonstrated that bone marrow stromal cells derived from pol θ knockout mice are sensitive to γ -irradiation and bleomycin (171). Higgins *et al.* (2010) also showed that several tumor cell lines depleted of pol θ exhibit sensitivity to ionizing radiation and contain an elevated number of γ -H2AX foci. Intriguingly, minimal effect of ionizing radiation was seen with normal fibroblast cell lines, suggesting that effective radiotherapy could be achieved by modulating pol θ expression (172).

An essential role of pol θ in the maintenance of genomic stability is highlighted by studies showing that dysregulation of pol θ expression leads to genomic instability. In human MRC5-SV cells that stably overexpress pol θ , the elongation of the replication fork is slower, and a 2- to 3-fold increase in the formation of γ -H2AX foci is observed.

These cells also display altered cell cycle progression; specifically, these cells accumulate in the S and G₂/M phases. Additionally, pol θ-overexpressing cells exhibit a higher number of phosphorylated CHK2 foci, suggesting that overexpression of pol θ results in the activation of the γ-H2AX-ATM-CHK2 DNA damage checkpoint. These cells also possess elevated chromosomal abnormalities, particularly end-to-end fusions and chromatid breaks. Finally, these cells exhibit sensitivity to *N*-nitroso-*N*-methylurea and methyl methane sulfonate (165).

The correlation between dysregulated pol θ expression and the emergence and survival of proliferating cancer cells is suggested by frequent pol θ dysregulation in tumors. In particular, pol θ transcript levels are 3- to 26-fold higher in breast carcinoma than in non-tumor breast tissue (165). Importantly, among several other TLS polymerases investigated, including pol η, pol ι, pol κ, pol ν, Rev1, and Rev3L, this increase was the highest. There is in fact a significant association between high expression of pol θ and poor survival of patients with breast cancers. Additionally, for patients who have tumors overexpressing pol θ, there is a 4.3-fold higher risk of death than those individuals with tumors expressing normal levels of pol θ. Furthermore, a significant association between pol θ expression and a number of prognostic indicators for breast cancer, such as estrogen receptor status, has been observed. For example, there is a frequent association between pol θ overexpression and triple-negative tumors (165). Pol θ is also overexpressed in other types of human cancers, including NSCLC, stomach and colon carcinomas. An association between high expression of pol θ and poor clinical prognosis has been found; patients expressing high levels of pol θ have a worse postoperative survival. In particular,

for lung and colon cancers, patients with high pol θ expression have significantly shorter survival based on a 5-year follow-up study, and Kaplan-Meier survival analyses show that patients with colon cancer expressing high levels of pol θ postoperatively survive for a significantly shorter period of time (173).

An important role of pol θ in maintaining genomic stability during cell cycle has been demonstrated in the chicken DT40 cell model. DT40 cells deficient in both the helicase and polymerase domains of the *pol* θ gene display a slower growth rate and a prolonged G₂ phase. Additionally, these cells have an elevated sub-G₁ fraction, as well as elevated levels of spontaneous chromosomal breaks and sister chromatid exchanges. Consistent with *in vitro* studies, pol θ -deficient cells are hypersensitive to hydrogen peroxide, further supporting a role in BER (170). A role for pol θ in generating immunoglobulin V gene diversity during an immune response has also been suggested (164).

1.3.3.2.3. Phenotype of *pol* θ knockout mice

Pol θ knockout mice are viable and fertile. However, their viability is severely compromised in an *Atm*-deficient background. Interestingly, these mice exhibit a delayed onset of thymic lymphomas. Additionally, pol θ knockout mice display an elevated frequency of micronuclei in their reticulocytes, a feature that occurs both spontaneously and as result of exposure to γ -irradiation (171,174). Furthermore, mice expressing a mutant form of pol θ , which is defective in its polymerase activity, exhibit a decrease in mutations, particularly at intrinsic C/G somatic hypermutation hotspots. In contrast to these mice, pol θ null mice exhibit a decrease in both C/G and A/T mutations in the

intronic sequence of the J_H4 region in germinal center B cells, while G to C transversions are increased. These results indicate a potential role of pol θ in somatic hypermutation of immunoglobulin genes (78,175,176). However, a recent report has shown that pol θ deficiency minimally alters the mutation spectrum in mice within the immunoglobulin loci (177)

1.4. COOPERATIVE ACTIONS OF MULTIPLE TLS POLYMERASES IN LESION BYPASS

The bypass of some DNA lesions can involve the actions of multiple TLS polymerases. For example, TLS past CPDs has been shown to require several TLS polymerases. When gapped plasmids carrying a site-specific T-T CPD were replicated in XP-V cells depleted of Rev3L, a 74% decrease in TLS was observed relative to cells transfected with the control siRNA (68). When pol ι and pol κ were simultaneously knocked down, TLS decreased by 65%. These results suggest that the bypass of T-T CPDs can be mediated by the cooperative action of pol ζ with pol κ and/or pol ι . Additionally, mutagenic TLS decreased by 84% when Rev3L was depleted in XP-V cells, and when both pol κ and pol ι were depleted, mutagenic TLS decreased by 76%. Similar results were obtained for accurate TLS, suggesting that these polymerases carry out both mutagenic and error-free TLS across T-T CPDs in the absence of pol η . Furthermore, the depletion of pol κ enhanced the sensitivity of XP-V cells to UV by 3.5-5-fold, suggesting that pol κ can protect XP-V cells against the cytotoxic effect of UV. In XPA cells, when either pol η or pol κ was knocked down, an up to 2-fold decrease in UV sensitivity was observed, and simultaneous depletion of both pol κ and pol η resulted in a 5 to 6-fold increase in UV

sensitivity; these data suggest that both pol η and pol ι can protect repair-defective XPA cells from the cytotoxic effect of UV (68). Similar complex cooperativity has been observed between different polymerases to bypass CPDs and (6-4) photoproducts using SV40-based vector systems (178,179). Moreover, the type I Burkitt's lymphoma BL2 cell lines deficient in pol η and pol ι are more sensitive to UV-induced killing than cells deficient in pol η alone (66). Furthermore, there is a significant decrease in the overall UV-induced mutagenesis in the absence of both pol η and pol ι compared to fibroblasts deficient in pol η alone, suggesting a role for pol ι in an error-prone TLS past UV-induced lesions in the absence of pol η . Since strand bias was abolished with the loss of both pol η and pol ι , it is reasonable to speculate that both polymerases play roles in generating strand bias (67). Fibroblasts from mice deficient in pol η and pol ι were also very sensitive to UV irradiation (77).

Double close mutations were significantly elevated in type I Burkitt's lymphoma cells deficient in pol η , pol ι , and pol η and pol ι . Other types of mutations were also observed; in the pol η and pol η /pol ι -deficient cells, an increase in misincorporation opposite the 3' T of a TT was observed, while a significant decrease in the mutations at the 5' TT was observed, suggesting that these polymerases may have a role in mutagenic bypass of 5' T-T dimers (66). Pol η -deficient cells, with a decreased level of pol ι , have a lower overall frequency of UV-induced mutations, indicating that pol ι introduces mutations in the absence of pol η in response to UV (180).

The bypass of cisplatin-induced dG-dG intrastrand cross-links also involves multiple TLS polymerases. When gapped plasmids containing this lesion were replicated in U2OS cells depleted of both pol η and Rev3L, a dramatic 80% reduction in TLS was observed, and depletion of both pol κ and pol η resulted in a 78% decrease in TLS. In addition, several TLS polymerases may function to cooperatively bypass (+)-*trans*-BPDE- N^2 -dG, as the depletion of both pol κ and Rev3L reduced mutagenic TLS by 3.9-fold (99).

1.5. TLS POLYMERASE INHIBITORS FOR CANCER PREVENTION AND THERAPY

Cancer cells generally have high levels of genomic instability characterized by point mutations, deletions, rearrangements, and abnormal ploidy relative to normal adjacent tissues. These differences in genomic stability cannot be adequately explained by the random accumulation of DNA damage, but rather by the indication that cancer cells have a strong mutator phenotype arising from deficiencies in DNA repair and tolerance mechanisms, cell cycle check points, and/or the dysregulation of error-prone DNA polymerases (181-184). It is estimated that during the ~100 cell divisions which take place during the life-time of stem cell replication, as few as one or two mutant genes would be produced (185). In humans, mutation rates have been calculated to be 5×10^{-11} mutations per base pair per replication (186).

In contrast, the frequency of randomly generated mutations in cancer cells averages 210×10^{-8} per base pair, which is greater than 200-fold higher when compared to the matching normal tissues (187). These studies illustrate the profound genetic instability of cancer

cells. This instability is also evident by a recent study showing that the genomes of cancer cells accumulate over 20,000 mutations (188-190). Since TLS polymerases can introduce massive numbers of mutations at the single nucleotide level and their expression is frequently dysregulated in tumors, TLS polymerases may play a causal or contributing role in genome-wide instability and carcinogenesis. Thus, inhibition of TLS polymerases may lead to a reduction in mutations and thus prevent the emergence of tumors.

Despite the continuous research efforts to combat cancers, chemotherapy resistance is still a major obstacle to successful cancer treatment. Multiple mechanisms have been implicated in drug-induced, acquired resistance, including decreased intracellular accumulation of the drug due to decreased uptake, increased efflux, or alteration in membrane lipids. These cellular adaptations can prevent apoptosis, increase the repair of DNA damage due to the upregulation of genes involved in repair, and alter cell cycle and checkpoint controls. Additional factors that may adversely affect chemotherapeutic efficacy are increased drug metabolism or compartmentalization, limiting access of the drug to sites of action (191).

As mentioned above, the ability of tumor cells to acquire resistance to chemotherapeutic agents has been proposed to be caused by both enhanced replication bypass and the low fidelity of the TLS polymerases (71,132,133,135,143,149,192). TLS polymerases can catalyze both error-free and error-prone TLS past a number of lesions. The error-free replication bypass can enhance the capacity of preexisting tumors to tolerate the drug-induced lesions. Error-prone bypass may not only promote tumorigenesis, but may also

provide an additional mutation load that results in secondary tumor initiation or the development of drug resistance. Thus, the identification of specific inhibitors of TLS polymerases may be useful as novel anticancer agents, since TLS polymerases do not only introduce mutations, but can decrease the efficacy of treatments involving DNA-damaging agents (Figure 2).

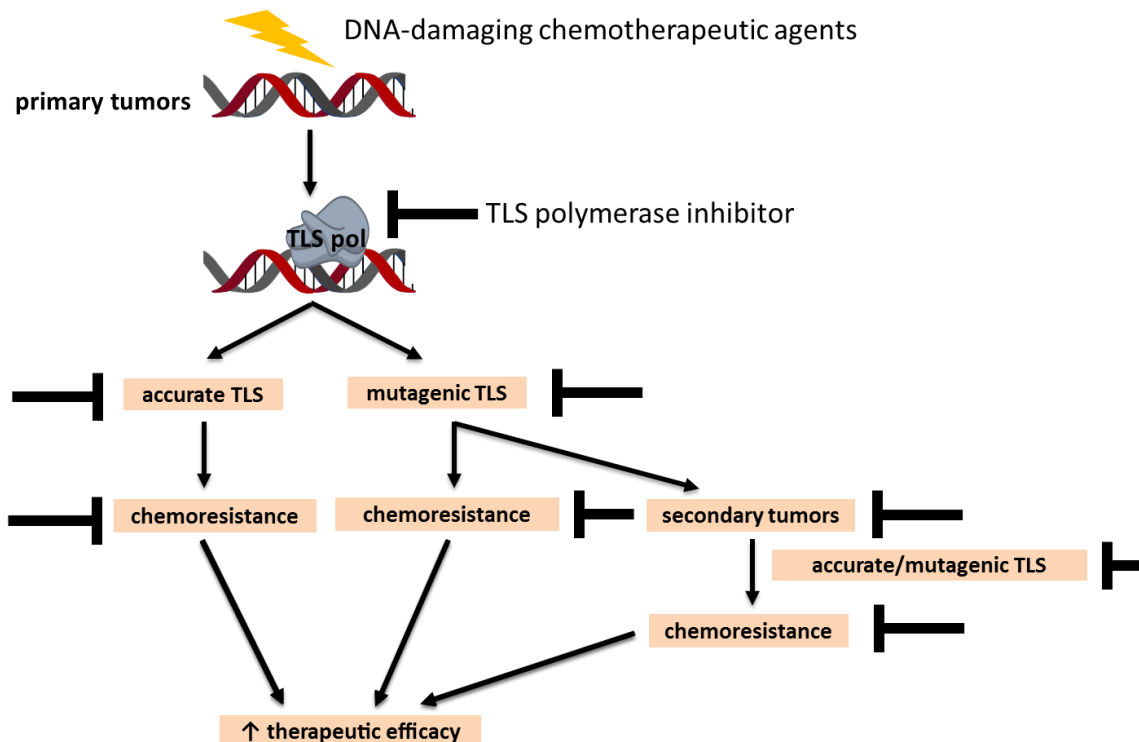


Figure 2. Model of new combination chemotherapy. Treatment of primary tumors with chemotherapeutic agents in combination with a TLS polymerase inhibitor is proposed to prevent chemoresistance, leading to an increase in therapeutic efficacy of chemotherapeutic agents.

Although the search for compounds targeting TLS polymerases has received modest attention, a number of inhibitors are emerging. For example, 3-*O*-methylfunicone (Figure 3A) is the most selective Y-family polymerase inhibitor identified to date. It is a natural product isolated and purified from marine fungal strains found in Australian sea salt. 3-*O*-methylfunicone is most potent against pol κ , with an IC₅₀ value of 12.5 μ M, in contrast to

34.3 μM and 50.1 μM against pol ι and η , respectively (Table 1). This compound is hypothesized to interact with the DNA template-primer-binding site of pol κ , rather than the dNTP substrate-binding site, since the mode of inhibition was shown to be competitive with the DNA template-primer and non-competitive with the dNTP substrate. In cell culture experiments, 3-*O*-methylfunicone was found to suppress the growth of two cancer cell lines, HCT116 and HeLa cells, with an LD_{50} value of 63.8 μM and 63.3 μM , respectively. Interestingly, 3-*O*-methylfunicone does not have an effect on cell proliferation and growth of normal human cells, such as HUVEC and HDF cells. These data suggest that this compound can be a selective anti-cancer agent with minimal toxicity to non-tumorous tissues. Additionally, 3-*O*-methylfunicone significantly enhanced HeLa cell UV-sensitivity, where the clonogenic survival was decreased by 4.3-fold upon treatment with the compound and UV irradiation. These data suggest that 3-*O*-methylfunicone inhibits the activities of Y family polymerases that cope with this specific genotoxic challenge. Whether the effects observed are due to inhibition of pol κ or another Y-family polymerase, for example pol η , needs to be determined (193).

Mizushina *et al.* reported the discovery of a compound (1S*,4aS*,8aS*)-17-(1,4,4a,5,6,7,8,8a-octahydro-2,5,5,8a-tetramethylnaphthalen-1-yl)heptadecanoic acid, a derivative of a natural product kohamaic acid A (Figure 3B), as a inhibitor of several mammalian polymerases, including pol η , pol ι , and pol κ , with IC_{50} values in the range of 7-8 μM (Table 1). Cellular studies show that this compound can inhibit the growth of HL-60 cancer cells, demonstrating its potential as a chemotherapeutic agent (194). Other natural compounds, such as penicilliols A (Figure 3C) and B (Figure 3D), isolated from a

fungus strain derived from a sea moss, also selectively inhibit Y-family polymerases, namely pol η , ι , and κ . These inhibitors are most potent against mouse pol ι , with an IC_{50} of 19.8 μ M and 32.5 μ M for penicilliol A and B, respectively (Table 1). The mode of inhibition of pol ι by these compounds is non-competitive for both the DNA template-primer and the dNTP substrate (195).

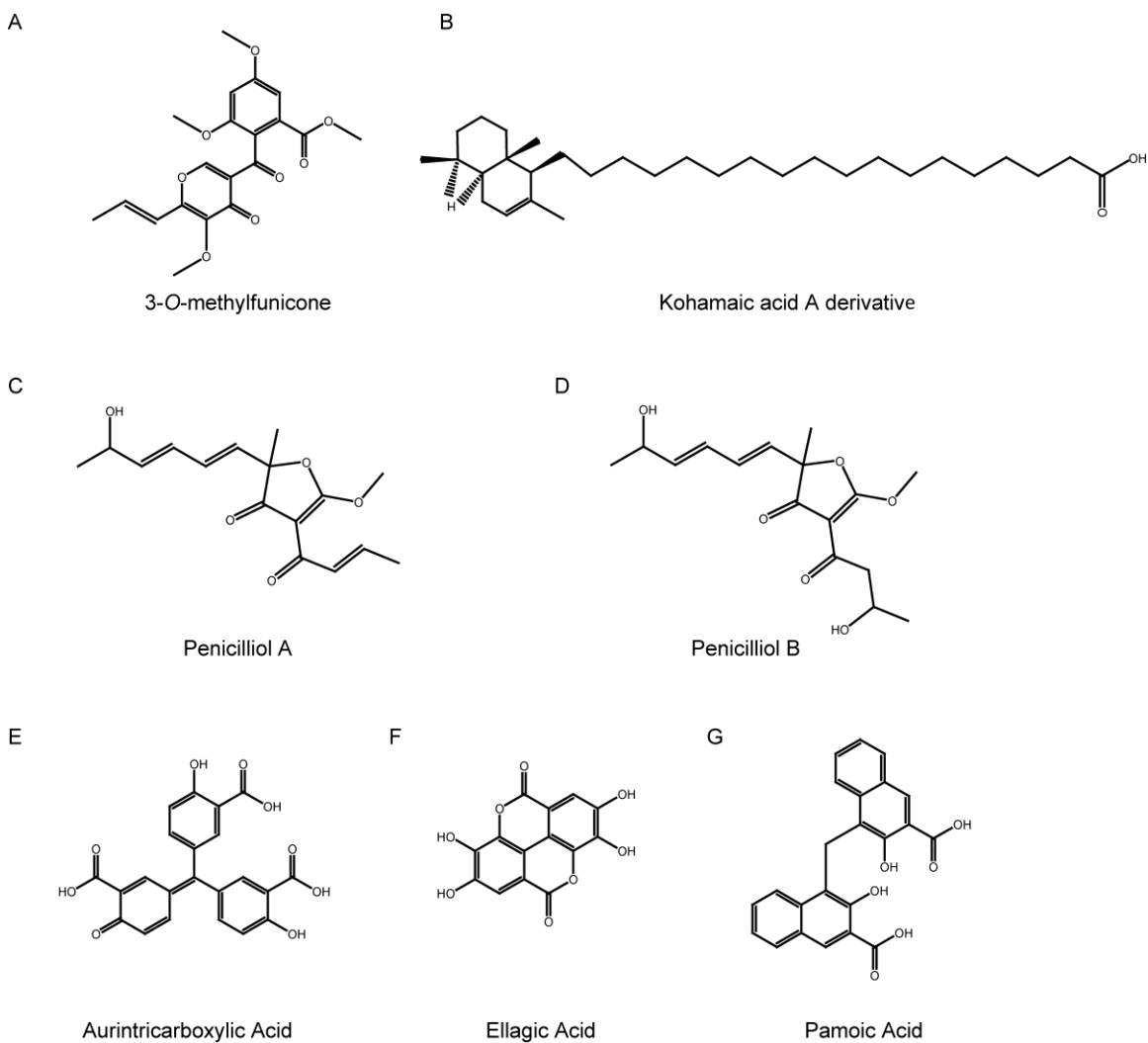


Figure 3. Structures of small molecule inhibitors of various TLS polymerases.

(A) 3-*O*-methylfunicone (193). (B) Kohamaic acid A derivative ((1*S**,4*aS**,8*aS**)-17-(1,4,4*a*,5,6,7,8,8*a* octahydro-2,5,5,8*a*-tetramethylnaphthalen-1-yl)heptadecanoic acid) (194). (C) Penicilliol A (195). (D) Penicilliol B (195). (E) Aurintricarboxylic acid (196). (F) Ellagic acid (196). (G) Pamoic acid (196).

inhibitor names	IC ₅₀ or K _d (μM)		
	pol η	pol ι	pol κ
3-O-methylfunicone	50.1	34.3	12.5
kohamaic acid A derivative	7.45	7.84	7.20
penicilliol A	ND	19.8	ND
penicilliol B	ND	32.5	ND
aurintricarboxylic acid	0.075	0.099	ND
ellagic acid	0.062	0.081	ND
pamoic acid	79	4.9	ND
aptamer 25	ND	ND	0.5
aptamer 32	ND	ND	0.41
aptamer 45	ND	ND	0.75

Table 1. Summary of inhibitors of TLS polymerases¹

¹ND: not determined; Kohamaic acid A derivative: (1S*,4aS*,8aS*)-17-(1,4,4a,5,6,7,8,8a-octahydro 2,5,5,8a-tetramethylnaphthalen-1-yl)heptadecanoic acid. For aptamers, values of dissociation constant (K_d) are shown instead of IC₅₀. The sequences of the aptamers are given in (197).

In contrast to the targeted methods used to identify natural product inhibitors as described above, a high-throughput screening procedure has been developed for the identification of small molecule inhibitors of TLS polymerases from large library sets (196). This assay utilizes polymerase-catalyzed strand displacement synthesis of a fluorescently-labeled oligodeoxynucleotide, in which the rhodamine fluorophore (TAMRA) is fully quenched in a duplex substrate by the quencher (BHQ-2). In the absence of an effective polymerase inhibitor, replication displaces the TAMRA-labeled reporter, resulting in a large increase in fluorescence; reactions containing inhibitors will retain the background fluorescence. With this methodology, inhibitors of pol η and pol ι have been identified using a 1,536-well plate screening format (196). Aurintricarboxylic acid (Figure 3E) and ellagic acid (Figure 3F) inhibit these enzymes with the nanomolar potency; the former compound has an IC₅₀ of 99 nM and 75 nM against pol ι and pol η, respectively, while the latter compound has an IC₅₀ of 81 nM and 62 nM against pol ι and pol η, respectively. Pamoic acid (Figure 3G) also inhibits these polymerases, though with lower potency (IC₅₀ of 4.9 μM and 79 μM against pol ι and pol η, respectively) (Table 1). Although

aurintricarboxylic acid and ellagic acid have improved potency relative to the previously identified compounds, they have other targets such as apurinic/apyrimidinic endonuclease, APE1 for aurintricarboxylic acid and casein kinase 2 for ellagic acid, and thus do not serve as selective Y-family polymerase inhibitors (198-204). Therefore, future studies require the development of potent compounds that selectively inhibit specific TLS polymerases.

In addition to small molecules, RNA aptamers could potentially be used to target TLS polymerases. RNA aptamers are RNA oligomers that have tight and specific binding to their targets. RNA aptamers that bind and inhibit pol κ have been described. These aptamers were originally discovered by screening a RNA library consisting of $\sim 8 \times 10^{12}$ molecules in an effort to identify aptamers that bind to and inhibit pol β . These aptamers have low selectivity as they bind to pol κ with similar affinities as to pol β ; the dissociation constant of aptamer 25 is 430 nM and 500 nM for pol β and pol κ , respectively; aptamer 32 is 290 nM and 410 nM for pol β and pol κ , respectively; and aptamer 45 is 490 nM and 750 nM for pol β and pol κ , respectively (Table 1) (197).

Germane to these studies and as extensively discussed above, RNAi (siRNA or shRNA) against specific TLS polymerase used to deplete specific enzymes can modulate the cellular activities of these polymerases. The naked RNAi cannot cross the cellular membrane and enter the intracellular environment. However, recently, a novel RNAi delivery technology has been developed that couples RNAi to molecules such as pegylated immunoliposome, polyethylenimine, or myristoylated polyarginine peptides to

enhance cellular uptake. With this technology, RNAi has been successfully delivered to tumors (205-208). Therefore, RNAi could be potentially used for the treatment of cancers. Additionally, gene-specific ribozymes could be employed for prevention of cancers, such as carcinogen-induced lung cancer, as demonstrated by Dumstorf and colleagues (134).

In summary, TLS polymerases function to bypass drug-induced DNA lesions and can introduce mutations in the genomes during this process. Thus, inhibitors of TLS polymerases can sensitize tumor cells to DNA-damaging agents and reduce the level of drug-induced mutagenesis. In this regard, a combination therapy with a relevant DNA-damaging agent and TLS polymerase inhibitor could improve the therapeutic efficacy of chemotherapeutic agents by rendering tumor cells more susceptible to the cytotoxic effect of the drug and reducing the establishment of drug-resistant mutant cells. A strategy for such adjuvant chemotherapy would require that the agents have minimal cytotoxicity on their own, but enhanced cytotoxicity when combined. Furthermore, selective inhibitors that are toxic only to tumor cells would limit undesirable side effects. With an ongoing effort to develop highly potent and selective TLS polymerase inhibitors, the utilization of TLS polymerase inhibitors could be a novel therapy to combat cancers in the future.

CHAPTER 2: NOVEL ENZYMATIC FUNCTION OF DNA POLYMERASE ν IN TRANSLESION DNA SYNTHESIS PAST MAJOR GROOVE DNA–PEPTIDE AND DNA–DNA CROSS-LINKS

Kinrin Yamanaka^{1,2}, Irina G. Minko¹, Kei-ichi Takata⁴, Alexandar Kolbanovskiy⁵, Ivan D. Kozekov⁵, Richard D. Wood⁴, Carmelo J. Rizzo⁵, and R. Stephen Lloyd^{1,3} (2010)
Novel Enzymatic Function of DNA Polymerase ν in Translesion DNA Synthesis Past Major Groove DNA–Peptide and DNA–DNA Cross-Links, *Chem. Res. Toxicol.* 23, 689-695.

¹Center for Research on Occupational and Environmental Toxicology, ²Department of Physiology and Pharmacology, and ³Department of Molecular and Medical Genetics, Oregon Health & Science University, Portland, OR 97239

⁴Department of Carcinogenesis, The University of Texas Graduate School of Biomedical Sciences at Houston, The University of Texas M. D. Anderson Cancer Center, Science Park-Research Division, Smithville, TX 78957

⁵Department of Chemistry, Center in Molecular Toxicology, VU Station B, 351822, Vanderbilt University, Nashville, TN 37235

2.1. PREFACE

This work is published in *Chemical Research in Toxicology*.

My contributions to this work included the conception of this project, design and performance of experiments, data analyses, and writing of the manuscript.

Irina G. Minko contributed to the conception of this project, design and performance of experiments for Figure 7B, data analyses, and the editing and critical reading of the manuscript.

Kei-ichi Takata and Richard D. Wood provided pol v and contributed to the critical reading of the manuscript.

Alexander Kolbanovskiy, Ivan D. Kozekov, and Carmelo J. Rizzo provided oligodeoxynucleotides adducted with γ -HOPdA, N^6 -dA- N^6 -dA ICL, or γ -HOPdG and contributed to the critical reading of the manuscript.

R. Stephen Lloyd contributed to the conception of this project, experimental design, the editing and critical reading of the manuscript, and provided funding and lab space for the execution of this work.

Adapted and modified with permission from

Kinrin Yamanaka, Irina G. Minko, Kei-ichi Takata, Alexandar Kolbanovskiy, Ivan D. Kozekov, Richard D. Wood, Carmelo J. Rizzo, and R. Stephen Lloyd (2010) Novel Enzymatic Function of DNA Polymerase ν in Translesion DNA Synthesis Past Major Groove DNA–Peptide and DNA–DNA Cross-Links, *Chem. Res. Toxicol.* 23, 689-695. Copyright (2010) American Chemical Society.

2.2. INTRODUCTION

TLS is a significant DNA damage tolerance mechanism to overcome replication blocks caused by DNA lesions or to seal gaps opposite lesions (3,4). In the past decade, numerous DNA polymerases have been discovered that possess lesion bypass activity. Recently, a new human DNA polymerase has been identified, POLN or pol ν , and falls in the A-family of DNA polymerases (160). This family includes *E. coli* pol I and human pol θ . Pol ν is a moderately processive enzyme and is able to carry out strand displacement DNA synthesis with much higher efficiency than the Klenow fragment, the polymerase-proficient portion of *E. coli* pol I. It also replicates ND DNA with low fidelity; specifically, it frequently misincorporates dT opposite template dG with about half the efficiency of incorporation of the correct nucleotide dC opposite template dG (158,159). Because low fidelity of DNA synthesis is common for TLS polymerases and pol ν lacks 3'-5' exonuclease proofreading activity, a role of pol ν in the bypass of specific DNA lesions has been proposed (158,159). Indeed, this polymerase can carry out TLS *in vitro*, being specifically proficient in accurate bypass of thymine glycols, the major groove DNA lesions (158). However, it is completely blocked by a number of other DNA modifications, including a cisplatin-induced dG-dG intrastrand cross-link, an AP site, a CPD, and a (6-4) photoproduct (158).

A function of pol ν in DNA cross-link repair in mammalian cells has been proposed (163). In particular, the data suggested that pol ν is involved in HR in response to various DNA cross-linking agents and potentially interacts with multiple proteins in the Fanconi anemia pathway, which are relevant to DNA cross-link repair. However, a cellular role

for pol ν in HR-independent, TLS-dependent repair of DNA cross-links has not yet been addressed. Additionally, as already mentioned, thymine glycol is the only lesion that pol ν has been reported to be able to bypass *in vitro* (158). To understand the cellular function of pol ν in TLS, it is crucial to identify types of DNA lesions that this polymerase can bypass. Because it has been previously established that both the exo^+ and the exo^- Klenow fragment can catalyze TLS past certain major groove DNA adducts (209,210), we hypothesized that in addition to thymine glycols, pol ν may catalyze replication bypass of additional major groove DNA lesions. This study was designed to test this hypothesis to facilitate insight into the cellular function of pol ν in TLS.

2.3. MATERIALS AND METHODS

Materials

$[\gamma\text{-}^{32}\text{P}]\text{ATP}$ was obtained from PerkinElmer Life Sciences (Waltham, MA). P-6 Bio-Spin columns were obtained from Bio-Rad (Hercules, CA). Uracil DNA glycosylase, T4 DNA ligase, and T4 polynucleotide kinase were purchased from New England BioLabs (Beverly, MA). Sodium cyanoborohydride (NaCNBH_3) was obtained from Sigma (St. Louis, MO). Slide-A-Lyzer dialysis cassettes with a molecular weight cutoff of 10,000 were purchased from Thermo Scientific (Rockford, IL). Human pol ν was purified as described (158). Yeast pol δ and PCNA were purified as previously described (211) and were generous gifts from Dr. Peter M. J. Burgers (Washington University, St. Louis, MO). Human pol η and yeast pol ζ were purchased from Enzymax, LLC (Lexington, KY). The Lys-Trp-Lys-Lys and Lys-Phe-His-Glu-Lys-His-His-Ser-His-Arg-Gly-Tyr peptides were obtained from Sigma-Genosys (St. Louis, MO).

Oligodeoxynucleotide synthesis

(a) All ND oligodeoxynucleotides were synthesized by the Molecular Microbiology and Immunology Research Core Facility at Oregon Health & Science University (Portland, OR). (b) Oligodeoxynucleotides containing γ -hydroxypropano-deoxyadenosine (γ -HOPdA) or γ -HOPdG were synthesized as previously described (212). DNAs containing DNA-peptide cross-links (Figure 4A and 4C) were prepared by the reaction of the γ -HOPdA- or γ -HOPdG-containing oligodeoxynucleotides with either 20 nmol of Lys-Trp-Lys-Lys or 4 nmol of Lys-Phe-His-Glu-Lys-His-His-Ser-His-Arg-Gly-Tyr in the presence of 50 mM NaCNBH₃ according to the previously published procedure (213). The sequences of oligodeoxynucleotides containing a N^6 -dA peptide cross-link and a N^2 -dG peptide cross-link are shown in Table 2, column 2, rows 1 and 2, respectively.

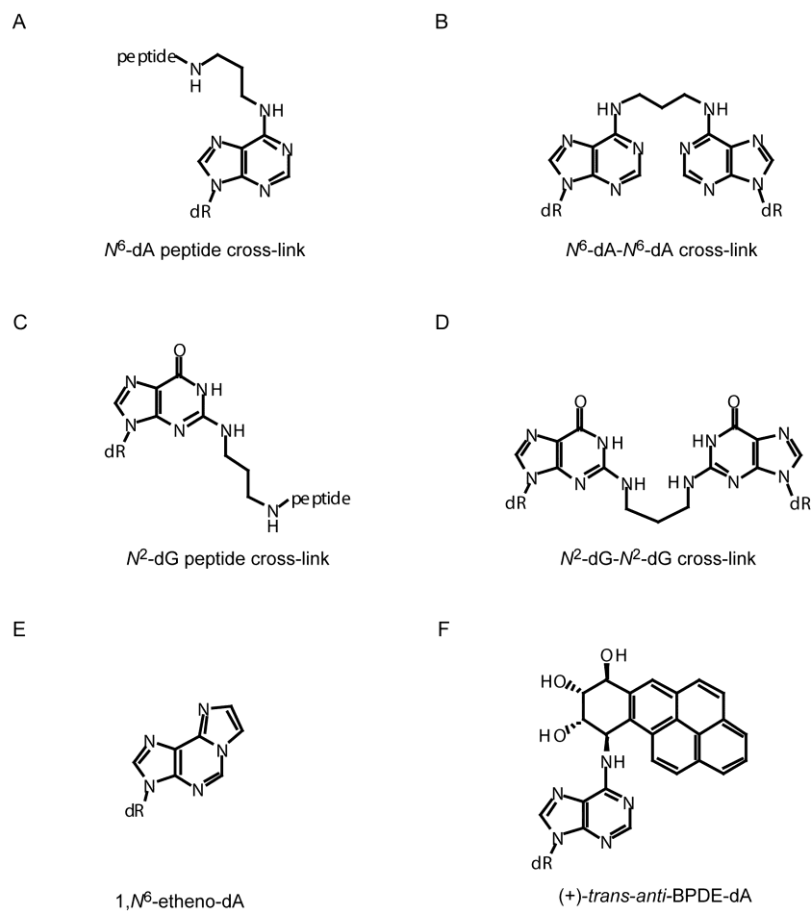


Figure 4. Structures of DNA adducts. The DNA-peptide cross-links consist of either a tetra (Lys-Trp-Lys-Lys) or dodecyl (Lys-Phe-His-Glu-Lys-His-His-Ser-His-Arg-Gly-Tyr) peptide attached via an acrolein moiety at the N^6 position of dA (A) or N^2 position of dG (C). The resulting DNA-peptide cross-links are referred to as N^6 -dA PCL4, N^6 -dA PCL12, N^2 -dG PCL4, and N^2 -dG PCL12. (B) Structure of N^6 -dA- N^6 -dA ICL. (D) Structure of N^2 -dG- N^2 -dG ICL. (E) Structure of ϵ dA. (F) Structure of (+)-BPDE-dA.

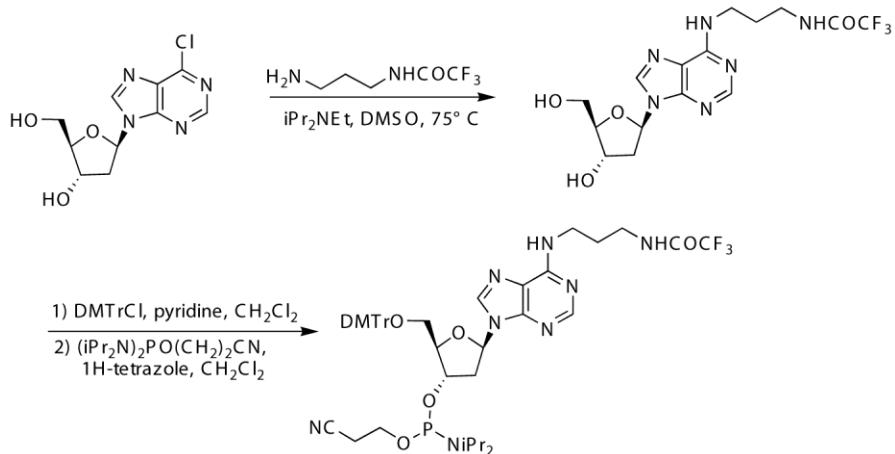
	Adducted Template	Template Sequence	Primer Sequence
1	N^6 -dA PCLs	5'-GCTAGTACTCGT <u>C</u> GACAATTCGGTATCCAT-3'	(-1) 5'-AAAATGGATACGGAATTG-3' (-3) 5'-AAAATGGATACGGAAT-3'
2	N^2 -dG PCLs	5'-GCTAGTACTCGT <u>C</u> GACAATTCGGTATCCAT-3'	(-4) 5'-AAAATGGATACGGAAT-3'
3	N^6 -dA ICL1	3'-gl-AUTATCGTA-5' 5'-AGCGATAGACAT <u>A</u> ATAGCATCGCTGGTACCGACTCG-3'	(-9) 5'-AAACGAGTCGGTACCAGC-3'
4	pre- N^6 -dA ICL2	3'-gl-AUTATCGTAGCGACCA-5' 5'-AGCGATAGACAT <u>A</u> ATAGCATCGCTGGTACCGACTCG-3'	N/A
5	N^6 -dA ICL2	3'-gl-A-5' 5'-AGCGATAGACAT <u>A</u> ATAGCATCGCTGGTACCGACTCG-3'	(-1) 5'-CGAGTCGGTACCAGCGATGCTAT-3' (-9) 5'-AAACGAGTCGGTACCAGC-3'
6	N^2 -dG ICL1	3'-(dd)CTGTGCTATCGTAG-5' 5'-AGCGATAGACAC <u>G</u> ATAGCATCGCTGGTACCGACTCG-3'	(-10) 5'-CGAGTCGGTACCAG-3'
7	N^2 -dG ICL2	3'-(dd)CTGTGC-5' 5'-AGCGATAGACAC <u>G</u> ATAGCATCGCTGGTACCGACTCG-3'	(-10) 5'-CGAGTCGGTACCAG-3'
8	N^2 -dG ICL3	3'-gl-GTATCGTAG-5' 5'-AGCGATAGACAC <u>G</u> ATAGCATCGCTGGTACCGACTCG-3'	(-10) 5'-CGAGTCGGTACCAG-3'
9	N^2 -dG ICL4	3'-gl-GC-5' 5'-AGCGATAGACAC <u>G</u> ATAGCATCGCTGGTACCGACTCG-3'	(-10) 5'-CGAGTCGGTACCAG-3'
10	edA	5'-GCTAGTACTCGT <u>C</u> GACAATTCGGTATCCAT-3'	(-3) 5'-AAAATGGATACGGAAT-3'
11	(+)-BPDE-dA	5'-CTCTC <u>A</u> CTTCCATTCCGTATCCATTTT-3'	(-1) 5'-ATGGATACGGAATGGAAG-3' (-6) 5'-AAAATGGATACGGAAT-3'

Table 2. Sequences of DNA primers and lesion-containing templates¹

¹Modified bases are underlined. A 3'-glycerol unit (gl) or a dideoxycytidine (dd) were incorporated to prevent DNA synthesis off of the shorter strand of the ICL-containing oligodeoxynucleotides. The number in the parentheses in front of the primer sequence indicates the position of the primer 3'-OH.

(c) The synthesis of the oligodeoxynucleotides containing ICL between N^6 -dAs of complementary strands (Figure 4B) is described under *Synthesis and characterization of oligodeoxynucleotides containing a N^6 -dA- N^6 -dA ICL*. The sequences of a N^6 -dA ICL1 and a N^6 -dA ICL2 are shown in Table 2, column 2, rows 3 and 5, respectively. The N^6 -dA ICL2 oligodeoxynucleotide was generated from a precursor oligodeoxynucleotide (pre- N^6 -dA ICL2, Table 2, column 2, row 4) as described previously (92).

Scheme 1



Synthesis and characterization of oligodeoxynucleotides containing a N^6 -dA- N^6 -dA ICL

Reagents for the synthesis and purification of oligodeoxynucleotides containing ICL between N^6 -dAs of complementary strands (Figure 4B) were purchased from Aldrich Chemical Co. unless otherwise noted, and used without further purification. The synthesis of an N^6 -(3-aminopropyl)-dA phosphoramidite reagent is shown in Scheme 1 and described below. NMR spectra were recorded using solutions in CD_2Cl_2 or $\text{DMSO-}d_6$. ^1H NMR spectra were recorded on Bruker spectrometers at 300 and 400 MHz, and ^{31}P NMR was recorded at 300 MHz.

N^6 -(3-Trifluoromethylcarbonylamino)propyl)-2'-deoxyadenosine

9-(2-deoxy- β -D-erythro-pento-furanosyl)-6-chloropurine (100 mg, 0.37 mmol), N -(3-aminopropyl)-2,2,2-trifluoroacetamide (125.7 mg, 0.74 mmol) (214), diisopropylethylamine (500 μl), and 500 μl of dry DMSO were mixed in a glass tube. The tube was flushed with argon and sealed; the mixture was heated at 75°C for 24 hrs. The volatiles were removed (centrifugal evaporator), and the residue was purified by medium pressure chromatography with a Biotage SP1 apparatus (Biotage, Charlottesville, VA), eluting with 3 to 15% gradient of CH_3OH in CH_2Cl_2 on an Si-25M silica gel

column to afford *N*⁶-(3-trifluoromethylcarbonylaminopropyl)-2'-deoxyadenosine (105 mg, 70% yield): ¹H NMR (400 MHz, DMSO-*d*₆): δ 9.49 (s, 1H, NH-COCF₃), 8.34 (s, 1H, H-8), 8.20 (s, 1H, H-2), 7.87 (bs, 1H, NH), 6.35 (dd, 1H, H-1', *J* = 6.3 Hz, *J* = 7.7 Hz), 5.29 (d, 1H, 3'-OH, *J* = 3.9 Hz), 5.21 (dd, 1H, 5'-OH, *J* = 5.1 Hz, *J* = 6.6 Hz), 4.41 (m, 1H, H-3'), 3.88 (m, 1H, H-4'), 3.64-3.59 (m, 1H, H-5'), 3.55-3.49 (m, 3H, H-5'', N-CH₂), 3.25 (q, 2H, CH₂-NHCO, *J* = 6.6 Hz, *J* = 13.0 Hz), 2.75-2.69 (m, 1H, H-2'), 2.28-2.22 (m, 1H, H-2''); 1.81 (m, 2H, CH₂).

5'-*O*-(4,4'-Dimethoxytrityl)-*N*⁶-(3-trifluoromethylcarbonylaminopropyl)-2'-deoxyadenosine

*N*⁶-(3-trifluoromethylcarbonylaminopropyl)-2'-deoxyadenosine (105 mg, 0.26 mmol) was evaporated from anhydrous pyridine (3 × 3 ml) and then dissolved in anhydrous pyridine (5 ml). 4,4'-Dimethoxytrityl chloride (132 mg, 0.39 mmol) was added and the reaction was stirred for 5 hrs at room temperature under an argon atmosphere. The solvent was removed (rotary evaporator), and the residue was purified by medium pressure chromatography with a Biotage SP1 apparatus, eluting with a 2 to 10% gradient of CH₃OH in CH₂Cl₂ containing 1% (v/v) triethylamine on a Si-25M silica gel column to afford the desired 5'-*O*-dimethoxytritylated nucleoside (140 mg, 76% yield): ¹H NMR (400 MHz, DMSO-*d*₆): δ 9.43 (s, 1H, NH-COCF₃), 8.24 (s, 1H, H-8), 8.14 (s, 1H, H-2), 7.83 (bs, 1H, NH), 7.34-7.30 (m, 2H, aromatic), 7.24-7.17 (m, 7H, aromatic), 6.82-6.77 (m, 4H, aromatic), 6.36 (t, 1H, H-1', *J* = 6.4 Hz), 5.35 (d, 1H, 3'-OH, *J* = 4.6 Hz), 4.48 (m, 1H, H-3'), 3.98 (m, 1H, H-4'), 3.72 and 3.71 (s, 6H, CH₃), 3.50 (m, 2H, N-CH₂), 3.25 (q, 2H, CH₂-NHCO, *J* = 6.8 Hz, *J* = 13.2 Hz), 3.15 (m, 2H, H-5' and H-5''), 2.90-2.84 (m, 1H, H-2'), 2.35-2.28 (m, 1H, H-2''); 1.81 (m, 2H, CH₂).

3'-O-[(*N,N*-Diisopropylamino)-2-cyanoethoxyphosphinyl]-5'-O-(4,4'-dimethoxytrityl)-*N*⁶-(3-trifluoromethylcarbonylamino)propyl)-2'-deoxyadenosine

The dimethoxytrityl nucleoside from above (60 mg, 0.085 mmol) was evaporated from anhydrous pyridine (3 × 3 ml) and then dissolved in freshly distilled CH₂Cl₂ (3 ml). A solution of anhydrous 1H-tetrazole (283 μL of a 0.45 M solution in CH₃CN, 8.9 mg, 0.127 mmol) and 2-cyanoethyl-*N,N,N',N'*-tetraisopropylphosphoramidite (35 μl, 33.3 mg, 0.11 mmol) were added, and the reaction was stirred for 2 hrs at room temperature under an argon atmosphere. The solvent was removed (rotary evaporator), and the residue was purified by medium pressure chromatography with a Biotage SP1, eluting with a 2 to 8% gradient of CH₃OH in CH₂Cl₂ containing 1% (v/v) triethylamine on a Si-25M silica gel column to afford the desired phosphoramidite (51 mg, 66% yield): ¹H NMR (300 MHz, CD₂Cl₂): δ 9.28 (bs, 1H, NH-COCF₃), 8.20 (m, 1H, H-8), 7.97-7.94 (m, 2H, H-2 and NH), 7.41-7.37 (m, 1H, aromatic), 7.30-7.20 (m, 8H, aromatic), 6.81-6.75 (m, 4H, aromatic), 6.40 (t, 1H, H-1', *J* = 6.3 Hz), 4.78 (m, 1H, H-3'), 4.26 (m, 1H, H-4'), 4.17-4.11 (m, 4H, N-CH₂ and NCH), 3.77 and 3.76 (s, 6H, CH₃), 3.55-3.45 (m, 4H, CH₂-NHCO and POCH₂), 3.40-3.31 (m, 2H, H-5' and H-5''), 2.95-2.90 (m, 1H, H-2'), 2.64-2.60 (m, 2H, CH₂CN), 2.52-2.46 (m, 1H, H-2''); 1.84 (m, 2H, CH₂), 1.26-1.20 (m, 12H, CH(CH₃)₂). ³¹P NMR (CD₂Cl₂, 121 MHz): δ 148.6, 148.4.

Oligodeoxynucleotide synthesis

Modified oligodeoxynucleotides were synthesized on a Perseptive Biosystems Model 8909 DNA synthesizer using Glen Research reagents with the standard synthetic protocol on a 1-μmol scale. The 6-chloropurine modified oligodeoxynucleotide was prepared using a standard DNA synthesizer cycle with p-(tert-butylphenoxy)-acetyl-protected

phosphoramidites. The modified oligodeoxynucleotide was cleaved from the solid support, and the exocyclic amino groups were deprotected in a single step using 0.1 M aq NaOH. The 6-chloropurine modified 36-mer oligodeoxynucleotide (5'-AGCGATAGACATA^{6Cl}ATAGCATCGCTGGTACCGACTCG-3') was purified by polyacrylamide gel electrophoresis (PAGE) and judged to be 99.5% pure by capillary gel electrophoresis (CGE). From MALDI-TOF MS, the calculated value of [M-H]⁻ was 11092.3, while the actual value of [M-H]⁻ was 11080.6 (0.104% difference between calculated and actual value).

HPLC separations

The purification of oligodeoxynucleotides and the analysis of reaction mixtures were performed on a Beckman HPLC system (32 Karat software version 7.0, pump module 125) with a diode array UV detector (module 168) monitoring at 260 nm using Waters YMC ODS-AQ columns (250 mm x 4.6 mm i.d., 1.5 ml/min for analysis and 250 mm x 10 mm i.d., 5 ml/min for purification) with 0.1 M aqueous ammonium formate and CH₃CN as a solvent system. HPLC gradient was as follows: 1-10% acetonitrile over 15 min, 10-20% acetonitrile over 5 min, hold for 5 min, 100% acetonitrile over 3 min, hold for 2 min, and then to 1% acetonitrile over 3 min.

PAGE separations

Oligodeoxynucleotides were purified by PAGE on a model Biorad Sequi-gen GT system. Following separation, bands were excised and the oligodeoxynucleotides were eluted from crushed gel overnight in 0.05 M TEAA buffer, pH 7.0 followed by Millipore water desalted system.

CGE

Electrophoretic analyses were carried out using a Beckman P/ACE MDQ instrument system (using 32 Karat software, version 5.0) monitored at 260 nm on a 31.2 cm x 100 μ m eCAP capillary with samples applied at 10 kV and run at 9 kV. The capillary was packed with their 100-R gel (for ss-DNA) using the Tris-borate buffer system containing 7 M urea.

Mass spectrometry

MALDI-TOF mass spectra (negative ion) of modified oligodeoxynucleotides were obtained on a Voyager Elite DE instrument (Perseptive Biosystems) at the Vanderbilt Mass Spectrometry Facility using a 3-hydroxypicolinic acid matrix containing ammonium hydrogen citrate (7 mg/ml) to suppress multiple sodium and potassium adducts.

*N*⁶-(3-aminopropyl)-dA-containing oligodeoxynucleotides

Using the *N*⁶-(3-trifluoromethyl-carbonylamino-propyl)-2'-deoxyadenosine phosphoramidite the modified oligodeoxynucleotides were prepared on DNA synthesizer and were purified by HPLC. To block the 3'-end of the oligodeoxynucleotides, a 3'-glyceryl (gl) CPG support (Glenn Research, 20-2902-XX) was used. The modified oligodeoxynucleotides were cleaved from the solid support and the exocyclic amino groups were deprotected in a single step using 14.8 N aq NH₄OH. The oligodeoxynucleotides were judged to be 100% and 94.7% pure by CGE. From MALDI-TOF MS, the calculated value of [M-H]⁻ for 3'-gl-A^{(CH₂)₃NH₂}UTATCGTA-5', gl= 3'-glycerol, 2,3-dihydroxypropyl was 2909.06, while the actual value of [M-H]⁻ was 2910.0 (0.014% difference between calculated and actual value). The calculated value of

[M-H]⁻ for 3'-gl-A^{(CH₂)₃NH₂}UTATCGTAGCGACCA-5' was 5063.3, while the actual value of [M-H]⁻ was 5062.9 (0.008% difference between calculated and actual value).

Cross-linked oligodeoxynucleotides

The oligodeoxynucleotide containing the *N*⁶-3-aminopropyl-dA modification and its complementary oligodeoxynucleotides containing 6-chloropurine were mixed in a plastic test tube with 100 μl 0.05 M sodium borate buffer, pH 9.0. The reaction mixtures were stirred at 0-4°C and the reaction was followed by HPLC and CGE. After 3 month, the cross-linked oligodeoxynucleotides were purified by PAGE and desalted. The cross-linked product was also characterized by MALDI and their purity estimated to be 88.2% and 100% as judged by CGE. From MALDI-TOF MS, the calculated value of [M-H]⁻ for an oligodeoxynucleotide containing a *N*⁶-dA-*N*⁶-dA ICL with short 5' nucleotide flap (*N*⁶-dA ICL1) shown in Table 2, column 2, row 3 was 13989.2, while the actual value of [M-H]⁻ was 13982.7 (0.046% difference between calculated and actual value), and the obtained yield was 8%.

From MALDI-TOF MS, the calculated value of [M-H]⁻ for an oligodeoxynucleotide containing a *N*⁶-dA-*N*⁶-dA ICL with long 5' nucleotide flap (pre-*N*⁶-dA ICL2) shown in Table 2, column 2, row 4 was 16141.6, while the actual value of [M-H]⁻ was 16144.4 (0.017% difference between calculated and actual value), and the obtained yield was 30%.

(d) Oligodeoxynucleotides containing an ICL between *N*²-dGs (Figure 4D) were synthesized as previously described (92,215,216), and the sequences of the oligodeoxynucleotides containing each *N*²-dG-*N*²-dG ICL (*N*²-dG ICL1, *N*²-dG ICL2, *N*²-dG ICL3, and *N*²-dG ICL4) are shown in Table 2, column 2, rows 6-9. A detailed description of each type of *N*²-dG ICLs has been reported previously (92). (e) An

oligodeoxynucleotide containing ϵ dA (Figure 4E and Table 2, column 2, row 10) was synthesized by the Molecular Microbiology and Immunology Research Core Facility at Oregon Health & Science University (Portland, OR). (f) An oligodeoxynucleotide (5'-CTCTCACTTCC-3') containing (+)-BPDE-dA (Figure 4F) at the underlined nucleotide was synthesized as previously described (217) and was a generous gift from Dr. Nicholas E. Geacintov (New York University, NY). This oligodeoxynucleotide was ligated to 16-mer oligodeoxynucleotide (5'-ATTCCGTATCCATTTT-3') using 800 units of T4 DNA ligase at 12°C overnight in the presence of 23-mer scaffold oligodeoxynucleotide (5'-TGGATACGGAATGGAAGTGAGAG-3'). The ligation reaction was terminated by the addition of an equal volume of formamide dye solution [95% (v/v) formamide, 10 mM EDTA, 0.03% (w/v) xylene cyanol, and 0.03% (w/v) bromphenol blue], and the products were separated on a 10% acrylamide gel containing 8 M urea. DNA was eluted from the gel with 0.5 M ammonium acetate/10 mM magnesium acetate solution, dialyzed against 10 mM Tris-HCl, pH 7.4 buffer containing 1 mM EDTA in Slide-A-Lyzer dialysis cassette (MWCO of 10,000), and further purified through a P-6 Bio-Spin column. The resulting 27-mer was used for DNA replication assays (Table 2, column 2, row 11).

DNA replication assays

For replication assays, primers were designed for reactions under a running or standing start condition. In the former case, the primer 3'-OH was positioned several nucleotides upstream of the lesion site. In latter case, the primer 3'-OH was positioned immediately prior to the lesion site (-1 primer). The sequences of primers are listed in Table 2, column 3. DNA replication assays were carried out in the following buffers: For pol ν , the reaction mixture contained 25 mM Tris-HCl, pH 7.5, 8 mM MgCl₂, 10% glycerol, 100

$\mu\text{g/ml}$ bovine serum albumin (BSA), and 5 mM dithiothreitol (DTT). For reaction with pol ν with N^2 -dG- N^2 -dG ICLs, Mg-acetate was used instead of MgCl_2 . For pol δ , the reaction mixture contained 40 mM Hepes-KOH, pH 6.8, 10% glycerol, 200 $\mu\text{g/ml}$ BSA, 1 mM DTT, and 8 mM MgCl_2 . All reactions were carried out at 37°C. DNA substrate, polymerase, and dNTP(s) concentrations, as well as reaction times, are given in figure legends. Reaction products were resolved through 15% acrylamide gel containing 8 M urea and visualized using a PhosphorImager screen. The percentage of primer extended in extension reactions was determined by taking the ratio of extended primer beyond the adducted base to the total amount of primer (unextended primer + extended primer up to and opposite the lesion + extended primer beyond the lesion). The percentage of primer extended in single nucleotide incorporations was determined by taking the ratio of extended primer to the total amount of primer (unextended primer + extended primer). Quantifications were done using ImageQuant 5.2 software.

2.4. RESULTS

Replication bypass of N^6 -dA peptide cross-links by pol ν

To address the hypothesis that pol ν can catalyze replication bypass of additional major groove DNA lesions, we utilized N^6 -dA acrolein-mediated peptide cross-links as a model for the bulky major groove DNA adducts (213). Specifically, tetra- and dodecylpeptide cross-links (Figure 4A, N^6 -dA PCL4 and N^6 -dA PCL12, respectively) were used. The molecular masses of these peptide cross-link-modified bases were 763 Da for N^6 -dA PCL4 and 1738 Da for N^6 -dA PCL12 versus 135 Da for unmodified adenine. These lesions were positioned 15 nucleotides from the 5' end of the 30-mer template and

annealed with a 16-mer radiolabeled primer in which the 3'-OH was three nucleotides upstream of the lesion site. Data in Figure 5A revealed that pol ν could fully extend primers annealed to these adducted templates; under the conditions used, very minimal blockage to DNA synthesis was observed one nucleotide prior to the lesion. To assess the identity of the nucleotides incorporated opposite the lesion, single nucleotide incorporations were conducted. Because N^6 -dA PCL12 is bulkier than N^6 -dA PCL4, further assays used only substrate containing this lesion. Data showed that pol ν incorporated only the correct nucleotide, dT, opposite N^6 -dA PCL12 (Figure 5B), suggesting that it catalyzed error-free bypass of this adduct. It is of interest to note that two nucleotides were incorporated for both the ND and the N^6 -dA PCL12 substrates when only dTTP was present. It has been reported that pol ν catalyzes error-prone insertion of dT opposite dG (158,159). Because the templating nucleotide immediately downstream of the adducted base is a dG, this specific sequence context likely accounts for the observed incorporation of the second dT. To quantitatively evaluate the extent of the blockage posed by N^6 -dA PCL12 for the pol ν -catalyzed nucleotide insertion, dTTP titration assays (6.4 nM to 100 μ M dTTP at 5-fold incrementally increased concentrations, left to right) were performed (Figure 5C). These results demonstrated that pol ν could incorporate approximately an equal amount of dT opposite the adducted base at concentrations only 5-fold higher relative to ND dA; specifically, 20% of primers were extended at 800 nM dTTP using ND substrate and at 4 μ M dTTP using damaged substrate.

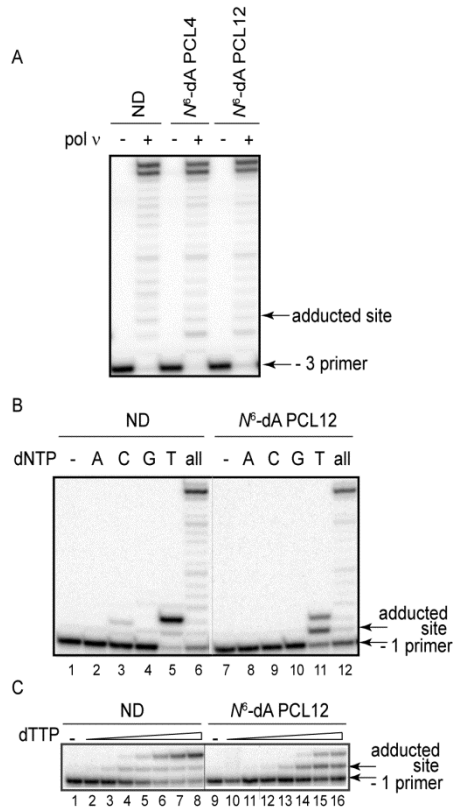


Figure 5. Replication bypass of *N*⁶-dA peptide cross-links by human pol v. (A) Primer extensions were catalyzed by 50 nM human pol v under running start conditions (-3 primer) in the presence of 5 nM primer template containing ND, *N*⁶-dA PCL4, or *N*⁶-dA PCL12 for 30 min at 37°C. (B) Single nucleotide incorporations and primer extensions were catalyzed by 5 nM human pol v under standing start conditions (-1 primer) in the presence of 2 nM primer template containing ND or *N*⁶-dA PCL12 for 15 min at 37°C. Reactions shown in lanes 1-6 and lanes 7-12 were conducted side-by-side, and products were separated on the same gel. The reactions shown in panels A and B were carried out in the presence of 100 μM individual or all dNTPs. (C) dTTP titration assays with 2 nM primer template were catalyzed by 5 nM human pol v under standing start conditions (-1 primer) for 10 min at 37°C using the same substrates as described in panel B. dTTP concentration ranges from 6.4 nM to 100 μM (5-fold incremental increase). Reactions shown in lanes 1-8 and lanes 9-16 were conducted side-by-side, and products were separated on the same gel.

Replication bypass of N⁶-dA-N⁶-dA DNA interstrand cross-links by pol v

Having demonstrated that pol v can readily bypass N⁶-dA peptide cross-links, we hypothesized that it may also be able to carry out TLS past other N⁶-dA major groove adducts, including N⁶-dA-N⁶-dA ICLs (Figure 4B). Although ICLs had been previously thought to pose an insurmountable block to replication, our laboratory has recently demonstrated that human DNA pol κ and *E. coli* DNA pol IV can catalyze replication bypass of an ICL between the N²-positions of dGs, which models the ICL formed by acrolein in a CpG sequence context (92,218). Related ICLs were constructed between the N⁶-positions of dA placing the cross-link in the major groove (Figure 4B and Table 2, rows 3 and 5). An N⁶-dA ICL1 was designed to model for a potential intermediate of ICL processing that could be generated by exo/endonucleolytic removal of DNA patch 3' to the ICL site. Even though N⁶-dA ICL1 contains an eight nucleotide duplex region 5' to the ICL site, it was anticipated that pol v would efficiently catalyze strand displacement DNA synthesis due to its intrinsic high strand displacement activity (158), a property that is useful for replicating this type of DNA lesion. A N⁶-dA ICL2 was constructed to model another potential intermediate of ICL processing; this could be generated by removal of DNA patches both 3' and 5' to the ICL site. When these major groove ICL-containing DNAs were used in primer extension reactions, pol v could extend primers and generate full-length products (Figure 6A and B). For both types of ICLs, the amount of primers extended beyond the adducted site was less as compared to ND substrate; specifically, a 10- and 4-fold decrease was observed for N⁶-dA-ICL1 and N⁶-dA-ICL2, respectively. As expected, pol v catalyzed strand displacement synthesis on the N⁶-dA ICL1 template (Figure 6A). When the identity of nucleotides incorporated opposite the cross-linked site

was examined by single nucleotide incorporations using the N^6 -dA ICL2 template, the data indicated that pol v preferentially incorporated the correct nucleotide, dT, opposite the N^6 -modified dA (Figure 6C).

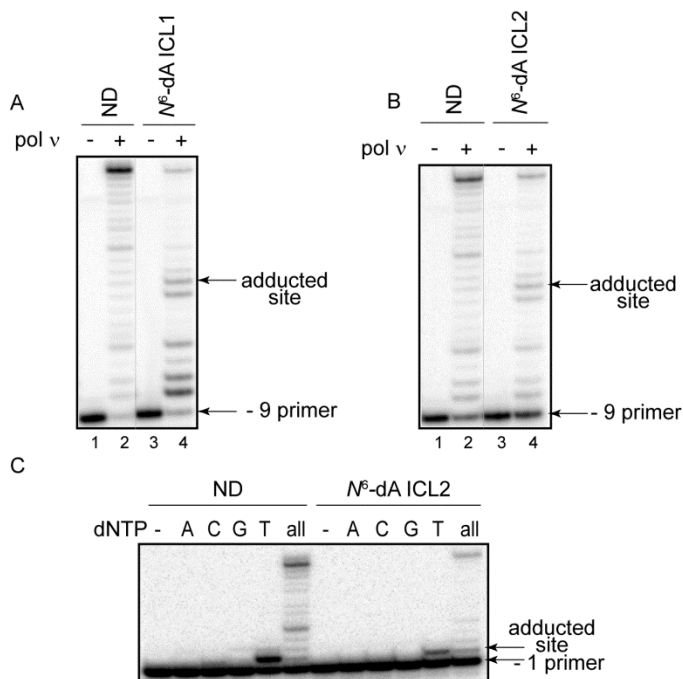


Figure 6. Replication bypass of N^6 -dA- N^6 -dA ICLs by human pol v. Primer extensions were catalyzed by 10 nM human pol v under running start conditions (-9 primer) using ND, N^6 -dA ICL1 (A), or N^6 -dA ICL2 (B). Reactions shown in lanes 1-2 and lanes 3-4 were conducted side-by-side, and products were separated on the same gel. (C) Single nucleotide incorporations and primer extensions were catalyzed by 5 nM human pol v under standing start conditions (-1 primer) using ND and N^6 -dA ICL2. All reactions were carried out in the presence of 5 nM primer template and 100 μ M individual or all dNTPs for 15 min at 37°C.

Pol v-catalyzed replication is blocked by N^2 -dG peptide and DNA interstrand cross-links

Given that pol v was able to bypass the extremely bulky major groove N^6 -dA peptide cross-links and ICLs, we tested whether it could replicate past chemically identical peptide cross-link and ICL lesions except situated in the minor groove through a linkage with the N^2 position of dG (Figure 4C and 4D). Primer extensions using these N^2 -dG linked peptide cross-links revealed that pol v was strongly blocked one nucleotide prior

to both peptide cross-links and was completely blocked at the site opposite the lesion, with no further primer extension observed (Figure 7A).

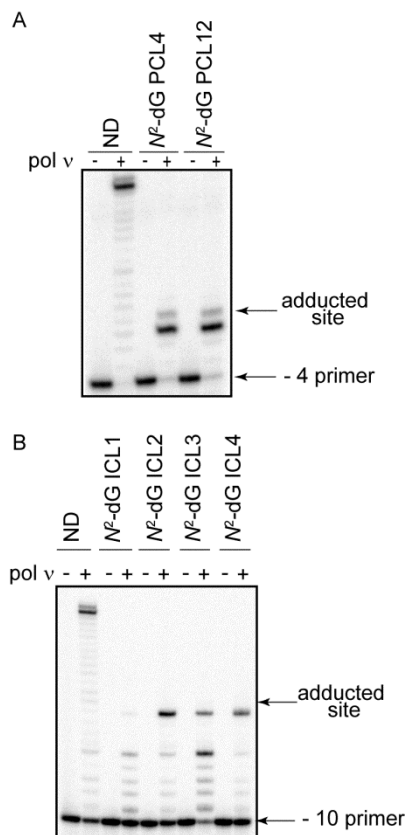


Figure 7. Replication bypass of N^2 -dG peptide and interstrand cross-links by human pol v. (A) Primer extensions were catalyzed by 10 nM human pol v under running start conditions (-4 primer) in the presence of 5 nM primer template containing ND, N^2 -dG PCL4, or N^2 -dG PCL12 for 30 min at 37°C. (B) Primer extensions were catalyzed by 25 nM human pol v under running start conditions (-10 primer) in the presence of 7.5 nM primer template containing ND, N^2 -dG ICL1, N^2 -dG ICL2, N^2 -dG ICL3, or N^2 -dG ICL4 for 10 min at 37°C. All reactions were carried out in the presence of 100 μ M dNTPs.

The identity of the nucleotide(s) incorporated opposite the peptide cross-links was not determined due to the limited nucleotide incorporation. Even though pol v could not replicate past the N^2 -dG peptide cross-links, suggesting an inability to replicate past minor groove DNA adducts, we tested whether pol v could catalyze TLS past N^2 -dG- N^2 -dG ICLs (Figure 4D and Table 2, rows 6-9). No incorporation opposite the lesion site

was observed for these ICL-containing DNAs (Figure 7B). Thus, similar to the observations made using peptide cross-link-containing DNAs, pol ν has much higher tolerance for the major groove N^6 -dA ICLs than the minor groove N^2 -dG ICLs.

Substrate limitations of pol ν -catalyzed bypass of major groove-linked DNA lesions

Since pol ν was able to accurately replicate past major groove N^6 -dA peptide cross-link and ICL lesions, we wanted to further explore the substrate range of pol ν and address the question concerning pol ν ability to bypass dA adducts in which both N1 and N^6 sites are blocked by modification. Thus, the ability of pol ν to bypass an ϵ dA (Figure 4E) was examined. ϵ dA is a promutagenic lesion that can be formed by exposure to industrial toxicants such as vinyl chloride and by the reaction of DNA with bis-electrophiles produced by lipid peroxidation (41). The running start primer extensions demonstrated that pol ν was severely blocked one nucleotide prior to the ϵ dA adduct, with only a very small amount of full-length product formed (Figure 8A). However, the nucleotide incorporation opposite the lesion appeared to be quite accurate. Under the conditions used, the primers were extended in the presence of dTTP but not other dNTPs (Figure 8B). On the basis of these data, we conclude that relatively nonbulky modifications at both N1 and N^6 of dA are sufficient to inhibit pol ν -catalyzed TLS.

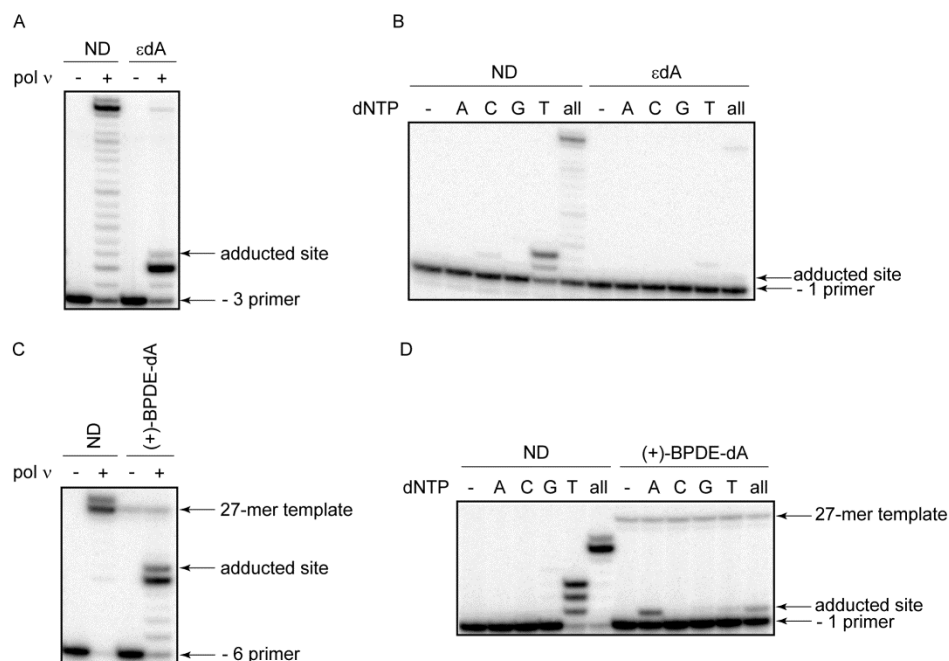


Figure 8. Replication bypass of ϵ dA and (+)-BPDE-dA by human pol v. (A) Primer extensions were catalyzed by 10 nM human pol v under running start conditions (-3 primer) in the presence of 5 nM primer template containing ND or ϵ dA. (B) Single nucleotide incorporations and primer extensions were catalyzed by 5 nM human pol v under standing start conditions (-1 primer) in the presence of 5 nM primer template using the same substrates as described in panel A. (C) Primer extensions were catalyzed by 10 nM human pol v under running start conditions (-6 primer) in the presence of 2 nM primer template containing ND or (+)-BPDE-dA. (D) Single nucleotide incorporations and primer extensions were catalyzed by 5 nM human pol v under standing start conditions (-1 primer) in the presence of 2 nM primer template using the same substrates as described in panel C. All reactions were carried out in the presence of 100 μ M individual or all dNTPs for 15 min at 37°C.

We also investigated the ability of pol v to carry out TLS past (+)-BPDE-dA (Figure 4F), one of the adducts formed by the active metabolite of the prevalent environmental pollutant, B[a]P (219). To construct an oligodeoxynucleotide of sufficient length for TLS analyses, an 11-mer oligodeoxynucleotide containing the (+)-BPDE-dA was 32 P-labeled, ligated to a 16-mer oligodeoxynucleotide, and gel-purified. Residual radioactive signals of the resulting 27-mer template are evident in all lanes [Figure 8C and 8D, (+)-BPDE-dA-27-mer template]. Primer extensions revealed that pol v could not fully extend the -6 primer and was severely blocked one nucleotide prior to the adducted site (Figure 8C). In

addition, pol ν displayed error-prone patterns of nucleotide incorporation opposite the lesion (Figure 8D); in the presence of dATP, 16% of primers were extended, while only 1% of primers were extended in the presence of the correct dTTP. A limited primer extension (<1%) was also observed in the presence of dGTP. Overall, pol ν -catalyzed TLS past (+)-BPDE-dA was inefficient, incomplete, and error-prone.

2.5. DISCUSSION

Although very significant progress has been made in both structural analyses of many of the TLS polymerases and the range of damaged DNA substrates that these polymerases can bypass, in the majority of cases, the biological role of these enzymes can only be inferred by changes in efficiency and mutagenic rates of TLS in their absence. Little data have been gathered concerning the role of these enzymes in developmental biology, their tissue-specific expression and steady-state distribution in adult organisms, the mechanism(s) for recruitment to sites of DNA damage, and the processes that regulate their expressions in response to environmental toxicant exposures and/or endogenous stresses. In the case of pol ν , the initial characterizations have demonstrated a very limited repertoire of lesions that pol ν can efficiently bypass (158). Although a cellular role of pol ν in TLS has not yet been established, its high frequency of misincorporation of dT opposite dG suggests that its expression would be tightly regulated. Thus, understanding the potential substrate specificity of pol ν may help to guide future investigations of its biological role in TLS and circumstances for induction or activation.

In this regard, we demonstrated that although pol ν could carry out TLS past bulky major groove DNA lesions such as N^6 -dA peptide cross-links and N^6 -dA- N^6 -dA ICLs, it failed to replicate DNAs containing chemically similar minor groove DNA lesions. Thus, the location of the lesion within DNA is one important structural determinant that influences the ability of pol ν to bypass the lesion.

We also discovered that pol ν could not efficiently bypass ϵ dA, and we speculate that this may be either due to pol ν requirement for the Watson-Crick edge for efficient dA templating or structural heterogeneity of the lesion within the active site. Regarding the former possibility, pol ν may fail to catalyze efficient TLS past ϵ dA because the Watson-Crick edge of this adduct is blocked by the modification. The majority of DNA polymerases utilize the geometry of the canonical Watson-Crick pairs for the nucleotide selection (220), but some TLS polymerases utilize alternative mechanisms. For example, pol τ induces a *syn* conformation on template purines, which results in a Hoogsteen base pairing with the correctly matched incoming nucleotide and enables bypass of lesions that disrupt the Watson-Crick edge, but not the Hoogsteen edge (221). The diminished capability of pol ν to bypass ϵ dA strongly suggests that the accessibility of the Watson-Crick edge of the template dA is important for the efficient replication by this polymerase; thus, it is likely that pol ν -catalyzed polymerization involves the recognition of the Watson-Crick geometry.

With regard to structural heterogeneity of ϵ dA adduct, NMR analyses have revealed that orientation of the base around the glycosidic bond is affected by identity of nucleotide

opposite the lesion (222,223). When paired with dT, the ϵ dA is in a normal *anti* conformation; however, the ϵ dA base prefers the *syn* conformation when placed opposite a mispaired dG. Additionally, the cocrystal structure of DNA containing an ϵ dA bound to pol ι also revealed that the lesion adopted a *syn* conformation (221). Thus, ϵ dA can adopt a *syn* or *anti* conformation depending on the base it is paired with, as well as interactions with the polymerase. There is a possibility that similar to pol ι , the adducted base is in a *syn* conformation in the pol ν active site. However, it is unclear whether either orientation of the ϵ -modified base can be efficiently utilized for nucleotide insertion.

Intriguingly, pol ν also could not fully bypass a (+)-BPDE-dA. The NMR solution structure of this lesion opposite dT in duplex DNA showed complex conformational heterogeneity (23). Computational studies using an NMR structure of duplex DNA where dT was placed opposite the modified dA have revealed that the glycosidic bond of (+)-BPDE-dA was in *syn-anti* equilibrium; therefore, the modified dA has a diminished capability to participate in Watson-Crick base pairing (224). It is possible that the glycosidic bond of modified dA rotates and adopts a *syn* conformation at the primer-template junction and therefore cannot participate in Watson-Crick base pairing. An alternative explanation may be that the structure of the active site of pol ν is significantly distorted by bulky aromatic ring system of this lesion. It has been shown that the BPDE moiety of this lesion is intercalated into the double helix, on the 3' side of the adducted dA, and thus causes significant structural distortions at the active site of T7 pol (225). Since the T7 pol is also a member of the A-family polymerases, the inability of pol ν to bypass this lesion may be due to the active site distortions, similar to those shown for T7

pol. With regard to the low fidelity synthesis past this lesion by pol ν , it has been shown that the adducted dA is displaced from the active site of T7 pol as a result of steric hindrance between the BPDE moiety and the primer template. Among the four dNTPs, dATP fits best into the dNTP binding pocket that is enlarged due to the displacement of adducted dA (225). This structural change provides a likely explanation for the predominant misincorporation of dA by pol ν .

Recently, we reported a comparative study of the mutagenic consequences of identical lesions linked in the major groove via N^6 -dA versus the minor groove linkage via N^2 -dG during the replication of single-stranded pMS2 shuttle vectors in African green monkey kidney cells (COS7 cells) (213); these lesions were the same site-specific PCL4 substrates used in this investigation. These data revealed that DNA containing either lesion could be replicated, with the N^2 -dG PCL4 being moderately mutagenic, while the N^6 -dA PCL4 showed very low mutagenic potential. Although it is anticipated that the extremely bulky nature of the N^6 -dA peptide cross-link lesions would block replicative polymerases, we carried out *in vitro* replication assays using pol δ (Figure 9). The primer extensions and single nucleotide incorporations showed some limited bypass of N^6 -dA PCL12 at very high dNTP concentrations (100 μ M) (Figure 9A), while the titration experiment with varying concentrations of dTTP (from 6.4 nM to 100 μ M) revealed the severity of the blockage posed by this lesion for the pol δ -catalyzed nucleotide insertion (Figure 9B). Specifically, pol δ could incorporate dT opposite the ND dA at concentrations as low as 6.4 nM with 8% of primers being extended, while even at 100 μ M dTTP, only 2% of primers were extended on the N^6 -dA PCL12-containing substrate.

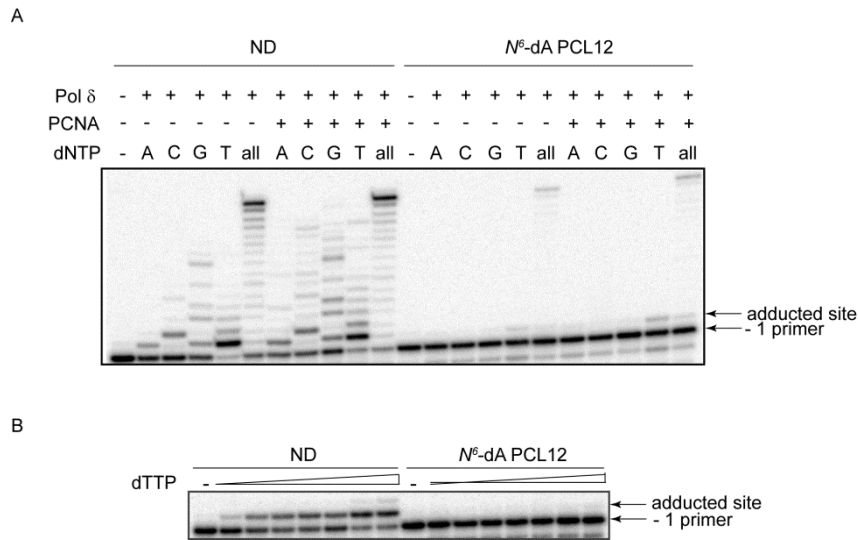


Figure 9. Replication bypass of *N*⁶-dA peptide cross-link by yeast pol δ. (A) Single nucleotide incorporations and primer extensions were catalyzed by 0.5 nM yeast pol δ with 2 nM primer template containing ND or *N*⁶-dA PCL12 under standing start conditions (-1 primer) in the presence or absence of 5 nM PCNA for 20 min at 37°C. Reactions were carried out in the presence of 100 μM individual or all dNTPs. (B) dTTP titration assays with 2 nM primer template were catalyzed by 0.5 nM yeast pol δ under standing start conditions (-1 primer) in the absence of PCNA for 10 min at 37°C using the same substrates as described in panel A. dTTP concentration ranges from 6.4 nM to 100 μM (5-fold incremental increase).

These results suggest that although *in vitro* conditions could be manipulated to observe bypass of *N*⁶-dA peptide cross-links by pol δ, the block to replication is likely to occur when pol δ encounters such bulky lesions; therefore, specialized polymerases may be recruited to carry out TLS. In order to examine whether pol ν is the major TLS polymerase responsible for the replication bypass of these lesions, *in vitro* replication assays were carried out also with other TLS polymerases, pol η and pol ζ. The results showed that both polymerases could not efficiently bypass the lesions (Figure 10 and Figure 11).

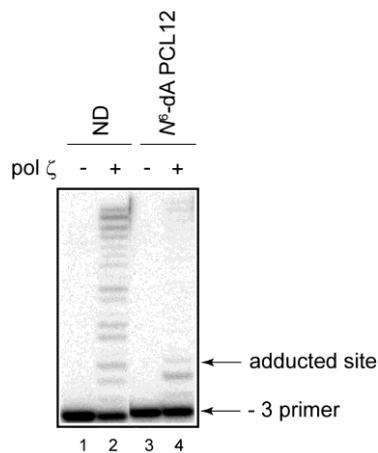


Figure 10. Replication bypass of N^6 -dA peptide cross-link by yeast pol ζ . Primer extensions were catalyzed by 5 nM yeast pol ζ under running start conditions (-3 primer) in the presence of 2 nM primer template containing ND or N^6 -dA PCL12 and 100 μ M dNTPs for 30 min at 37°C. Reactions shown in lanes 1-2 and lanes 3-4 were conducted side-by-side, and products were separated on the same gel.

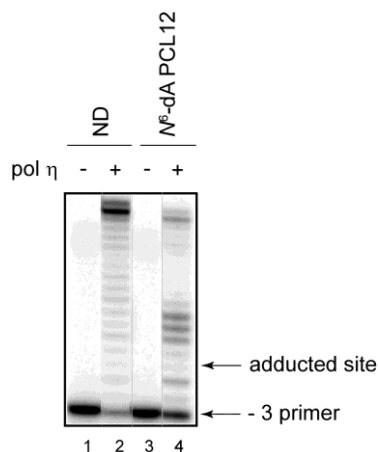


Figure 11. Replication bypass of N^6 -dA peptide cross-links by human pol η . Primer extensions were catalyzed by 10 nM human pol η under running start conditions (-3 primer) in the presence of 5 nM primer template containing ND or N^6 -dA PCL12 and 100 μ M dNTPs for 30 min at 37°C. Reactions shown in lanes 1-2 and lanes 3-4 were conducted side-by-side, and products were separated on the same gel.

The data presented herein suggest that pol ν is a likely candidate to perform TLS past a variety of major groove lesions. At present, the structural basis is unknown why pol ν could efficiently bypass peptide cross-link and ICL as large as 3025 Da, but fails to

bypass less bulky BPDE adduct. However, we speculate that the lesions that are readily bypassed by pol ν may have significant conformational flexibility and thus, can be accommodated without distorting DNA-enzyme interactions within the polymerase active site. Overall, our data suggest that since pol ν is capable of bypassing extremely large major (but not minor) groove lesions, it may play a role in TLS following toxicant challenges that result in the formation of such lesions in the cells.

CHAPTER 3: ROLE OF HIGH-FIDELITY *ESCHERICHIA COLI* DNA POLYMERASE I IN REPLICATION BYPASS OF A DEOXYADENOSINE DNA–PEPTIDE CROSS- LINK

Kinrin Yamanaka^{1,2}, Irina G. Minko¹, Steven E. Finkel⁴, Myron F. Goodman^{4,5}, and R. Stephen Lloyd^{1,3} (2011) Role of High-Fidelity *Escherichia coli* DNA Polymerase I in Replication Bypass of a Deoxyadenosine DNA–Peptide Cross-Link, *J. Bacteriol.*193, 3815-3821.

¹Center for Research on Occupational and Environmental Toxicology, ²Department of Physiology and Pharmacology, and ³Department of Molecular and Medical Genetics, Oregon Health & Science University, Portland, OR 97239

⁴Department of Biological Sciences and ⁵Department of Chemistry, University of Southern California, Los Angeles, CA 90089

3.1. PREFACE

This work is published in the *Journal of Bacteriology*.

My contributions to this work included the conception of this project, design and performance of experiments, data analyses, and writing of the manuscript.

Irina G. Minko contributed to the conception of this project, experimental design, data analyses, and the editing and critical reading of the manuscript.

Steven E. Finkel and Myron F. Goodman provided the pol II-, IV-, and V-deficient *E. coli* strain SF2018 (ZK126 *polB::Sp^c dinB::Kan^r umuDC::Cam^r*) and contributed to the design of the related experiments and critical reading of the manuscript.

R. Stephen Lloyd contributed to the conception of this project, experimental design, the editing and critical reading of the manuscript, and provided funding and lab space for the execution of this work.

Adapted and modified with permission from American Society for Microbiology.

Copyright © American Society for Microbiology, *Journal of Bacteriology*, 193, 2011, 3815-3821, DOI: 10.1128/JB.01550-10.

3.2. INTRODUCTION

DNA–protein cross-links represent a class of DNA lesions that are formed as a consequence of endogenous metabolic processes and exposure to various chemical toxicants, such as acrolein (2,226). Although the prokaryotic NER machinery can function directly on a subset of DNA–protein cross-links, it has been demonstrated to act more efficiently on DNA–peptide cross-links, the proteolytic degradation products of DNA–protein cross-links (227,228). However, little is known about the replication past DNA–peptide cross-link lesions. This lack of knowledge is an obstacle to understanding how cells tolerate these lesions.

Unrepaired DNA–peptide cross-links are hypothesized to be substrates for replication bypass by DNA polymerases. Previously, we demonstrated that when a single-stranded shuttle vector containing a major groove-linked DNA–peptide cross-link was replicated in COS7 cells, this lesion was only marginally miscoding (213). Such data show that in a mammalian system, a subset of DNA–peptide cross-links can be bypassed in a relatively error-free manner. Germane to these observations, we recently demonstrated that pol ν , an A family human polymerase possessing *in vitro* TLS activity, can efficiently and accurately bypass an N^6 -dA PCL12 (Figure 12) (162).

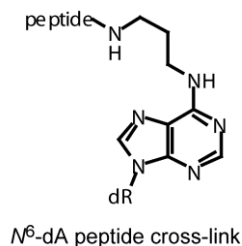


Figure 12. Structure of a γ -HOPdA-derived peptide cross-link. The DNA–peptide cross-link consists of a dodecyl-(Lys-Phe-His-Glu-Lys-His-His-Ser-His-Arg-Gly-Tyr) peptide attached via an acrolein moiety at the N-6 position of dA.

In *E. coli*, pol III carries out DNA synthesis at the replication fork, while specialized DNA damage-inducible polymerases, i.e., pol II, pol IV, and pol V, mainly conduct replication bypass of DNA lesions (6). Pol I, a member of the A family of DNA polymerases, is the most abundant DNA polymerase in *E. coli* in the absence of exogenous stressors and has many important cellular functions, including the processing of Okazaki fragments and DNA repair (229). In addition, pol I has been shown to be capable of catalyzing replication bypass of various N^6 -dA-linked DNA lesions, ranging from a small styrene oxide-induced DNA adduct to more bulky B[a]P-induced DNA adducts (209,210).

To determine if high-fidelity bypass of an N^6 -dA PCL12 by human pol ν could be extrapolated to other A family polymerases, we evaluated the ability of *E. coli* pol I and its exonuclease-deficient Klenow fragment (KFexo⁻) to replicate past this lesion *in vitro*, and for comparative purposes, we conducted similar analyses with all other *E. coli* DNA polymerases. In addition, the efficiency and fidelity of intracellular TLS past the cross-link were assessed using either wild-type *E. coli* or an isogenic triple mutant that lacks DNA damage-inducible polymerases.

3.3. MATERIALS AND METHODS

Materials

[γ -³²P]ATP was purchased from PerkinElmer Life Sciences (Waltham, MA). P-6 Bio-Spin columns were obtained from Bio-Rad (Hercules, CA). T4 polynucleotide kinase, pol I (10,000 U/ml), and KFexo⁻ (5,000 U/ml) were purchased from New England BioLabs

(Beverly, MA). Qiagen plasmid miniprep kits were obtained from Qiagen (Valencia, CA). ScaI was purchased from Fermentas (Glen Burnie, MD). NaCNBH₃ was obtained from Sigma (St. Louis, MO). Slide-A-Lyzer dialysis cassettes with a molecular weight cutoff of 10,000 were purchased from Thermo Scientific (Rockford, IL). The peptide Lys-Phe-His-Glu-Lys-His-His-Ser-His-Arg-Gly-Tyr (KFHEKHHSHRGY) was obtained from Sigma-Genosys (St. Louis, MO). *E. coli* pol II (230), pol IV (231,232), UmuD'₂C (233), and RecA (234) were purified as previously described. The pol III replicase (pol III*), a holoenzyme that contains two molecules of pol III core connected by the γ complex clamp loader but lacks the β subunit sliding clamp, was a generous gift from Michael E. O'Donnell (Rockefeller University, New York, NY) and was purified and reconstituted as previously described (90,235-237). Pol κ was purchased from Enzymax, LLC (Lexington, KY).

Bacterial strains

The pol II-, IV-, and V-deficient strain SF2018 (ZK126 *polB::Spc^r dinB::Kan^r umuDC::Cam^r*) is derived from the *E. coli* K-12 strain ZK126 (W3110 Δ *lacUI169 tna-2*) (238). This triple mutant strain was constructed by bacteriophage P1 transduction into ZK126, using the following donor strains: SF2003 (*polB::Spc^r*), SF2006 (*dinB::Kan^r*), and SF2009 (*umuDC::Cam^r*) (239). The original donor alleles and strains for the polymerase mutants mentioned above were as follows: for SF2003, SH2101 (*polB Δ 1:: Ω Sm-Sp*) (240); for SF2006, RW626 (*dinB::Kan*); and for SF2009, RW82 (*umuDC::Cam*) (both RW626 and RW82 were generous gifts from Roger Woodgate [National Institutes of Health, Bethesda, MD]). The triple mutant was selected by growing cells in the

presence of spectinomycin (100 µg/ml), chloramphenicol (30 µg/ml), and kanamycin (50 µg/ml).

Oligodeoxynucleotide synthesis

ND oligodeoxynucleotides were synthesized by the Molecular Microbiology and Immunology Research Core Facility at Oregon Health & Science University (Portland, OR). An oligodeoxynucleotide containing γ -HOPdA was a generous gift from Carmelo J. Rizzo (Vanderbilt University, Nashville, TN).

An oligodeoxynucleotide containing an N^6 -dA PCL12 (Figure 12) (5'-GCTAGTACTCGTCGACAATTCCGTATCCAT-3') at the underlined nucleotide was prepared according to a previously published procedure (162).

DNA replication assays

For replication assays, primers were designed for conditions with either a running or standing start, where the primer 3'-OH was positioned three nucleotides upstream of the lesion site (-3 primer) or immediately prior to the lesion site (-1 primer), respectively. The sequences of the -3 and -1 primers were 5'-AAAATGGATACGGAAT-3' and 5'-AAAATGGATACGGAATTG-3', respectively. DNA replication assays with pol III*, pol I, KFex^o-, pol II, pol IV, and human pol κ were carried out in reaction mixtures containing 25 mM Tris-HCl, pH 7.5, 10% (v/v) glycerol, 100 µg/ml BSA, and 5 mM DTT. The pol III*-, pol I-, KFex^o-, and pol κ -catalyzed reactions were carried out in the presence of 8 mM MgCl₂; the pol II- and pol IV-catalyzed reactions were carried out in the presence of 5 mM MgCl₂. DNA replication assays with UmuD'₂C were carried out in reaction mixtures containing 20 mM Tris-HCl, pH 7.5, 8 mM MgCl₂, 4% (v/v) glycerol, 10 mM sodium glutamate, 5 mM DTT, 100 µM EDTA, 1 µM single-stranded 36-mer

oligodeoxynucleotide, 6 μ M RecA, and 0.5 mM adenosine 5'-[γ -thio]triphosphate. The single-stranded 36-mer oligodeoxynucleotide and RecA were preincubated in reaction buffer in the presence of adenosine 5'-[γ -thio]triphosphate at 37°C for 3 min. Reactions were initiated by the addition of dNTPs and UmuD'₂C. All reactions were carried out at 37°C. DNA substrate, DNA polymerase, and dNTP concentrations, as well as reaction times, are given in the figure legends. Reaction products were resolved through 15% acrylamide denaturing gels containing 8 M urea and were visualized using a PhosphorImager screen. The percentage of primer extension was determined by calculating the ratio of the amount of extended primers beyond the adducted or corresponding unadducted base to the total amount of primers (unextended primers plus extended primers up to and opposite the site of the adduct plus extended primers beyond the site of the adduct). Quantifications were done using ImageQuant 5.2 software.

Replication of DNAs containing site-specific N⁶-dA PCL12 in E. coli

The pMS2 shuttle vector was the generous gift of Masaaki Moriya (State University of New York, Stony Brook, NY). A single-stranded pMS2 vector containing a site-specific N⁶-dA PCL12 (pMS2-XL12) was constructed following a previously published protocol (90). Initially, individual transformations with either unadducted reference pBR322 plasmid or pMS2-XL12 plasmid were carried out using a wild-type *E. coli* strain to determine the ratio of plasmid concentrations that would result in approximately equal numbers of transformants. The exact ratio of plasmids used for the transformations was not possible to calculate because following ligation of the lesion-containing insert into the pMS2 vector, the percentage of closed circular plasmids with the insert could not be determined accurately.

Following determination of a desirable ratio, the unadducted pBR322 and lesion-containing pMS2-XL12 plasmids were mixed and used to transform wild-type *E. coli* and an isogenic strain (SF2018 [pol II⁻ pol IV⁻ pol V⁻]). The transformants were selected overnight on LB agar plates containing ampicillin, and individual colonies were grown first in LB broth containing ampicillin (100 µg/ml) in 96-well plates at 37°C. After 6 hrs of incubation, a 20-µl aliquot from each well was transferred to other plates containing LB broth with tetracycline (12.5 µg/ml) and incubated overnight at 37°C. This procedure allowed the distinction of the tetracycline-sensitive pMS2 transformants from the tetracycline-resistant pBR322 transformants. In order to identify the population of transformants that originated from insert-containing pMS2-XL12 vectors, tetracycline-sensitive colonies were subjected to differential hybridization as previously described (90). As a probe, we used the oligodeoxynucleotide 5'-TACCAGCGATGCTAGTACT-3', which hybridizes to the 5' junction of the pMS2 backbone and the lesion-containing 30-mer oligodeoxynucleotide insert. To ensure the accuracy of this hybridization screen, plasmids from approximately 10% of colonies that did not hybridize with this probe were isolated and sequenced. The numbers of pBR322 and pMS2-XL12 transformants in the wild-type and pol II⁻ pol IV⁻ pol V⁻ strains were determined, and the relative transformation efficiency of pMS2-XL12 in each strain was calculated by normalizing the transformation efficiency of pMS2-XL12 to that of pBR322. Mutational analyses were carried out by transforming the wild-type and pol II⁻ pol IV⁻ pol V⁻ strains with a pMS2 vector containing either an unmodified or N⁶-dA PCL12-containing 30-mer oligonucleotide. The probe that was complementary to the DNA sequences encompassing the lesion, assuming no mutations were introduced, was used for differential

hybridization. Vectors that did not hybridize to the probe were isolated by use of Qiagen plasmid miniprep kits and digested with ScaI restriction endonuclease. Since both the original pMS2 vector and the insert had an ScaI recognition site, two DNA fragments were generated (~1.9 and ~3.2 kb) from vectors that contained inserted sequences. Subsequently, such vectors were analyzed by DNA sequencing.

3.4. RESULTS

Pol III-catalyzed replication is blocked by N⁶-dA PCL12 in vitro*

It has been shown previously that *Saccharomyces cerevisiae* replicative pol δ cannot efficiently bypass an N⁶-dA PCL12 (162). However, the ability of prokaryotic replicative polymerases to bypass this lesion has not been investigated. Therefore, primer extension reactions were conducted using ND and N⁶-dA PCL12-containing templates with pol III* (holoenzyme that lacks the β subunit sliding clamp). The results revealed that pol III* could not bypass the cross-link because it was severely blocked at a site one nucleotide prior to the lesion, with only 2% of primers extended beyond the adducted site, compared to 65% with an unadducted template (Figure 13).

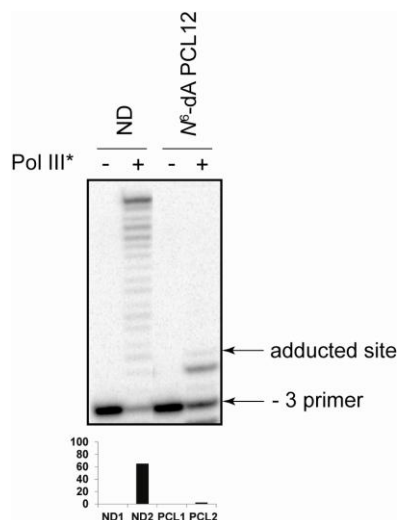


Figure 13. Replication blockage of pol III* by N^6 -dA PCL12. Primer extension reactions were catalyzed by 2 nM pol III* under running start conditions (-3 primer), using ND and N^6 -dA PCL12 substrates. Reactions were carried out in the presence of 2 nM primer template and a 200 μ M concentration of each dNTP for 20 min at 37°C. The bar graph indicates the percentage of primers extended beyond the unadducted or adducted site. ND1, primer extension reactions with ND substrate in the absence of pol III*; ND2, primer extension reactions with ND substrate in the presence of pol III*; PCL1, primer extension reactions with N^6 -dA dodecylpeptide cross-linked substrate in the absence of pol III*; PCL2, primer extension reactions with N^6 -dA dodecylpeptide cross-linked substrate in the presence of pol III*.

Replication bypass of N^6 -dA PCL12 by pol I and KFlexo⁺ in vitro

In order to test the hypothesis that pol I could be involved in replication bypass of the N^6 -dA PCL12, primer extension reactions were carried out using pol I. As shown in Figure 14A, pol I fully extended the primers annealed to the adducted template; under the conditions used, minimal blockage of DNA synthesis was observed one nucleotide prior to the lesion. As evident from the bar graph, the percentages of primers that were extended beyond the adducted site and the corresponding unadducted site were comparable; specifically, 63% and 51% primer extension was observed with a low concentration of pol I on unadducted and adducted templates, respectively. Thus, pol I can catalyze replication bypass of a large N^6 -dA peptide cross-link.

In order to assess the identity of the nucleotide incorporated opposite the lesion, single nucleotide incorporation reactions were conducted with KFlexo⁻. KFlexo⁻ was used instead of pol I in this experiment because the proofreading exonuclease activity of pol I could potentially remove the misincorporated nucleotide, and thus the fidelity of nucleotide incorporation would be overestimated. In the presence of a 1 μM concentration of each dNTP individually, only the correct nucleotide, dT, was incorporated opposite the lesion (Figure 14B), demonstrating that this cross-link can be bypassed accurately by KFlexo⁻ and suggesting that pol I-catalyzed replication past the lesion is error-free.

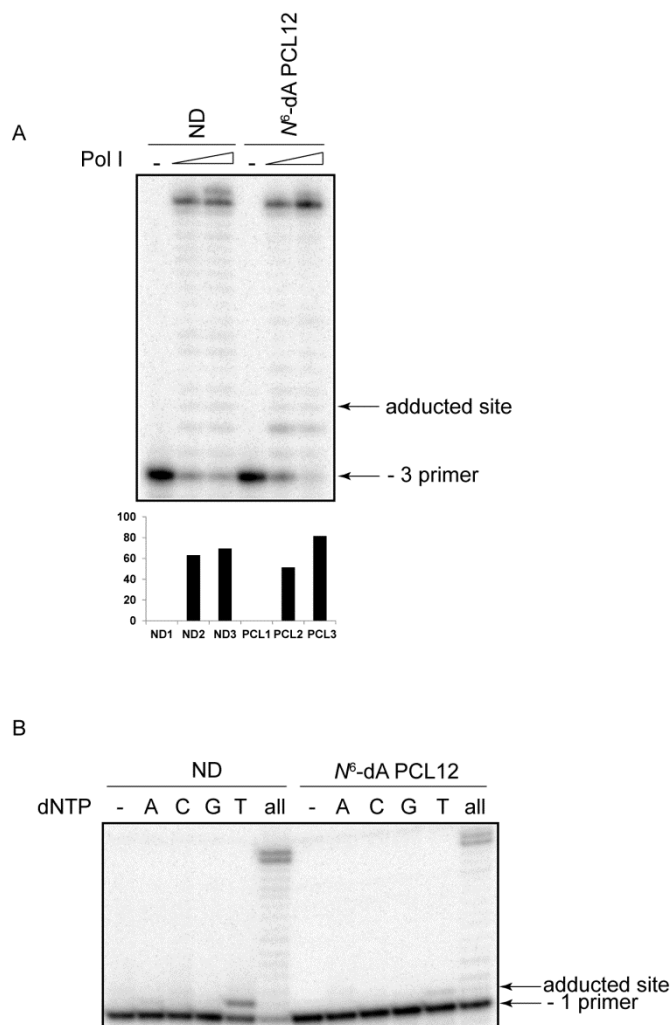


Figure 14. Replication bypass of N^6 -dA PCL12 by pol I and $KFexo^-$. (A) Primer extension reactions were catalyzed by 0.32 mU or 1.6 mU pol I under running start conditions (-3 primer), using ND and N^6 -dA PCL12 substrates in the presence of a 200 μ M concentration of each dNTP. The bar graph indicates the percentage of primers extended beyond the unadducted or adducted site. ND1, primer extension reactions with ND substrate in the absence of pol I; ND2, primer extension reactions with ND substrate in the presence of 0.32 mU pol I; ND3, primer extension reactions with ND substrate in the presence of 1.6 mU pol I; PCL1, primer extension reactions with N^6 -dA dodecylpeptide cross-linked substrate in the absence of pol I; PCL2, primer extension reactions with N^6 -dA dodecylpeptide cross-linked substrate in the presence of 0.32 mU pol I; PCL3, primer extension reactions with N^6 -dA dodecylpeptide cross-linked substrate in the presence of 1.6 mU pol I. (B) Single nucleotide incorporation reactions and primer extension reactions were catalyzed by 0.1 mU $KFexo^-$ under standing start conditions (-1 primer), using the same substrates as those described for panel A in the presence of a 1 μ M concentration of individual or all dNTPs. All reactions were carried out in the presence of 2 nM primer template for 30 min at 37°C.

Replication bypass of N^6 -dA PCL12 by DNA damage-inducible polymerases pol II, pol IV, and pol V in vitro

Since DNA damage-inducible polymerases are known to be involved in bypass of many lesions, the ability of these polymerases to bypass DNAs containing an N^6 -dA PCL12 was examined. Primer extension reactions were carried out with pol II, pol IV, and pol V (UmuD'₂C and RecA complex). Pol IV could not efficiently bypass this lesion. It was strongly blocked at a site one nucleotide prior to the lesion, with only 11% of primers being extended beyond the adducted site, even at the highest concentration of pol IV used. This is in contrast to 90% primer extension beyond the corresponding unadducted site (Figure 15).

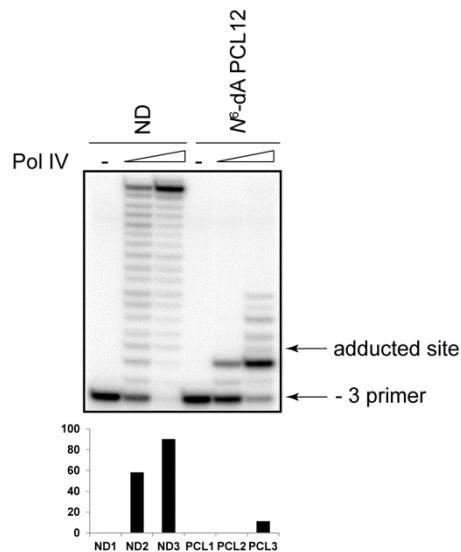


Figure 15. Replication blockage of pol IV by N^6 -dA PCL12. Primer extension reactions were catalyzed by 1.25 nM and 5 nM Pol IV under running start conditions (-3 primer), using ND and N^6 -dA PCL12 substrates. Reactions were carried out in the presence of 5 nM primer template and a 100 μ M concentration of each dNTP for 20 min at 37°C. The bar graph indicates the percentage of primers extended beyond the unadducted or adducted site. ND1, primer extension reactions with ND substrate in the absence of pol IV; ND2, primer extension reactions with ND substrate in the presence of 1.25 nM pol IV; ND3, primer extension reactions with ND substrate in the presence of 5 nM pol IV; PCL1, primer extension reactions with N^6 -dA dodecylpeptide cross-linked substrate in the absence of pol IV; PCL2, primer extension reactions with N^6 -dA dodecylpeptide cross-linked substrate in the presence of 1.25 nM pol IV; PCL3, primer extension reactions with N^6 -dA dodecylpeptide cross-linked substrate in the presence of 5 nM pol IV.

Pol V also catalyzed inefficient bypass of the N^6 -dA PCL12. It could extend primers annealed to the adducted template up to the lesion, but the percentage of primers extended beyond the adducted site was only 4%, compared to 44% beyond the unadducted site (Figure 16A). However, this limited replication bypass appeared to be accurate, because only the correct nucleotide, dT, was incorporated opposite the lesion (Figure 16B).

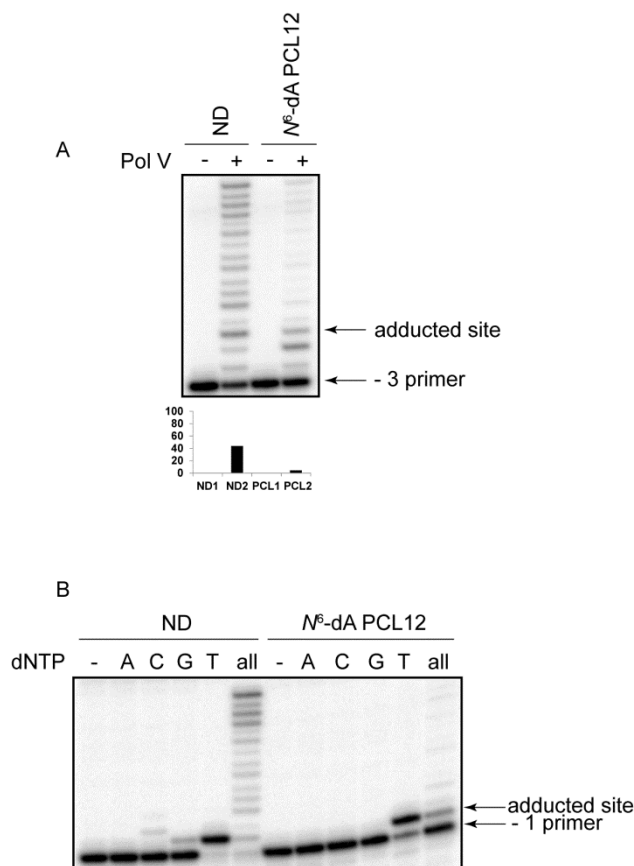


Figure 16. Replication bypass of N^6 -dA PCL12 by pol V. (A) Primer extension reactions were catalyzed by 200 nM UmuD'₂C under running start conditions (-3 primer), using ND and N^6 -dA PCL12 substrates in the presence of a 500 μ M concentration of each dNTP, activated RecA, and 5 nM primer template. The bar graph indicates the percentage of primers extended beyond the unadducted or adducted site. ND1, primer extension reactions with ND substrate in the absence of UmuD'₂C; ND2, primer extension reactions with ND substrate in the presence of UmuD'₂C; PCL1, primer extension reactions with N^6 -dA dodecylpeptide cross-linked substrate in the absence of UmuD'₂C; PCL2, primer extension reactions with N^6 -dA dodecylpeptide cross-linked substrate in the presence of UmuD'₂C. (B) Single nucleotide incorporation reactions and primer extension reactions were catalyzed by 200 nM UmuD'₂C under standing start conditions (-1 primer), using the same substrates as those described for panel A in the presence of a 100 μ M concentration of individual or all dNTPs, activated RecA, and 2 nM primer template. All reactions were carried out for 20 min at 37°C.

Relative to pol IV and pol V, pol II was significantly more competent in bypass of the N^6 -dA PCL12. In particular, using a low concentration of pol II, the percentages of primers extended beyond the corresponding unadducted and adducted sites were 48% and 13%, respectively (Figure 17A). As shown in Figure 17B, single nucleotide incorporation

reactions revealed that only the correct nucleotide, dT, was incorporated opposite the lesion. Collectively, these data suggest that pol II could be another polymerase involved in replication bypass of the N^6 -dA PCL12.

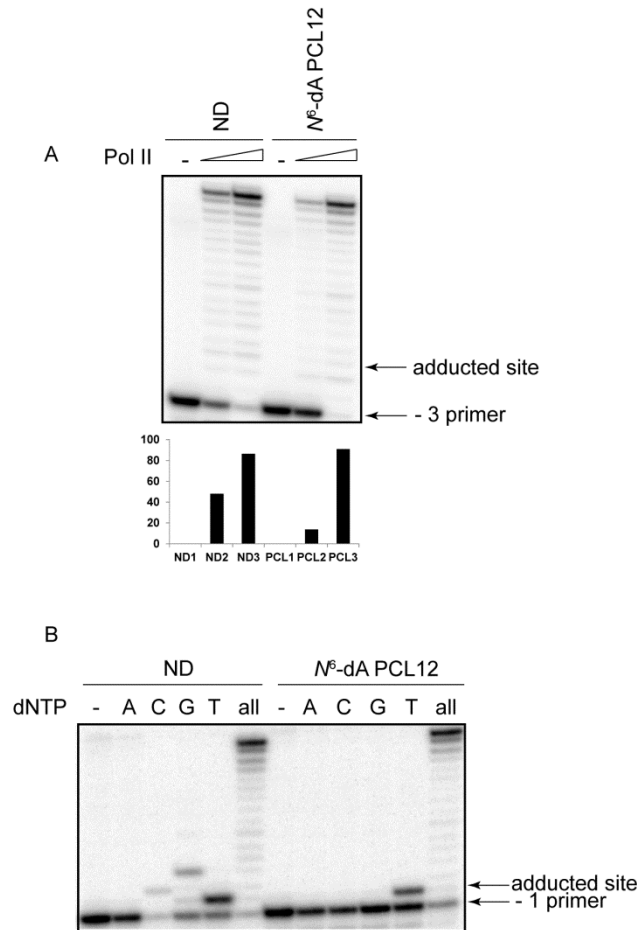


Figure 17. Replication bypass of N^6 -dA PCL12 by pol II. (A) Primer extension reactions were catalyzed by 0.5 nM and 5 nM pol II under running start conditions (-3 primer), using ND and N^6 -dA PCL12 substrates in the presence of a 250 μ M concentration of each dNTP and 5 nM primer template. The bar graph indicates the percentage of primers extended beyond the unadducted or adducted site. ND1, primer extension reactions with ND substrate in the absence of pol II; ND2, primer extension reactions with ND substrate in the presence of 0.5 nM pol II; ND3, primer extension reactions with ND substrate in the presence of 5 nM pol II; PCL1, primer extension reactions with N^6 -dA dodecylpeptide cross-linked substrate in the absence of pol II; PCL2, primer extension reactions with N^6 -dA dodecylpeptide cross-linked substrate in the presence of 0.5 nM pol II; PCL3, primer extension reactions with N^6 -dA dodecylpeptide cross-linked substrate in the presence of 5 nM pol II. (B) Single nucleotide incorporation reactions and primer extension reactions were catalyzed by 0.5 nM pol II under standing start conditions (-1 primer), using the same substrates as those described for panel A in the presence of a 250 μ M concentration of individual or all dNTPs. All reactions were carried out with 2 nM primer template for 20 min at 37°C.

Efficiency and accuracy of replication of plasmid DNAs containing N⁶-dA PCL12 in vivo

Although our *in vitro* results showed that pol II was able to bypass the N⁶-dA PCL12 lesion, pol I manifested a greater ability. In contrast to pol II, pol I is known to be expressed constitutively. Therefore, DNA damage-inducible polymerases may not be required for the replication bypass of this lesion, and pol I may play a major intracellular role in catalyzing replication bypass of such large peptide cross-links.

In order to test whether DNA damage-inducible polymerases are required for replication bypass of the N⁶-dA PCL12, 30-mer oligodeoxynucleotides containing this lesion were ligated into the single-stranded pMS2 vector. A mixture of lesion-containing pMS2-XL12 vector and pBR322 ND reference vector was prepared and transformed into either wild-type or pol II⁻ polIV⁻ polV⁻ *E. coli*. The transformants were then selected for ampicillin resistance and tested for tetracycline resistance to identify tetracycline-sensitive pMS2-containing clones. Furthermore, colonies were identified by differential hybridization using a probe that hybridizes to the 5' junction of pMS2 DNA and the insert sequence. The colonies containing the progeny of either pBR322 or pMS2-XL12 were counted, and the transformation efficiency of pMS2-XL12 vector relative to that of pBR322 vector was calculated for each strain. No differences in the transformation efficiency of pMS2-XL12 vector were observed between the wild-type and pol II⁻ polIV⁻ polV⁻ strains (Figure 18). These data demonstrate that DNA damage-inducible polymerases, including pol II, are dispensable for bypass of an N⁶-dA PCL12 *in vivo*.

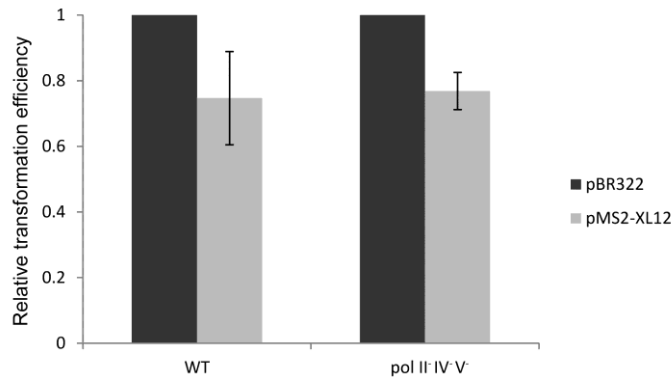


Figure 18. Ability of *E. coli* strains to replicate DNA containing N^6 -dA PCL12. A mixture of ND pBR322 vector and site-specifically modified single-stranded pMS2 vector (pMS2-XL12) was transformed into an *E. coli* wild-type strain and a mutant strain lacking all DNA damage-inducible polymerases (pol II⁻ pol IV⁻ pol V⁻). The transformation efficiency of pMS2-XL12 vector (a function of the replication bypass efficiency) was measured for each strain. The data were normalized using the transformation efficiency of pBR322 vector as a reference. The data were obtained from three independent experiments. Error bars represent standard errors.

In vitro, pol I bypassed the N^6 -dA PCL12 in an error-free manner. In order to test whether accurate bypass of this lesion also takes place within cells, mutational analyses were conducted by transforming pMS2-XL12 vector into the wild type or the pol II⁻ polIV⁻ polV⁻ strain. After overnight selection in the presence of ampicillin, 95 and 96 colonies of wild-type and pol II⁻ polIV⁻ polV⁻ cells, respectively, were analyzed for mutations as described in Materials and Methods. In parallel experiments, 89 and 96 individual clones of wild-type and pol II⁻ polIV⁻ polV⁻ cells, respectively, were tested following replication of the corresponding ND control vectors. The results revealed that no mutations were introduced opposite either ND or damaged dA, demonstrating the accuracy of TLS past the N^6 -dA PCL12 *in vivo*.

Pol I is known to be essential for ColE1-type plasmid replication (241,242). Since pMS2 possesses a ColE1 origin (243), a pol I-defective strain could not be used for the plasmid-based approach described above to directly assess the role of pol I in bypass of DNA lesions. However, given the strong inhibitory effect of the N^6 -dA PCL12 on pol III*-catalyzed DNA synthesis *in vitro* (Figure 13) and the efficient replication of plasmids containing this lesion in the pol II⁻ polIV⁻ polV⁻ strain (Figure 18), it can be inferred that pol I likely plays a key role in bypass of such large major groove peptide cross-links.

3.5. DISCUSSION

In the current investigation, we demonstrated that pol I and pol II could replicate DNAs containing an N^6 -dA PCL12 in an error-free manner *in vitro*, while pol III* and pol IV were strongly inhibited by this type of lesion. Although pol V could fully and accurately extend a primer on a damaged substrate, its efficiency was low. Since pol I is expressed constitutively, we proposed that pol I in cells can carry out TLS past an N^6 -dA PCL12 and that the DNA damage-inducible polymerases are not required. Consistent with this idea, *in vivo* studies using wild-type and pol II⁻ pol IV⁻ pol V⁻ *E. coli* strains revealed that DNA damage-inducible polymerases were dispensable.

Although these data suggested the essential role of pol I in replication bypass of the N^6 -dA PCL12, an involvement of alternative DNA polymerases in this process cannot be ruled out completely. In particular, pol III and possibly other DNA polymerases may manifest higher bypass efficiencies in cells than those observed *in vitro* due to stimulation of bypass by the β sliding clamp and additional accessory factors. It is also

important to recognize that the division of labor between DNA polymerases in replication bypass is expected to be more complex in the context of chromosomal DNA, as opposed to a site-specific single lesion on plasmid DNA. Following chemical exposure, multiple structurally different DNA lesions are likely to be formed that may trigger the SOS response. The contribution of pol II to TLS past N^6 -dA polypeptide cross-links could be quite prominent under such conditions, since its intracellular levels are significantly increased (10). Pol IV, the most abundant *E. coli* DNA polymerase in stressed cells (10), may also be involved in replication bypass of lesions, displacing more efficient but less abundant DNA polymerases from the primer termini. Such a phenomenon was recently observed during DSB repair (244). In addition, the location of the lesions on the chromosome may also influence the choice of polymerase, similar to a site-specific polymerase switch during spontaneous mutagenesis (245).

The active site of pol I is constrained, and pol I has a stringent requirement for accommodating nucleobase pairs with the correct Watson-Crick geometry (246,247). Therefore, it is intriguing that pol I was capable of bypassing a very large N^6 -dA PCL12 that not only blocked replicative polymerases (*E. coli* pol III* and yeast pol δ) but also blocked the low-fidelity polymerases specialized in lesion bypass (*E. coli* pol IV and pol V and human pol κ (Figure 19)).

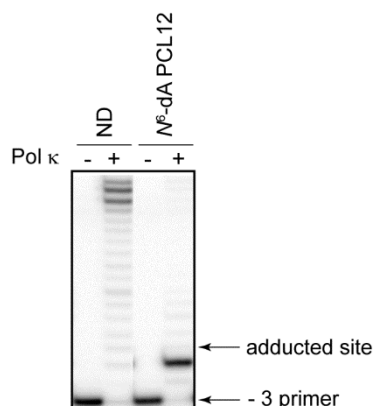


Figure 19. Replication blockage of human pol κ by N^6 -dA PCL12. Primer extension reactions were catalyzed by 1 nM pol κ under running start conditions (-3 primer), using ND and N^6 -dA PCL12 substrates. Reactions were carried out in the presence of a 100 μ M concentration of each dNTP and 5 nM primer template for 30 min at 37°C.

One possible explanation may be that this lesion has conformational flexibility, with the bulky dodecylpeptide pointed away from the active site of pol I, and has no effect on the Watson-Crick geometry. The DNA-peptide structure might resemble that of Lys-Trp-Lys-Lys linked at N^2 -dG via the N-terminal Lys through an acrolein moiety. In the latter structure, the Trp indolyl group does not intercalate into the DNA, while the C-terminal Lys is exposed to solvent, interacting minimally with the DNA (248). However, a detailed analysis of the mechanism of action of pol I in the bypass of the N^6 -dA PCL12 awaits the co-crystal structure determination of pol I in complex with this lesion.

With regard to the biological significance of N^6 -dA peptide cross-links, a previous report focused exclusively on the identification of *E. coli* DNA polymerases that can catalyze replication bypass of N^2 -dG peptide cross-links (90). The polymerases responsible for the replication bypass of N^6 -dA peptide cross-links, however, were not studied. The N^6 -dA peptide lesion used in this study was derived from the ring-opened aldehydic form of the acrolein-induced γ -HOPdA adduct. NMR analyses showed that γ -HOPdA in the ring-

opened form can be detected readily (212). This suggests that γ -HOPdA could potentially interact with peptides, resulting in the formation of DNA–peptide cross-links. Such a mechanism would be conceptually similar to that for the aldehydic group of ring-opened γ -HOPdG, which reacts with peptides and yields chemically identical lesions, except that the lesions are located in the minor groove of DNA (249). Consistent with this prediction, it was demonstrated that the peptide Lys-Trp-Lys-Lys is trapped efficiently and stably with oligodeoxynucleotides containing γ -HOPdA in the presence of a reducing agent (213). Thus, although N^6 -dA peptide cross-links have not been identified *in vivo* to date, their biological relevance cannot be disregarded, and therefore the present investigation examining the identity of polymerases involved in the processing of these lesions has importance.

It is worth noting that in *E. coli*, TLS past N^2 -dG peptide cross-links requires the DNA damage-inducible polymerase pol IV (90). In contrast, such specialized polymerases were not essential for replication bypass of the N^6 -dA PCL12. This is interesting given the fact that the previously investigated N^2 -dG PCL12 is chemically identical to the N^6 -dA PCL12 used here, except that the former lesion is positioned in the minor, not the major, groove of DNA. Germane to this observation, DNA polymerases of the A family interact with DNA at the minor groove (250). Thus, pol I may have evolved to be particularly proficient in the bypass of major groove lesions, including relatively small adducts (209,210) and large degradation products of DNA–protein cross-links.

In summary, we have shown the ability of *E. coli* pol I to accurately replicate past an N^6 -dA PCL12 *in vitro* and have generated data suggesting its role in bypass of this lesion *in vivo*. Since no data about the identity of *E. coli* DNA polymerases responsible for processing the major groove cross-links are available to date, the findings reported here promote our understanding of how cells maintain genome integrity upon induction of DNA-peptide and DNA-protein cross-links.

CHAPTER 4: REPLICATION BYPASS OF THE ACROLEIN-MEDIATED DEOXYGUANINE DNA–PEPTIDE CROSS-LINKS BY DNA POLYMERASES OF THE DINB FAMILY

Irina G. Minko¹, **Kinrin Yamanaka**¹, Ivan D. Kozekov², Albena Kozekova², Chiara Indiani³, Michael E. O'Donnell³, Qingfei Jiang⁴, Myron F. Goodman⁴, Carmelo J. Rizzo², and R. Stephen Lloyd¹ (2008) Replication Bypass of the Acrolein-Mediated Deoxyguanine DNA–Peptide Cross-Links by DNA Polymerases of the DinB Family, *Chem. Res. Toxicol.* 21, 1983-1990.

¹Center for Research on Occupational and Environmental Toxicology, Oregon Health & Science University, Portland, OR 97239

²Departments of Chemistry and Biochemistry, Center in Molecular Toxicology, Vanderbilt University, Nashville, TN 37235

³Rockefeller University, New York, NY 10021

⁴Department of Biological Sciences and Chemistry, University of Southern California, Los Angeles, CA 90089

4.1. PREFACE

This work is published in *Chemical Research in Toxicology*.

My contributions to this work were in generating the data shown in Table 3 and writing of the manuscript.

Irina G. Minko contributed to the conception of this project, design and performance of the experiments, data analyses, and writing of the manuscript.

Ivan D. Kozekov, Albena Kozekova, and Carmelo J. Rizzo synthesized oligodeoxynucleotides containing γ -HOPdG and provided expertise on the chemistry of this DNA adduct.

Chiara Indiani and Michael E. O'Donnell provided pol III replicase and contributed to the design of the related experiments.

Qingfei Jiang and Myron F. Goodman provided pol II, pol IV, pol V, RecA and contributed to the design of the related experiments.

R. Stephen Lloyd contributed to the conception of this project, experimental design, the editing and critical reading of the manuscript, and provided funding and lab space for the execution of this work.

Adapted and modified with permission from

Irina G. Minko, Kinrin Yamanaka, Ivan D. Kozekov, Albena Kozekova, Chiara Indiani, Michael E. O'Donnell, Qingfei Jiang, Myron F. Goodman, Carmelo J. Rizzo, and R. Stephen Lloyd (2008) Replication Bypass of the Acrolein-Mediated Deoxyguanine DNA–Peptide Cross-Links by DNA Polymerases of the DinB Family, *Chem. Res. Toxicol.* 21, 1983-1990.

Copyright (2008) American Chemical Society.

4.2. INTRODUCTION

DNA–protein cross-links are formed in cells not only as a consequence of routine DNA metabolism but also from exposure to a variety of chemical toxicants and metals (226). In particular, these lesions have been detected in DNA following treatment of cultured human cells with an α,β -unsaturated aldehyde, acrolein (251,252). Among aldehydes that can induce DNA–protein cross-links *in vitro*, acrolein is one of the most potent (253). It is cytotoxic and mutagenic (254-256) and has tumor-initiating activity (257). Acrolein is ubiquitous in the environment, but more importantly, it is generated *in vivo*, mainly as a product of peroxidation of fatty acids (258-260). Thus, acrolein may represent a significant endogenous causative factor for induction of DNA–protein cross-links.

Being a highly reactive bifunctional electrophile, acrolein reacts with DNA to modify nucleobases at various positions, in particular, at N^2 of dG (261-265). The major product of reaction between N^2 -dG and acrolein is γ -HOPdG (261), a mutagenic adduct (266) that has been detected in cellular DNA isolated from various tissues both following acrolein exposure and as an endogenous lesion (259,267-269). The γ -HOPdG adduct undergoes spontaneous ring opening and closing (Figure 20A) with the equilibrium being shifted toward the ring-opened form in duplex DNA (1,270). The free aldehyde of the ring-opened γ -HOPdG can further react with amines in peptides and proteins to yield Schiff base-mediated linkages (249,271). Similar to the acrolein adduct, N^2 -dG adducts of other biologically important α,β -unsaturated aldehydes, crotonaldehyde and *trans*-4-hydroxynonenal, have also been shown to form Schiff base-mediated DNA–peptide cross-links (249). Therefore, elucidation of a role for acrolein and other related

compounds in living organisms cannot be complete without detailed understanding of cellular processing of DNA–protein cross-links.

Although a subset of DNA–protein cross-links can undergo spontaneous reversal, others require active removal by DNA repair machinery or are processed through damage avoidance and tolerance pathways. Prokaryotic NER has been demonstrated to function on DNA–protein adducts as large as 16,000 Da (228), while comparably sized cross-linked protein adducts were refractory to excision by the human NER complex (272-274). However, these data showing a lack of repair of intact proteins by human NER do not rule out a role for this pathway in the ultimate processing of these lesions, since there is a literature precedent suggesting an initial proteolytic processing of these lesions prior to excision. In this regard, data obtained from the Zhitkovich's group (275) demonstrated that repair of formaldehyde-induced DNA–protein cross-links was significantly reduced in cells treated with lactacystin, a proteasome inhibitor. It was hypothesized that the cross-linked proteins were proteolytically degraded into substrates suitable for completion of the repair process. Consistent with these results, DNA–peptide cross-links serve as much better substrates relative to DNA–protein cross-links for both prokaryotic (227,228) and human NER (272-274). Baker *et al.* also demonstrated that incubation with the 26S proteasome inhibitor, MG132, resulted in a greater than 50% reduction in the intracellular repair of plasmids carrying site-specific DNA–protein cross-links (274). Collectively, these data indicate that biological processing of covalently linked protein adducts can proceed via a proteolytic degradative process, converting DNA–protein cross-links into DNA–peptide cross-links.

NER processing of DNA–peptide cross-links could be sufficiently delayed to make these lesions available for DNA replication bypass and potentially lead to mutations. Recently, we have assessed the mutagenic properties of Lys-Trp-Lys-Lys cross-links during extrachromosomal replication in mammalian cells. When this tetrapeptide was linked to the N^2 position of dG via the acrolein-derived γ -HOPdG, lesion bypass was only moderately mutagenic (213). Previous investigations have suggested that the efficient and nonmutagenic replication bypass of bulky N^2 -dG adducts can be performed by DNA polymerases of the DinB family, pol κ in mammalian cells, and its bacterial orthologue, pol IV, in *E. coli* (95,100,101,276-280). Here, we hypothesized that human pol κ as well as pol IV also function in replication bypass of N^2 -dG–peptide cross-links. To test this hypothesis, we have created site specifically modified oligodeoxynucleotides that contain either tetrapeptide (Lys-Trp-Lys-Lys) or dodecylpeptide (Lys-Phe-His-Glu-Lys-His-His-Ser-His-Arg-Gly-Tyr) γ -HOPdG-mediated cross-links (Figure 20) and performed replication assays *in vitro*.

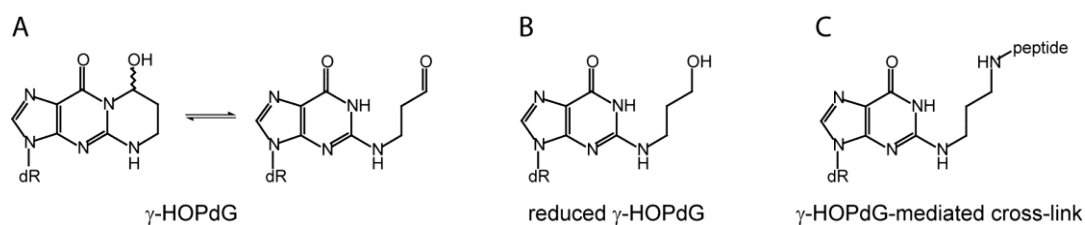


Figure 20. Structure of DNA adducts used in the current study. (A) γ -HOPdG shown as the equilibrium between the ring-closed and the ring-opened forms. (B) Reduced γ -HOPdG. (C) Reduced γ -HOPdG-mediated peptide cross-link.

Additionally, the DNA–peptide cross-links were introduced into a single-stranded DNA vector (pMS2) (281) and the consequences of replication past these lesions were investigated in both the wild-type and the pol IV-deficient *E. coli* strains.

4.3. MATERIALS AND METHODS

DNA polymerases

Human pol κ was purchased from Enzymax Inc. (Lexington, KY). The polymerase was full length and tagged at its N termini with the calmodulin-binding peptide. Subunits of the pol III replicase were purified as described before (237,282). The pol III core was reconstituted by mixing α , ϵ , and θ subunits (1:1.5:3 molar ratio, respectively) and incubating for 30 min at 15°C. The pol III core was resolved from unbound proteins by chromatography on MonoQ as described previously (235). The pol III replicase, containing two molecules of pol III core connected by the clamp loader, was reconstituted as follows. A mixture of γ and τ (2.5:1 molar ratio, respectively) was incubated for 90 min at 15°C, followed by the addition of δ , δ' , χ , and ψ (3-fold molar excess of each subunit over τ) followed by a further 1 hr incubation. The $\tau_2\gamma_1\delta\delta'\chi\psi$ complex was resolved from other species ($\tau_3\delta\delta'\chi\psi$, $\tau_1\gamma_2\delta\delta'\chi\psi$, and $\gamma_3\delta\delta'\chi\psi$) using a 1 ml MonoS column by elution with a 0.0-0.5 M NaCl gradient as described before (236). The $\tau_2\gamma_1\delta\delta'\chi\psi$ clamp loader was incubated with a 4-fold molar excess of pol III core, and pol III replicase was purified from excess pol III core by MonoQ anion exchange chromatography as reported previously (237). *E. coli* pol II (230), pol IV (231,232), pol V (233), and RecA (234) were purified as previously described.

Bacterial strains

The *E. coli* strains ZK126 (W3110 *DlacU169 tna2*) and its pol IV-deficient derivative (ZK126 *dinB::Kan*) (239) used in this study were the generous gift of Dr. Steven E. Finkel (University of Southern California, Los Angeles, CA).

DNA substrates

DNA oligodeoxynucleotides containing a site-specific γ -HOPdG (Figure 20A) were synthesized and purified as previously described (212). This 30-mer had the following sequence: GCTAGTACTCGTCGACAATTCCGTATCCAT, where the underlined G denotes the position of the γ -HOPdG. Procedures to convert γ -HOPdG into the permanently ring-opened adduct, the reduced γ -HOPdG (Figure 20B), were performed as previously described (213). The Lys-Trp-Lys-Lys tetrapeptide was synthesized by Sigma-Genosys.

The Lys-Phe-His-Glu-Lys-His-His-Ser-His-Arg-Gly-Tyr dodecylpeptide was purchased from Sigma-Genosys. The generation of the DNA-peptide cross-links (Figure 20C) and purification of the DNA-peptide cross-link-containing oligodeoxynucleotides was carried out according to a published protocol (213). These 30-mer oligodeoxynucleotides were used as templates in replication reactions *in vitro* and also for preparation of site specifically modified vectors for cellular studies. All other oligodeoxynucleotides were obtained from the Molecular Microbiology and Immunology Research Core Facility (Oregon Health & Science University, Portland, OR).

Replication assays in vitro

Preparations of primer template DNA substrates were performed as previously described (33). Polymerase bypass assays with human pol κ and *E. coli* pol II, pol III, and pol IV were carried out using 5 nM primer template DNA substrates in the presence of 25 mM

Tris-HCl, pH 7.5, 5 mM MgCl₂, 10% (v/v) glycerol, 10 mM NaCl, 0.1 mg/ml BSA, and 5 mM DTT at 37°C. Polymerase bypass assays with *E. coli* pol V were carried out using 5 nM primer template DNA substrates in the presence of 20 mM Tris-HCl, pH 7.5, 8 mM MgCl₂, 4% (v/v) glycerol, 10 mM sodium glutamate, 5 mM DTT, 100 μM EDTA, 2 μM single-stranded 36-mer oligodeoxynucleotide, 12 μM RecA, and 1 mM adenosine 5'[γ-thio]triphosphate.

Prior to pol V-catalyzed reactions, single-stranded oligodeoxynucleotide and RecA were preincubated in reaction buffer in the presence of adenosine 5'[γ-thio]triphosphate at 37°C for 3 min and then added to the primer template DNA substrates. The reactions were initiated by addition of dNTPs and pol V and conducted at 37°C. Protein concentrations, dNTPs concentrations, and incubation times are given in the figure legends. Polymerase reactions were terminated by the addition of an equal volume of a solution of 95% (v/v) formamide, 20 mM EDTA, 0.2% (w/v) bromphenol blue, and 0.2% (w/v) xylene cyanol. Products were resolved through a 15% denaturing polyacrylamide gel in the presence of 8 M urea and visualized using a PhosphorImager screen.

Replication of DNAs containing site-specific DNA-peptide cross-links in E. coli

The pMS2 phagemid shuttle vector (281) was a gift from Dr. Masaaki Moriya (State University of New York, Stony Brook, NY). Single-stranded, site specifically modified pMS2 vectors were constructed as in previous studies (213,266,281). Transformations of *E. coli* cells with these vectors and analyses of the progeny DNAs by differential hybridization were performed as previously described (213,266). Individual DNAs were isolated using Qiagen plasmid miniprep kits and tested by ScaI restriction endonuclease according to manufacturer's recommendations.

4.4. RESULTS

Preparation of DNA–peptide cross-links

Although there are multiple potential sites of adduction within both DNA and protein, we have chosen to model DNA–peptide cross-links via acrolein-modified DNA at N^2 -dG. Acrolein reacts with DNA primarily at N^2 -dG, yielding γ -HOPdG, a lesion that undergoes spontaneous ring opening and closing (Figure 20A) (270). In the presence of NaBH_4 , γ -HOPdG can be converted to its reduced derivative (Figure 20B) that serves in our assays as a model for the permanently ring-opened form of the adduct. The free aldehyde of the natural, unreduced γ -HOPdG can react with primary and secondary amines in peptides and proteins (249,271). When DNAs containing these lesions are incubated in the presence of peptides that contain both α and ϵ amino groups, the relative pK_a of the α amino group dominates the course of the cross-linking reaction, forming a carbinolamine linkage between the N-terminal α amino group and the aldehyde of the γ -HOPdG adduct. The initial carbinolamine linkage can dehydrate to a Schiff base that can be reductively trapped in the presence of a mild reducing agent such as NaCNBH_3 to form an irreversible cross-link (Figure 20C) (249). Thus, DNAs incubated as described above have stable peptide cross-links that are directly amenable to replication bypass analyses. These linkages through the α amino group are common intermediates for a variety of DNA glycosylase/abasic site lyases (283); thus, our DNA–peptide cross-links model biologically relevant lesions.

The 30-mer oligodeoxynucleotides containing DNA–peptide cross-links were prepared as previously described (213) and tested for purity using denaturing (8 M urea)

polyacrylamide gel. No bands were detected that would suggest either the presence of DNAs without cross-link or the decomposition of oligodeoxynucleotides.

Bypass of DNA-peptide cross-links by human pol κ

Our previous studies had indicated that both the γ -HOPdG adduct and its reduced derivative posed a severe block to DNA synthesis by eukaryotic replicative polymerases, pol δ and pol ϵ (93,266). On the basis of these observations, we considered it unlikely that either of them would be able to replicate past bulky γ -HOPdG-mediated DNA-peptide cross-links. In contrast to replicative polymerases, human pol κ could efficiently incorporate the correct nucleotide, dC, opposite the ring-opened reduced γ -HOPdG (93,94). Furthermore, pol κ will efficiently extend a 0 primer if the correct C has been placed opposite either γ -HOPdG or its reduced derivative (93,94). In the current study, we compared the ability of pol κ to carry out TLS past tetra- and dodecylpeptides linked to DNA via the ring-opened γ -HOPdG adduct vs control (unadducted) DNAs (Figure 20C).

Using a -4 primer, pol κ showed a significant processivity on ND DNA, with a large percentage of primers being extended to near full length (Figure 21, upper panel, lanes 2-5). Surprisingly, neither of the peptide-modified γ -HOPdG substrates blocked the progression of pol κ (Figure 21, upper panel, lanes 6-13). Although there was a minor pause site, two nucleotides prior to the adducted site, there was no evidence of even a minor replication pause at the site of the lesion, and primers could be extended to full length comparable with the control DNAs.

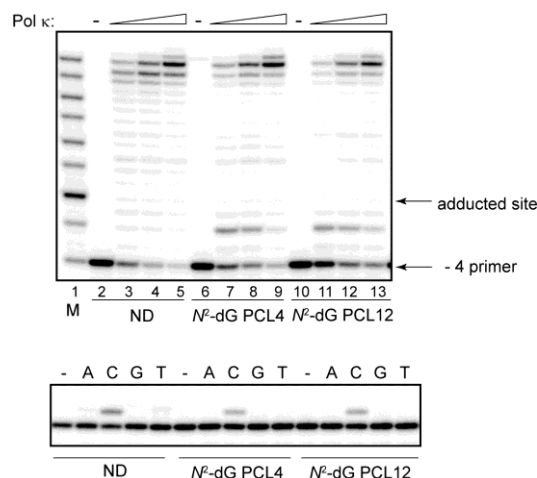


Figure 21. Replication bypass of DNA-peptide cross-links by human pol κ . Upper panel: Primer extensions by pol κ were carried out for 20 min in the presence of 100 μ M dNTPs at 1.25 (lanes 3, 7, and 11), 2.5 (lanes 4, 8, and 12) or 5 nM (lanes 5, 9, and 13) protein concentrations. Lower panel: Single nucleotide incorporations by pol κ (1 nM) were carried out for 5 min in the presence of 20 μ M individual dNTPs. M, oligodeoxynucleotide sizing markers; N^2 -dG PCL4, tetrapeptide cross-linked substrate; N^2 -dG PCL12, dodecylpeptide cross-linked substrate.

Since pol κ incorporated a nucleotide opposite both lesions, the relative fidelity of the reactions was examined by carrying out single nucleotide incorporation assays using a -1 primer (Figure 21, lower panel). These assays revealed that in addition to these DNA-peptide cross-links not posing a block, pol κ utilized dC with a very strong preference over any other of the dNTPs (Figure 21, lower panel). Taken together, these data indicate that pol κ has the capacity to accurately bypass the complex N^2 -dG acrolein-derived peptide adducts.

*Replication of DNAs containing DNA-peptide cross-links by *E. coli* DNA polymerases*

Whereas the blocking effect of γ -HOPdG and reduced γ -HOPdG has been shown for eukaryotic replicative polymerases (93,266), the replicative polymerase in *E. coli* cells, pol III, has not been previously tested with any of these adducts. Here, the primer extensions by pol III were conducted with -4 primers that were annealed with DNA

templates containing either γ -HOPdG, reduced γ -HOPdG, or γ -HOPdG-derived DNA-peptide cross-links (Figure 22). The form of the multisubunit pol III replicase employed here is the dimeric replicase that is utilized for chromosome replication; it contains two molecules of pol III core that attach to two τ subunits of the clamp loading assembly. The observed results reveal that while the pol III replicase could efficiently catalyze DNA synthesis utilizing the ND substrate (Figure 22, lanes 2 and 3), no bypass was detected in reactions containing any of the adducted templates; all primer extensions were terminated one nucleotide prior to the lesion, even at the highest enzyme concentrations (Figure 22, lanes 6, 9, 12, and 15). Previously, it has been shown that the KFlexo⁻, which is another major DNA polymerase in *E. coli*, catalyzed very inefficient and extremely error-prone DNA synthesis past the γ -HOPdG adduct (284,285). Collectively, these data suggest that similar to mammalian cells, DNA synthesis past γ -HOPdG-derived lesions in bacteria is likely to utilize specialized bypass polymerases.

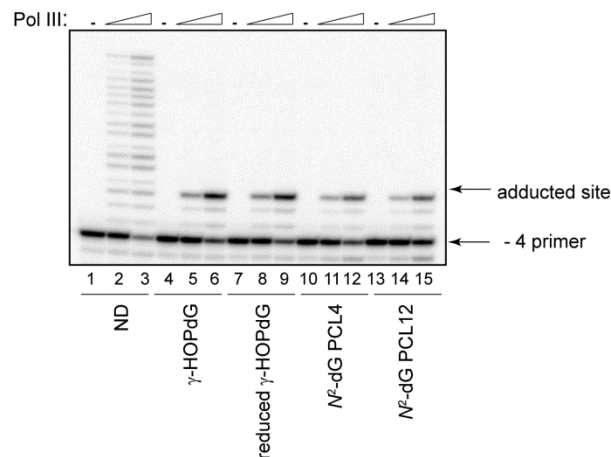


Figure 22. Replication bypass of γ -HOPdG, reduced γ -HOPdG, and DNA-peptide cross-links by *E. coli* pol III. Primer extensions by the pol III replicase were carried out for 20 min in the presence of 200 μ M dNTPs at 0.01 (lanes 2, 5, 8, 11, and 14) or 0.05 nM (lanes 3, 6, 9, 12, and 15) protein concentrations. N^2 -dG PCL4, tetrapeptide cross-linked substrate; N^2 -dG PCL12, dodecylpeptide cross-linked substrate.

Given that human pol κ could readily bypass these lesions, it was hypothesized that *E. coli* pol IV, which is an orthologue of mammalian pol κ (82), might be capable of catalyzing TLS past these adducts. As anticipated, pol IV extended a -4 primer annealed with an undamaged template to full length product (Figure 23, upper panel, lanes 2-5). In contrast, extension of the -4 primer annealed to the DNA template containing γ -HOPdG was significantly blocked one nucleotide prior to the lesion and modestly opposite the lesion (Figure 23, upper panel, lanes 6-9). However, given a sufficient number of enzyme-DNA encounters, extension could proceed to full length. Similar reactions, but using the reduced γ -HOPdG, showed only a modest pause site one nucleotide prior to the lesion (Figure 23, upper panel, lanes 10-13). Thus, the permanently ring-opened analogue of the lesion affords efficient bypass.

In contrast to these data, replication of the templates containing the γ -HOPdG adducts with tetra- and dodecylpeptide revealed different patterns of inhibition. For the DNA modified with tetrapeptide, the dominant pause site occurred following incorporation of a nucleotide opposite the lesion (Figure 23, upper panel, lanes 14-17). However, using increasing enzyme concentrations, blockage opposite the lesion could be overcome, only to encounter replication blockage one and three nucleotides beyond the lesion (Figure 23, upper panel, lanes 16 and 17). The block at the third position beyond the lesion was very poorly extended, suggesting that there are structural impediments to the passage of the bulky adducted duplex DNA through the backside of pol IV. Comparable analyses using the dodecylpeptide-containing substrate revealed a less significant blockage opposite the lesion but an equivalent pause site at the third position beyond the lesion (Figure 23,

upper panel, lanes 18-21). These data confirm that the presence of N^2 -dG-linked peptide inhibits pol IV-catalyzed processive synthesis several nucleotides past the site of the lesion. However, because the magnitude and site of the pause was not affected by the increased bulk of the larger peptide, these data suggest that the impeding interactions are localized to the first few amino acids of the adducted peptides.

Single nucleotide incorporation analyses revealed that pol IV preferentially incorporated the correct nucleotide, dC, opposite all of these lesions; however, misincorporations of dA and dT opposite the γ -HOPdG and reduced γ -HOPdG adducts were also observed (Figure 23, lower panel).

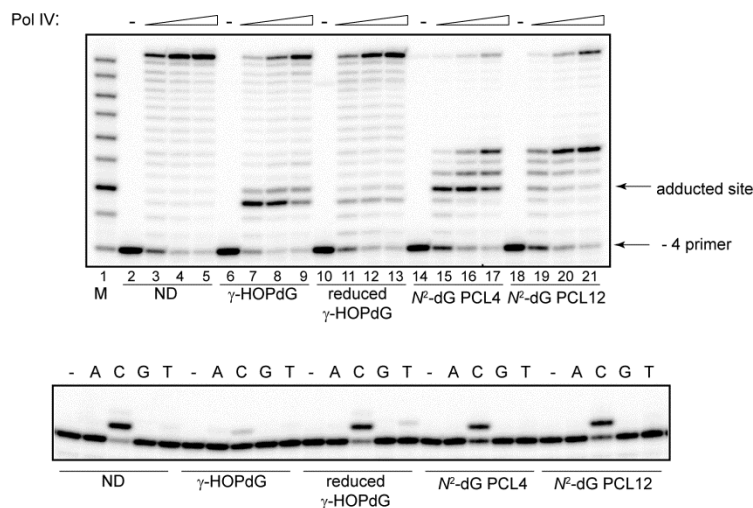


Figure 23. Replication bypass of γ -HOPdG, reduced γ -HOPdG, and DNA-peptide cross-links by *E. coli* pol IV. Upper panel: Primer extensions by pol IV were carried out for 20 min in the presence of 100 μ M dNTPs at 1.25 (lanes 3, 7, 11, 15, and 19), 2.5 (lanes 4, 8, 12, 16, and 20), or 5 nM (lanes 5, 9, 13, 17, and 21) protein concentrations. Lower panel: Single nucleotide incorporations by pol IV (1 nM) were carried out for 20 min in the presence of 20 μ M individual dNTPs. M, oligodeoxynucleotide sizing markers; N^2 -dG PCL4, tetrapeptide cross-linked substrate; N^2 -dG PCL12, dodecylpeptide cross-linked substrate.

In addition to pol IV, *E. coli* possesses two other DNA damage-induced polymerases, pol II and pol V (6). Here, the abilities of pol II and pol V to synthesize DNA past γ -HOPdG, reduced γ -HOPdG, and γ -HOPdG-derived DNA–peptide cross-links have been tested by conducting primer extension experiments similar to those described above. The data revealed that pol II was strongly inhibited by all of these lesions one nucleotide prior to the site of modification (Figure 24). The blockage was less severe on the DNA substrate containing the ring-opened reduced γ -HOPdG adduct with a significant percentage of primers being extended to the end of the template (Figure 24, lanes 8 and 9). In contrast, almost no full-length products were detected in reactions using substrates that contained either γ -HOPdG (Figure 24, lanes 5 and 6) or DNA–peptide cross-links (Figure 24, lanes 11, 12, 14, and 15). When pol V was examined with the same set of modified DNAs (Figure 25), patterns of inhibition of DNA synthesis appeared to be very similar to that observed for pol II, with the only exception that in pol V-catalyzed reactions, no bypass products were detected on substrates adducted with DNA–peptide cross-links (Figure 25, lanes 8 and 10). Thus, among *E. coli* DNA polymerases, pol IV was uniquely able to tolerate N^2 -dG linked DNA–peptide cross-links *in vitro*.

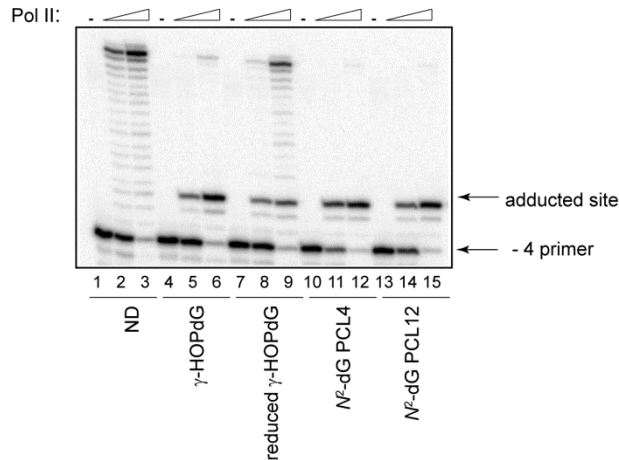


Figure 24. Replication bypass of γ -HOPdG, reduced γ -HOPdG, and DNA-peptide cross-links by *E. coli* pol II. Primer extensions by pol II were carried out for 20 min in the presence of 250 μ M dNTPs at 0.5 (lanes 2, 5, 8, 11, and 14) or 5.0 nM (lanes 3, 6, 9, 12, and 15) protein concentrations. N^2 -dG PCL4, tetrapeptide cross-linked substrate; N^2 -dG PCL12, dodecylpeptide cross-linked substrate.

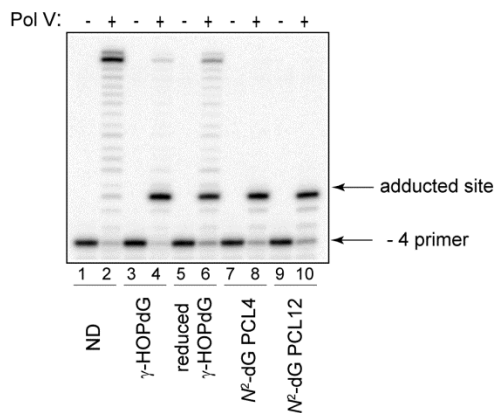


Figure 25. Replication bypass of γ -HOPdG, reduced γ -HOPdG, and DNA-peptide cross-links by *E. coli* pol V. Primer extensions by pol V (200 nM) were carried out for 20 min in the presence of 500 μ M dNTPs. N^2 -dG PCL4, tetrapeptide cross-linked substrate; N^2 -dG PCL12, dodecylpeptide cross-linked substrate.

Replication of plasmid DNA containing DNA-peptide cross-links in E. coli

Having observed replication bypass of the γ -HOPdG-derived DNA-peptide cross-links by pol IV *in vitro*, we hypothesized that this polymerase may function in such a process intracellularly. To test this hypothesis, 30-mer DNA oligodeoxynucleotides adducted with either tetrapeptide or dodecylpeptide or containing no damage were individually

inserted into a single-stranded pMS2 vector, and these vectors were used to transform the wild-type and pol IV-deficient *E. coli* cells. Following overnight selection on ampicillin-containing plates, colonies were counted, and the relative efficiency of transformation was calculated as the ratio of the number of clones originating from the adducted vectors to the number of clones originating from the ND control. The average relative efficiencies with their standard deviations obtained from three independent experiments are given in Table 3, third column. These data suggested that DNA-peptide cross-links represented a more severe block for replication in pol IV-deficient mutant than in wild-type cells. However, on the basis of our previous experience (213), it was possible that a substantial percentage of the progeny DNAs originated from ligated pMS2 vectors that did not contain the insert sequences; therefore, they should be excluded from the analyses. To evaluate the number of progeny DNAs having specific insert sequences, the following approach was utilized. A subpopulation of clones were individually grown in the 96-well plates, transferred onto Whatman 541 paper, and subjected to differential hybridization, utilizing the 5'-radiolabeled oligodeoxynucleotide probe G. This probe was designed to be complementary to the insert sequence, assuming no mutations were introduced. Additional 20-mer oligodeoxynucleotide probes, L and R, were designed to be complementary to the vector sequences located 60 and 52 nucleotides from the site of insertion. Hybridization with these probes allowed for the exclusion of the progeny DNAs with deletions involving the region of interest. Individual DNAs were isolated and analyzed further if they met the following criteria: hybridized with a mixture of L and R probes, but did not hybridize with G probe. Specifically, they were tested by cleavage with ScaI endonuclease. Because both the original pMS2 vector and the inserted DNAs

contain ScaI recognition sites, cleavage of progeny DNAs containing the insert sequences can be easily identified by the generation of DNA fragments, ~1.9 and ~3.2 kb in length. Thus, the combination of differential hybridization and analyses of isolated plasmids by cleavage with ScaI facilitated the determination of the percentage of the progeny DNAs having inserted sequences (Table 3, fifth column). Subsequently, these values were used to re-evaluate the relative efficiencies of transformation, taking into account only the transformants in which vectors with inserts, but not other products of ligation and/or intracellular DNA rearrangements, were replicated. These data indicated that relative to wild-type cells, the pol IV-deficient mutant was very inefficient in replicating the adducted vectors, thus confirming the intracellular role for pol IV in bypass of γ -HOPdG-derived DNA-peptide cross-links.

<i>E. coli</i> strain	Insert	Relative efficiency of transformation	Number of colonies tested	Colonies with inserts, %	Relative efficiency of transformation adjusted for number of colonies with inserts	Efficiency of transformation of pol IV ⁻ deficient mutant relative to wild type
Wild type	ND	1	106	97	1	
	Tetra-peptide cross-link	0.45 ± 0.04	136	85	0.39 ± 0.035	1
	Dodecyl-peptide cross-link	0.39 ± 0.15	128	93	0.37 ± 0.14	1
Pol IV ⁻	ND	1	136	98.5	1	
	Tetra-peptide cross-link	0.05 ± 0.01	67	37	0.02 ± 0.004	0.05
	Dodecyl-peptide cross-link	0.12 ± 0.07	80	56	0.07 ± 0.04	0.19

Table 3. Efficiency of *E. coli* transformation using vector DNAs containing DNA-peptide cross-links

Mutagenic properties of γ -HOPdG-mediated DNA-peptide cross-links in E. coli

Earlier reports (266,284,285) indicated that TLS past the γ -HOPdG adduct was essentially error-free in *E. coli*. Although these studies assayed bacterial strains with various genetic backgrounds and utilized different vector systems, mutations (G to T transversions) were consistently observed at less than 1% frequencies or not detected at all. In this report, we examined the potential of the γ -HOPdG-mediated DNA-peptide cross-links to cause mutations during extrachromosomal replication in *E. coli*. As described above, following intracellular replication of site specifically modified pMS2 vectors, individual clones were tested by differential hybridization using a probe that hybridized only when nonmutagenic replication bypass had occurred. Using this method, the progeny DNAs containing no mutations were readily identified. To verify the accuracy of hybridization procedure, approximately 10% of such clones were analyzed by DNA sequencing using oligodeoxynucleotide R as a primer. Among these DNAs, no clone had any sequence alteration. However, a few clones were identified that did not hybridize with probe G, but according to the ScaI cleavage analyses, they contained inserts. Targeted mutations were detected in these clones by DNA sequencing, indicating that in both the wild-type and the pol IV-deficient cells, the γ -HOPdG-mediated DNA-peptide cross-links were only marginally miscoding. Specifically, two mutations were observed in the wild-type cells: one G to A transition (caused by the tetrapeptide cross-link) and one G to T transversion (caused by the dodecylpeptide cross-link). In pol IV-deficient mutant, the only mutation found was G to C transversion (caused by the tetrapeptide cross-link).

4.5. DISCUSSION

Previous investigations have provided insights into the mechanisms by which DNA–protein cross-links are processed and removed (226). Although there have been inconsistent reports in the literature on the role of NER in the removal of these adducts, these apparent contradictions may potentially be explained by differences in both the damage-inducing agents and the assays used to assess repair capacity. With the advent of technologies to create site-specific DNA–protein and DNA–peptide adducts, a much clearer picture has emerged for the role of NER in processing of these lesions. Specifically, data in both bacterial and mammalian systems indicate that relative to DNA–protein cross-links, DNA–peptide cross-links are preferable substrates for the initiation of repair by NER proteins (227,228,272-274). These data are highly consistent with a role for proteolytic degradation of cross-linked proteins occurring prior to repair, since proteasomal inhibitors significantly reduce repair (275).

Because proteolytic processing of DNA–protein cross-links appears to be integral to the ultimate repair, these data raise the possibility that replication forks could encounter these intermediates prior to NER. Therefore, it is likely that replicative polymerases, such as pol δ and pol ϵ in mammalian cells and pol III in bacteria, would be blocked. In such a scenario, specialized TLS polymerases could be recruited to these sites. Germane to this hypothesis, the study presented herein shows that pol κ was able to catalyze high-fidelity efficient bypass of DNA–peptide cross-links, where the linkage of the peptide to DNA was via an acrolein-mediated bridge to N^2 -dG. These biochemical data suggest that pol κ contributes to the nonmutagenic bypass events during intracellular replication past N^2 -dG

DNA–peptide cross-links. Thus, the relatively accurate replication past the γ -HOPdG-mediated tetrapeptide cross-link that previously was observed in mammalian cells (213) may, at least partially, be catalyzed by pol κ . Pol κ has been shown to catalyze high-fidelity bypass of B[a]P and other bulky N^2 -dG adducts (95,100,101,276-279). Recently, we have extended the substrate repertoire of pol κ to include replication bypass of ICLs (92). In this study, DNAs were utilized containing site specifically engineered N^2 -dG- N^2 -dG ICLs that model DNA repair intermediates, hypothesized to be in a repair pathway not requiring HR. We demonstrated that pol κ could catalyze bypass of cross-linked substrates in which nucleotides 3' to the cross-link had been removed. Data were also obtained that demonstrated that loss or even reduction in cellular levels of pol κ resulted in increased cytotoxicity and chromosomal damage when cells were exposed to mitomycin C, an N^2 -dG- N^2 -dG cross-link-inducing agent.

Collectively, these data reveal a consistent pattern of pol κ being an efficient and high-fidelity enzyme in the bypass of extremely bulky N^2 -dG adducts. Relative to these and other catalytic bypass substrates, it is of interest that the cocrystal structure has been solved for the catalytic core of pol κ with a primer template complex and an incoming nucleotide (286). This structure clearly shows pol κ completely encircling the duplex DNA, using an N-terminal clasp. It was hypothesized that this structure would enhance the thermodynamic stability of the core complex, thus facilitating replication bypass. Given this tight-fitting encircling of the DNA, we hypothesized that there must be considerable flexibility in the hinge domains to allow such bulky lesions to pass through the core of the complex. Thus, it is of considerable interest to determine the structures of

additional complexes to reveal the conformational changes that must take place to permit these error-free reactions.

Our data also demonstrated that *E. coli* pol III, pol II, and pol V were all incapable of replicating past DNA–peptide cross-links as assayed herein but that pol IV was modestly efficient at the incorporation and extension steps; furthermore, the incorporation of the correct nucleotide opposite the lesions was highly preferred. However, unexpectedly, processive synthesis of pol IV was strongly inhibited beyond the site of the lesions. Such blocks were not observed with the γ -HOPdG, reduced γ -HOPdG (this study), or furfuryl N^2 -dG adducts (276). These data suggest that the ability of pol IV to continue processive synthesis is blocked via a physical obstruction of the peptide cross-link with a portion of pol IV in a location where the newly synthesized DNA exits the polymerase. Such downstream blockages have been previously observed with the HIV reverse transcriptase replicating N^2 -dG styrene oxide-modified DNAs (287,288). This blockage could be attributed directly to the interaction of α -helix H and I, tracking in the minor groove of the newly synthesized duplex DNA, such that site-directed mutagenesis of selected amino acid residues in the tracking face of α -helix H modulated the downstream pause sites (287,289). We hypothesize that similar “reading heads” of pol IV may monitor the newly synthesized duplex DNA. Insights into this mechanism await crystal and cocrystal structures of pol IV.

Although DNA synthesis past the γ -HOPdG-mediated DNA–peptide cross-links by pol IV *in vitro* was partially inhibited relative to the ND DNA, our cellular studies clearly

implicate pol IV as a major contributor to the replication bypass of these lesions *in vivo*. In its absence, we observed ~5- and 20-fold reduction in recovery of plasmids when the dodecylpeptide or tetrapeptide, respectively, was site specifically linked to the single-stranded vector DNAs, and these DNAs replicated in *E. coli* cells. Surprisingly, such cross-links appeared to be only marginally miscoding in both the wild-type and pol IV-deficient strains. In wild-type *E. coli*, mutations were observed at overall frequencies of ~1%, which is significantly less than the frequency of mutations caused by the identical tetrapeptide cross-link in mammalian cells, in which ~8% of bypass events resulted in targeted mutations (213). Interestingly, the γ -HOPdG adduct is also less miscoding in *E. coli* relative to mammalian system (266,284,285). Overall, these data give strong support for the role of DinB family polymerases in the bypass of very bulky N^2 -dG adducts.

CHAPTER 5: A COMPREHENSIVE STRATEGY TO DISCOVER INHIBITORS OF THE TRANSLESION SYNTHESIS DNA POLYMERASE κ

Kinrin Yamanaka^{1,2}, Dorjbal Dorjsuren⁴, Robert L. Eoff⁵, Martin Egli⁶, David J. Maloney⁴, Ajit Jadhav⁴, Anton Simeonov⁴, and R. Stephen Lloyd^{2,3}

¹Department of Physiology and Pharmacology, ²Center for Research on Occupational and Environmental Toxicology, and ³Department of Molecular and Medical Genetics, Oregon Health & Science University, Portland, OR 97239

⁴National Center for Advancing Translational Sciences, National Institutes of Health, Bethesda, MD 20892

⁵Department of Biochemistry and Molecular Biology, University of Arkansas for Medical Sciences, Little Rock, AR 72205

⁶Department of Biochemistry, Center in Molecular Toxicology and Vanderbilt Institute of Chemical Biology, Vanderbilt University School of Medicine, Nashville, TN 37232

5.1. PREFACE

Manuscript of this work has been submitted for review.

My contributions to this work included the conception of this project, design and performance of experiments, data analyses, and writing of the manuscript.

Dorjbal Dorjsuren, David J. Maloney, Ajit Jadhav, and Anton Simeonov contributed to conception, design, performance of experiments, and data analyses of high-throughput screening part of this project, as well as the writing of the manuscript.

Robert L. Eoff and Martin Egli provided human pol κ (residues 19-526) and contributed to the critical reading of the manuscript.

R. Stephen Lloyd contributed to the conception of this project, experimental design, the editing and critical reading of the manuscript, and provided funding and lab space for the execution of this work.

5.2. INTRODUCTION

Cells employ multiple mechanisms to repair or tolerate DNA lesions in order to maintain genomic integrity. TLS is one of the mechanisms used to tolerate unrepaired DNA lesions (2-6,290). Pol κ is a TLS polymerase that has been shown to catalyze TLS past a variety of DNA lesions, being particularly proficient in the bypass of minor groove N^2 -dG lesions, including the acrolein-derived adducts γ -HOPdG and its ring-opened reduced form, DNA-peptide cross-links, and ICLs, as well as adducts induced by activated polycyclic aromatic hydrocarbons such as BPDE (44,45,87,89,90,92-94). Importantly, pol κ has been demonstrated to be involved in the tolerance of ICLs induced by a chemotherapeutic agent, mitomycin C (92). In addition to its role in the bypass of N^2 -dG lesions, pol κ has also been shown to play a role in the processing of various UV light-induced DNA lesions (68,102,106).

Many clinically relevant chemotherapeutic agents, including mitomycin C, cisplatin, and nitrogen mustard, target tumor cells by virtue of their ability to covalently cross-link complementary DNA strands, introducing ICLs into the genome. These ICL-inducing agents are powerful chemotherapeutic agents as the ICL interferes with vital cellular processes such as DNA replication, RNA transcription, and recombination by preventing transient DNA strand separation (291-294). Therefore, although TLS is an essential process for cells to survive genotoxic stress, the ability of pol κ to bypass ICLs could limit the efficacy of these agents. Critical to this point are data demonstrating that the effectiveness of mitomycin C was increased when pol κ expression was suppressed by siRNA (92).

Germane to these observations, previous reports have suggested that pol κ may play a role in glioma development and therefore serve as a potential target for novel routes of therapies. Gliomas are the most common form of primary brain cancer and represent what is currently a generally incurable tumor in humans. These tumors are highly resistant to current treatment strategies, including chemotherapy with alkylating agents such as temozolomide, leading to median survival of patients with high-grade gliomas of only 1 year post diagnosis (295). Therefore, there is an urgent need for development of new therapies. Significantly, the level of pol κ has been shown to be upregulated in tumors from glioma patients, with its level being highly correlated with the grades of disease. Moreover, glioma patients expressing high levels of pol κ have an even poorer prognosis (107). Collectively, these data suggest a potential role for pol κ as an oncogene in glioma. Thus, the identification of small molecule inhibitors targeting pol κ may be crucial for improving the therapeutic efficacy of chemotherapeutic agents.

To the best of our knowledge, only one selective small molecule inhibitor of pol κ has been identified to date: a natural product, 3-*O*-methylfunicone (193). This compound exhibits selectivity against Y-family DNA polymerases, and importantly, among the Y-family polymerases investigated, it shows the highest potency towards pol κ at IC_{50} of 12.5 μ M. However, the utilization of 3-*O*-methylfunicone for therapeutic purposes is limited by its low potency. Additionally, given a lack of analogues and structure-activity relationship of this compound, it is unclear whether 3-*O*-methylfunicone-based agents can be developed into efficient therapeutics. Thus, in search for compounds with improved potency, a quantitative high-throughput screening (qHTS) of libraries of

bioactive molecules composed of 15,805 members was carried out. Here we report the identification of novel small molecule inhibitors of pol κ .

5.3. MATERIALS AND METHODS

Materials

1 M Tris-HCl and topoisomerase I were purchased from Invitrogen (Grand Island, NY), while Tween-20, KCl, MgCl₂, and DTT were purchased from Sigma–Aldrich (St. Louis, MO). Black 384-well and 1,536-well plates were purchased from Greiner Bio-One (Monroe, NC). [γ -³²P]ATP was obtained from PerkinElmer Life Sciences (Waltham, MA). P-6 Bio-Spin columns were obtained from Bio-Rad (Hercules, CA). T4 polynucleotide kinase and 100 bp DNA ladder were purchased from New England BioLabs (Beverly, MA). Human pol κ (residues 19-526) was purified as previously reported (96). Human pol η (residues 1-427) was purified following the same procedures as pol κ purification. Dimethyl sulfoxide (DMSO, certified ACS grade), paraformaldehyde, glacial acetic acid, crystal violet, and ethidium bromide were purchased from Fisher Scientific (Pittsburgh, PA). Clear 96-well plates and white/clear bottom 96-well plates were purchased from BD Falcon (Franklin Lakes, NJ) and Corning (Corning, NY), respectively. CellTiter-Glo Luminescent Cell Viability Assay was obtained from Promega (Madison, WI). XP-V, XP30RO cells were generously supplied by Dr. James E. Cleaver (University of California, San Francisco, San Francisco, CA).

Oligodeoxynucleotides synthesis

The three oligodeoxynucleotides used in the qHTS (see below under *qHTS*) were purchased from Biosearch Technologies, Inc., (Novato, CA). Control unadducted

oligodeoxynucleotides and an oligodeoxynucleotide adducted with acrolein-derived ring-opened reduced form of γ -HOPdG were the generous gifts of Dr. Carmelo J. Rizzo (Vanderbilt University, Nashville, TN).

qHTS

Fluorogenic substrate

The substrate used in qHTS was made by the annealing of unlabeled oligodeoxynucleotide primer and TAMRA-labeled reporter strand, respectively, to oligodeoxynucleotide template labeled with BHQ-2 as originally described by Dorjsuren *et al.* (196). The annealing mixture of unlabeled primer, TAMRA-labeled reporter, and BHQ-2-labeled template in buffer containing 50 mM Tris-HCl, pH 8.0, 100 mM NaCl, and 5 mM MgCl₂ was heated at 95°C for 5 min and allowed to cool gradually to room temperature. The substrate was then stored at -20°C as 50 μ M stock.

Compound libraries

The screening collection of 15,805 members included the following libraries with the number of compounds indicated in parentheses: NCGC Pharmaceutical Collection (NPC) (296), MicroSource Spectrum collection (2,031), TimTec natural products (400), the LOPAC¹²⁸⁰ collection from Sigma–Aldrich (1280), Tocris (1624), Prestwick (1597), BioMol (1943), Pharmacopeia (1648), and NCGC chemistry analogues and several additional small-size collections of bioactives.

Strand displacement reactions in 384-well and 1,536-well plates

The reactions in 384-well plate were carried out in 50 mM Tris-HCl, pH 8.0, 40 mM NaCl, 0.01% Tween-20, and 1 mM DTT. 7.5 μ l of solution containing pol κ and MgCl₂ at final concentration of 10 nM and 2 mM, respectively was added to the plate. The

strand displacement reactions were initiated by the addition of 2.5 μ l of solution containing 50 nM fluorogenic substrate and 100 μ M dTTP. The kinetic fluorescence read-out (excitation and emission wavelengths of 525 nm and 598 nm, respectively) was taken immediately with Infinite® M200 plate reader (Tecan, Durham, NC). The reactions in 1,536 plates were carried out as described below under qHTS assay protocol.

qHTS assay protocol

qHTS was performed in 50 mM Tris-HCl, pH 8.0, 40 mM NaCl, 1 mM MgCl₂, 0.01% Tween-20, 2 mM DTT, and 100 μ M dTTP. 3 μ l of reagents (buffer as negative control and pol κ in the remaining plate at 10 nM final concentration) were dispensed by Flying Reagent Dispenser™ (FRD) (Beckman Coulter, Inc., Fullerton, CA) into a 1,536-well plate. Compounds were delivered as 23 nl in DMSO solution via pintool transfer; vehicle-only control consisted of 23 nl DMSO. The plate was incubated for 15 min at room temperature, and then 1 μ l of substrate (50 nM final concentration) was added to initiate the reaction. The plate was immediately transferred into ViewLux reader for kinetic fluorescence data collection (excitation and emission wavelengths of 525 nm and 598 nm, respectively).

Radioactive gel-based primer extension assays

The reactions were carried out in the buffers containing 25 mM Tris-HCl, pH 7.5, 8 mM MgCl₂, 10% glycerol, 100 μ g/ml BSA, and 5 mM DTT. Final concentration of pol κ , pol η , or pol ι in the reaction was 0.25 nM, 1 nM, or 2.5 nM, respectively. In this assay, each polymerase was preincubated with the compound for 15 min at room temperature. Primer extensions were then initiated by the addition of DNA substrate at final concentration of 5 nM and carried out for 30 min at room temperature in the presence of

100 μ M dCTP and dGTP. The reactions were terminated by the addition of an equal volume of a dye solution containing 95% (v/v) formamide, 10 mM EDTA, 0.03% (w/v) xylene cyanol, and 0.03% (w/v) bromophenol blue. Reaction products were separated through a 15% acrylamide gel containing 8 M urea and visualized with a PhosphorImager screen. The ratio of extended primer to the total amount of primer was measured using ImageQuant 5.2 software to calculate the percentage of primer extended. IC₅₀ values were determined by fitting the data to variable slope four-parameter equations using GraphPad Prism 5.

Plasmid DNA relaxation assay

A total of 0.5 μ g of supercoiled plasmid DNA was preincubated with ethidium bromide or candesartan cilexetil at concentrations indicated in figure legends for 15 min at room temperature. Subsequently, 1 unit of topoisomerase I was added, and the reactions were carried out for 30 min at 37°C. The reactions were terminated by the addition of 1% SDS and 55 mM EDTA (final concentrations). Plasmid DNA was then extracted by phenol-chloroform-isoamylalcohol (25:24:1, v/v), followed by diethyl ether, and run on 1% agarose gel at 4°C overnight. The gel was stained with ethidium bromide (0.5 μ g/ml) for visualization.

DNA intercalation assay

Candesartan cilexetil or ethidium bromide was incubated with 1.5 nmol of double-stranded DNA ladder for 15 min at room temperature in the buffer containing 50 mM Tris-HCl, pH 8.0, 0.01% Tween-20, 1 mM DTT, and 40 mM NaCl. The reaction mixtures were run on 1% agarose gel and stained with ethidium bromide (0.5 μ g/ml) for

visualization. The amounts of candesartan cilexetil or ethidium bromide used for the reactions were indicated in figure legends.

Cell survival assays

Cell survival assays were carried out using crystal violet assays and CellTiter-Glo Luminescent Cell Viability Assays. In crystal violet assays, XP30RO cells were plated into clear 96-well plates at a density of 8000 cells/ml and incubated overnight at 37°C, 5% CO₂. The cells were treated with (1) inhibitor alone for 6 hrs or (2) UV alone or (3) inhibitor alone for 6 hrs followed by UV irradiation. After 2 days, cells were fixed with 4% paraformaldehyde and stained with 0.5% crystal violet dye. The dye was dissolved in 10% acetic acid and absorbance measurement was taken at OD₅₉₅ nm with Infinite® M200 plate reader. For the CellTiter-Glo Luminescent Cell Viability Assays, the same procedures as crystal violet assays were used except that white/clear bottom 96-well plates were used and cell viability was measured following manufacturer's recommendations. The concentration of candesartan cilexetil and the dose of UV were indicated in figure legends.

5.4. RESULTS

Development of TAMRA/BHQ-2 based strand displacement assays in 384- and 1,536-well plates using pol κ (residues 19-526)

A HTS assay utilizing TAMRA/BHQ-2 system to examine enzymatic activity of several DNA polymerases has been previously developed (Figure 26 and (196)). However, in this report, full-length pol κ from Enzymax, LLC was used. In order to determine whether pol κ (residues 19-526) was also amenable to this assay, the same strand displacement

reactions were carried out initially in 384-well plates. As shown in Figure 27A, a robust increase in fluorescence signal was observed in the presence of pol κ , while minimal fluorescence signal was maintained in the absence of pol κ . Similar results were obtained using 1,536-well plates (Figure 27B), indicating that HTS could be conducted with our enzyme using this fluorescence-based assays in 1,536-well plate format for the discovery of small molecule inhibitors of pol κ .

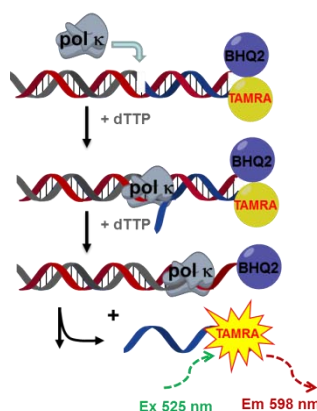


Figure 26. Principle of the fluorescence-based polymerase-catalyzed strand displacement assay. Pol κ -catalyzed DNA synthesis displaces TAMRA-labeled reporter strand. This process relieves the quenching effect of BHQ-2, leading to an increase in fluorescence signals.

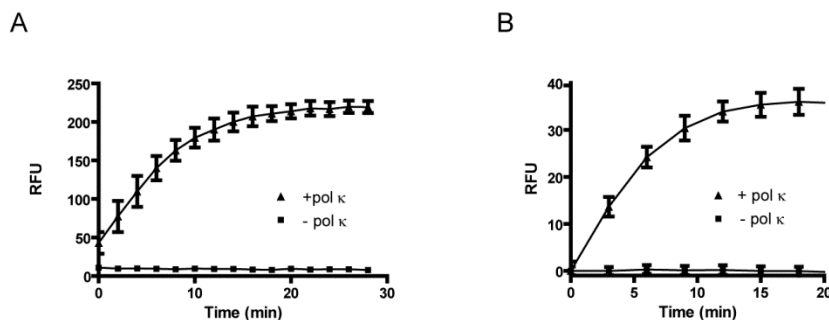


Figure 27. Miniaturized HTS assay. Reaction time course in (A) 384-well plate and (B) 1,536-well plate. The data in panel A were obtained from three independent experiments, and error bars represent standard deviations. Averages and standard deviations shown in panel B represent data from 32 replicate wells.

Stability and quality of TAMRA/BHQ-2 based strand displacement assays

Since assay stability is crucial for HTS, it is necessary to investigate the stability of reagents to be used. Thus, strand displacement reactions were performed either with fresh reagents or those stored at 4°C for various periods of time (3, 6, or 9 hrs). The results showed that both in the absence and presence of pol κ , the fluorescence signals remained constant upon reagent storage for at least 9 hrs (Figure 28A).

Additionally, HTS assays need to be of high quality. Thus, Z' factor was measured. Z' factor is defined as $Z' = 1 - (3\sigma_{c+} + 3\sigma_{c-}) / |\mu_{c+} - \mu_{c-}|$ where σ_{c+} and σ_{c-} are standard deviation of positive control and negative control, respectively, and μ_{c+} and μ_{c-} are mean signal of positive control and negative control, respectively. As evident from this equation, Z' factor assesses assay signal dynamic range, as well as data variation associated with the measurements of both the positive control and negative control samples, and the maximum Z' factor possible is 1.0, while values of greater than 0.5 are considered an indication of a highly stable, good quality screening assay (297). The results showed that high Z' factor of >0.75 was maintained (Figure 28B). Collectively, these results demonstrated that this assay is suitable for HTS.

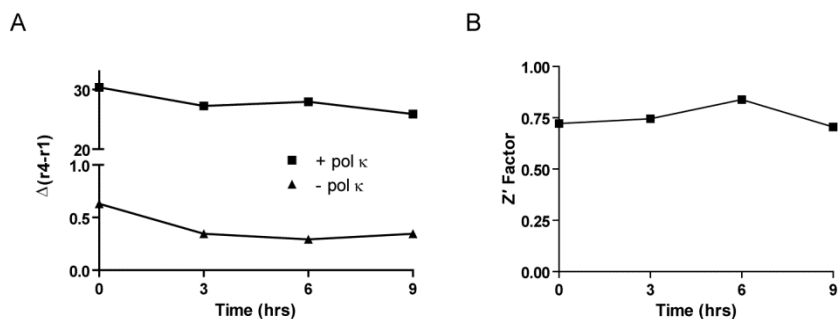


Figure 28. Reagent stability (A) and quality (B) of strand displacement assay. (A) Reagents at working concentrations were stored at 4°C for 0, 3, 6, or 9 hrs, and subsequently, strand displacement reactions were carried out. The fluorescence signals obtained at each time point during 9 min reactions were shown on y-axis. r1: fluorescence signal measured immediately after the reaction was initiated. r4: fluorescence signal measured 9 min after the reaction was initiated. (B) Excellent Z' factor of >0.75 was obtained at each time point.

qHTS

To discover novel inhibitors of pol κ and also to further validate our HTS assay on a robotic system, we carried out TAMRA/BHQ-2-based strand displacement assay (Figure 26 and (196)) in 1,536-well plate format.

The library of bioactive small molecules was tested as seven-point dilution series, with the final concentrations ranging from 2.9 nM to 57 μ M. The statistical performance of the screening assay as expressed by its Z' factor remained consistently high with only few deviations, at an average of 0.85 (Figure 29A).

The concentration-response screen paradigm used here (298) allowed for calculation of an inhibitory potency IC_{50} value for each positive hit in the primary screen, as well as an evaluation of the shape and other characteristics of the concentration response curve. A total of 60 hits displaying full concentration-response curves and IC_{50} values of less than 50 μ M were identified (the qHTS results are available in PubChem under Assay Identifier 588579, <http://pubchem.ncbi.nlm.nih.gov/> and Table 4), and concentration-response curves of representative top hits are shown in Figure 29B. The results from

these experiments were combined with the radioactive gel-based secondary primer extension assay described below in order to nominate a small subset of hits for detailed characterization.

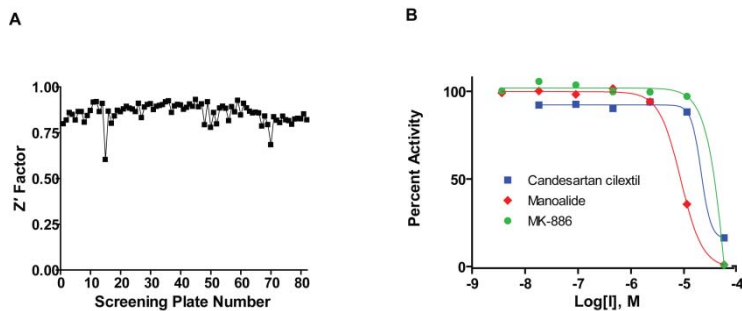


Figure 29. Summary of results from qHTS. (A) Excellent Z' factor of >0.75 was maintained throughout the screen. (B) Concentration-response curves of top hits derived from the screen.

Index	Sample ID	Gel Assay - % Inhibition at 80 μ M	qHTS IC ₅₀ (μ M)	qHTS % Inhibition at 57 μ M	Followup Comment
1	NCGC00015040-05	100%	0.12	95%	Used as a control, pan-DNA-enzyme inhibitor
2	NCGC00025307-01	100%	1.4	98%	Deprioritized - Undesirable functionality
3	NCGC00160408-01	100%	38	96%	Deprioritized - Promiscuous hit
4	NCGC00162249-02	100%	30	96%	**Selected for further followup**
5	NCGC00163463-01	100%	9.5	99%	**Selected for further followup**
6	NCGC00095123-01	98%	32	84%	**Selected for further followup**
7	NCGC00012520-01	82%	25	56%	Sample not available in sufficient quantity
8	NCGC00011126-01	65%	32	95%	Sample not available in sufficient quantity
9	NCGC00011665-01	52%	25	89%	Sample not available in sufficient quantity
10	NCGC00162223-02	100%	5.3	98%	Deprioritized - Promiscuous hit
11	NCGC00159481-02	96%	35	85%	Deprioritized - Undesirable functionality
12	NCGC00159698-01	100%	14	99%	Sample not available in sufficient quantity
13	NCGC00160033-01	100%	45	97%	Sample not available in sufficient quantity
14	NCGC00159834-01	97%	40	94%	Sample not available in sufficient quantity
15	NCGC00025080-01	92%	1.8	100%	Deprioritized - Undesirable functionality
16	NCGC00167823-01	77%	19	86%	Deprioritized - Promiscuous hit
17	NCGC00161415-01	76%	7.9	97%	Deprioritized - Promiscuous hit
18	NCGC00094270-02	73%	8.9	97%	Deprioritized - Promiscuous hit
19	NCGC00011768-01	58%	14	95%	Sample not available in sufficient quantity
20	NCGC00010749-01	49%	32	81%	Sample not available in sufficient quantity
21	NCGC00010004-01	48%	28	92%	Sample not available in sufficient quantity
22	NCGC00011866-01	34%	40	71%	Deprioritized - Weak in gel assay
23	NCGC00163453-01	15%	0.63	100%	Deprioritized - Promiscuous hit
24	NCGC00161677-01	100%	3.6	96%	Sample not available in sufficient quantity
25	NCGC00163348-01	100%	0.32	96%	Deprioritized - Promiscuous hit
26	NCGC00163464-01	100%	27	98%	Deprioritized - Undesirable functionality
27	NCGC00164581-01	100%	8.9	95%	Deprioritized - Undesirable functionality
28	NCGC00095922-01	76%	1.1	99%	Deprioritized - Undesirable functionality
29	NCGC00165741-01	71%	3.0	100%	Deprioritized - Weak in gel assay
30	NCGC00094031-02	68%	2.8	98%	Deprioritized - Promiscuous hit
31	NCGC00094857-01	59%	32	77%	Deprioritized - Promiscuous hit
32	NCGC00142585-02	45%	11	75%	Deprioritized - Weak in gel assay
33	NCGC00018292-04	43%	0.79	98%	Deprioritized - Undesirable functionality
34	NCGC00065934-02	25%	35	68%	Deprioritized - Weak in gel assay
35	NCGC00010079-01	18%	25	69%	Sample not available in sufficient quantity
36	NCGC00016050-04	100%	0.13	97%	Deprioritized - Undesirable functionality
37	NCGC00161304-02	100%	3.2	99%	Deprioritized - Undesirable functionality
38	NCGC00163605-01	100%	0.47	93%	Deprioritized - Promiscuous hit
39	NCGC00164537-01	100%	0.24	100%	Deprioritized - Undesirable functionality
40	NCGC00094959-03	90%	0.25	98%	Deprioritized - Undesirable functionality
41	NCGC00017245-02	88%	0.13	98%	Deprioritized - Undesirable functionality
42	NCGC00024695-01	88%	0.35	97%	Deprioritized - Undesirable functionality
43	NCGC00095723-01	83%	0.18	98%	Deprioritized - Undesirable functionality
44	NCGC00015384-02	72%	0.16	98%	Deprioritized - Undesirable functionality
45	NCGC00016054-04	70%	0.34	95%	Deprioritized - Undesirable functionality
46	NCGC00016467-01	64%	0.27	98%	Deprioritized - Undesirable functionality
47	NCGC00094901-01	61%	1.6	93%	Deprioritized - Promiscuous hit
48	NCGC00021152-02	58%	32	82%	Deprioritized - Undesirable functionality
49	NCGC00096056-01	57%	22	93%	Deprioritized - Weak in gel assay
50	NCGC00024700-01	47%	1.8	99%	Deprioritized - Undesirable functionality
51	NCGC00165811-01	42%	30	100%	Deprioritized - Undesirable functionality
52	NCGC00166170-01	13%	15	92%	Deprioritized - Undesirable functionality
53	NCGC00010056-01	0%	25	59%	Inactive in gel assay
54	NCGC00015950-02	0%	11	85%	Inactive in gel assay
55	NCGC00166399-01	0%	7.5	98%	Inactive in gel assay
56	NCGC00010341-01	ND	25	86%	Interfered with the migration of the DNA into the gel
57	NCGC00011382-01	ND	25	93%	Interfered with the migration of the DNA into the gel
58	NCGC00011739-01	ND	32	81%	Interfered with the migration of the DNA into the gel
59	NCGC00011886-01	ND	22	93%	Interfered with the migration of the DNA into the gel
60	NCGC00165782-01	ND	19	91%	Interfered with the migration of the DNA into the gel

Table 4. Summary of IC₅₀s of top 60 hits obtained from qHTS and radioactive gel-based primer extension assays using ND oligodeoxynucleotides¹

¹In both qHTS and the radioactive gel-based primer extension assays, values of % inhibition that are over 100% and below 0% are presented as 100% and 0%, respectively. ND: not determined.

Candesartan cilexetil, manoalide, and MK-886 inhibit pol κ -catalyzed primer extensions on ND DNA in vitro

In order to confirm the 60 top hits identified through qHTS by an orthogonal detection method, radioactive gel-based primer extension assays were performed. Initially, the assay was carried out at 80 μM of each compound in order to identify false-positive compounds that were inactive against pol κ even at this high concentration (Table 4). Using this assay, 3 compounds were shown to have minimal effect on pol κ and thus were not considered in further analyses. Additionally, 5 compounds interfered with the migration of the DNA into the gel, likely due to the precipitation of the compounds in the electrodes of the gel-running apparatus, and could not be assayed. Thus, these 8 compounds were excluded from further analyses. The remaining 52 compounds showed a range of inhibitory activity against pol κ at 80 μM . Based on the compounds' activity in the radioactive gel-based primer extension assay, the presence of reactive functional group(s) in the compounds, their tendency to appear as actives in a large number of internally-conducted screens (i.e., their promiscuity), and the commercial availability of the compounds to enable further studies, candesartan cilexetil, manoalide, and MK-886 were determined to be lead inhibitors, and the IC_{50} values of these compounds were examined by primer extension assays with various concentrations of the compounds. The results showed that these compounds inhibited pol κ activity in a dose-dependent manner, and the IC_{50} s of candesartan cilexetil, manoalide, and MK-886 on ND DNA were $9.2 \pm 0.5 \mu\text{M}$, $3.4 \pm 0.9 \mu\text{M}$, and $13 \pm 1.7 \mu\text{M}$, respectively (Figure 30 and Table 5). Despite significant differences between the fluorescence substrate-based HTS method and the

radioactive gel-based primer extension assay, IC_{50} s obtained from qHTS and primer extension assay were found to be well-correlated (Table 5).

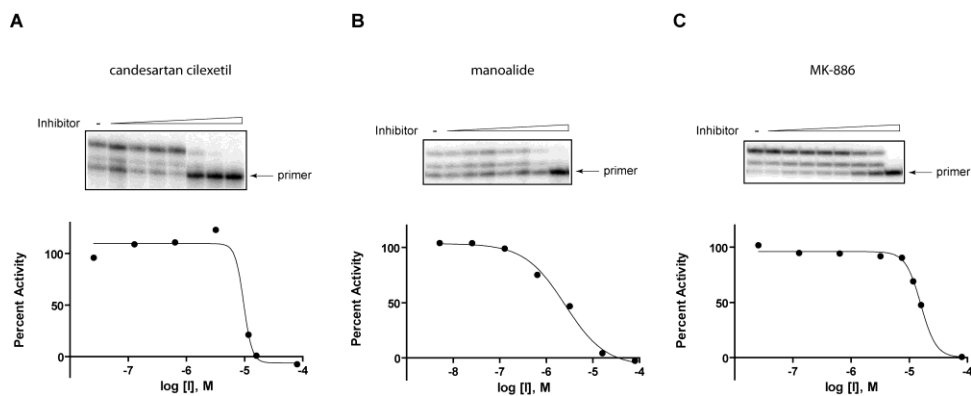


Figure 30. Dose-response activities of (A) candesartan cilexetil, (B) manoalide, and (C) MK-886 on pol κ -catalyzed primer extension reactions on ND DNAs. Representative data from three independent experiments are shown. The gels shown on the top panel were used to generate dose-response curves shown on the bottom panel.

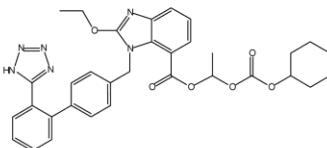
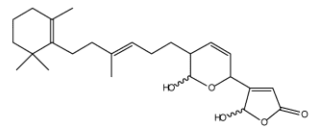
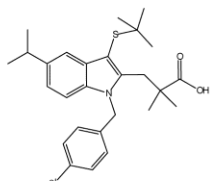
Inhibitor Name	qHTS: IC_{50} (μ M)	gel: ND: IC_{50} (μ M)	gel: ring-opened reduced form of γ -HOPdG: IC_{50} (μ M)
<p>candesartan cilexetil</p> 	32	9.2 ± 0.5	11 ± 1.5
<p>manoalide</p> 	9.5	3.4 ± 0.9	5.6 ± 0.9
<p>MK-886</p> 	30	13 ± 1.7	14 ± 0.9

Table 5. Summary of IC_{50} s of candesartan cilexetil, manoalide, and MK-886 obtained from qHTS and radioactive gel-based primer extension assays using oligodeoxynucleotides unadducted or adducted with acrolein-derived ring-opened reduced form of γ -HOPdG. In primer extension assays, three independent experiments were carried out, and IC_{50} s are shown as average \pm standard error.

Candesartan cilexetil, manoalide, and MK-886 inhibit pol κ -catalyzed TLS past acrolein-derived ring-opened reduced form of γ -HOPdG lesions in vitro

The primary role of pol κ is to bypass DNA lesions. Therefore, it was critical to investigate the capability of the lead compounds to inhibit lesion bypass activity of pol κ . Radioactive gel-based primer extension reactions were carried out using DNA substrate containing site-specific acrolein-derived ring-opened reduced form of γ -HOPdG, a lesion that pol κ can efficiently bypass *in vitro* (93). As shown in Figure 31 and Table 5, all these compounds were capable of inhibiting pol κ -catalyzed TLS past the lesion in a dose-dependent manner with similar potency as they inhibited pol κ -catalyzed primer extensions on ND DNA. The IC_{50} s obtained from these reactions were $11 \pm 1.5 \mu\text{M}$ for candesartan cilexetil, $5.6 \pm 0.9 \mu\text{M}$ for manoalide, and $14 \pm 0.9 \mu\text{M}$ for MK-886.

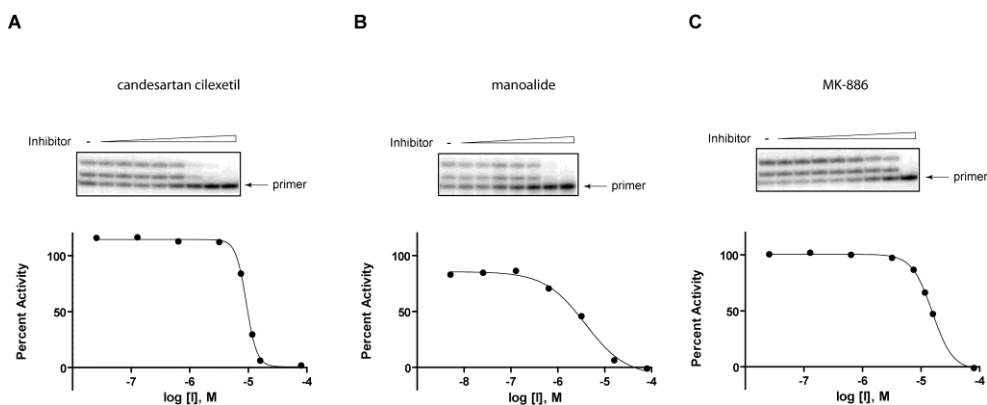


Figure 31. Dose-response activities of (A) candesartan cilexetil, (B) manoalide, and (C) MK-886 on pol κ -catalyzed primer extension reactions on DNAs adducted with acrolein-derived ring-opened reduced form of γ -HOPdG. Representative data from three independent experiments are shown. The gels shown on the top panel were used to generate dose-response curves shown on the bottom panel.

Candesartan cilexetil enhance UV-induced cellular toxicity

In order to demonstrate that at least a subset of these small molecule inhibitors could exhibit biological efficacy in a cytotoxicity assay, the following strategy was developed.

Previous reports have shown that XP-V cells had 3.5- to 5-fold enhanced sensitivity to UV irradiation when pol κ was depleted by siRNA versus control cells (68). Based on these data, we hypothesized that pol κ inhibitor should be capable of enhancing the cytotoxic effect of UV in XP-V cells. To test this hypothesis, XP-V cells were treated with candesartan cilexetil or UV alone, or in combination, and assayed for cell viability using a crystal violet staining assay. As shown in Figure 32, the inhibitor slightly potentiated the cytotoxicity of UV at higher UV doses (4.5 and 7.5 J/m²). The assay was repeated also with the CellTiter Glo Luminescent Cell Viability Assay, which measures ATP content of the cells, and comparable results were obtained (Figure 33). These data suggest that candesartan cilexetil may inhibit intracellular pol κ . Cell viability was also investigated with manoalide and MK-886. Although both compounds could inhibit pol κ activity *in vitro*, they failed to enhance UV toxicity in these cells under the conditions investigated.

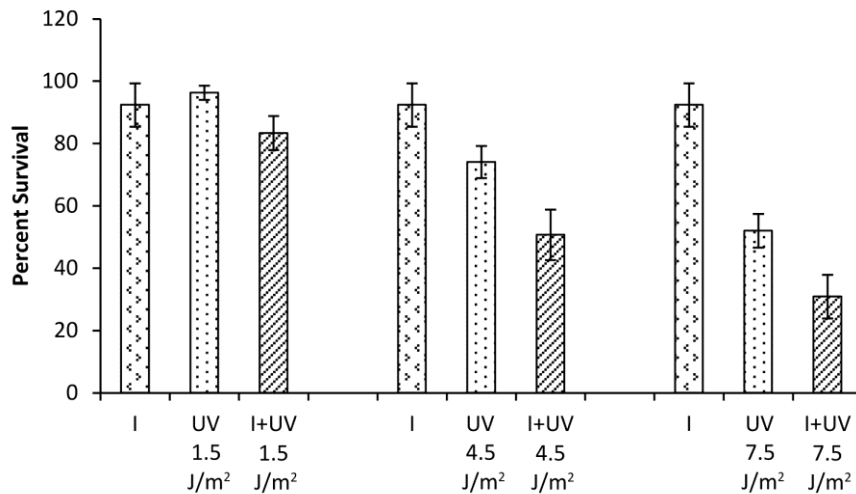


Figure 32. The effect of candesartan cilexetil on cytotoxicity of UV-treated XP30RO cells using crystal violet staining assay. Cells were treated with 24 μ M (the concentration that minimally affects cell survival) of candesartan cilexetil alone, UV alone at 1.5 J/m², 4.5 J/m², or 7.5 J/m², or in combination. Percent survival was calculated by normalizing the data using the cell survival of untreated cells. The data were obtained from three independent experiments. Error bars represent standard deviations. I: candesartan cilexetil.

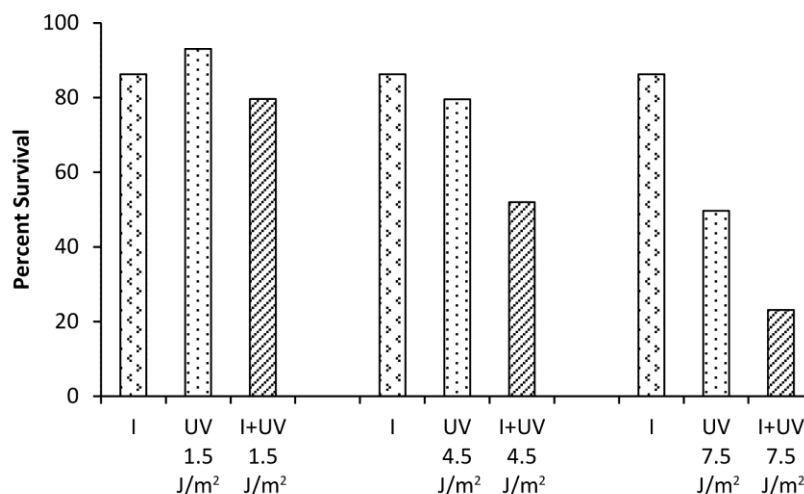


Figure 33. The effect of candesartan cilexetil on cytotoxicity of UV-treated XP30RO cells using CellTiter Glo Luminescent Cell Viability Assay. Cells were treated with 24 μM of candesartan cilexetil alone, UV alone at 1.5 J/m^2 , 4.5 J/m^2 , or 7.5 J/m^2 , or in combination. Percent survival was calculated by normalizing the data using the cell survival of untreated cells. I: candesartan cilexetil.

Candesartan cilexetil does not bind to or intercalate into DNA

It is possible that the compounds inhibited pol κ activity by blocking the access of this enzyme to DNA. As mentioned above, only candesartan cilexetil exhibited cellular effect against pol κ . Thus, the property of this compound to bind to or intercalate into DNA was investigated. The results of plasmid DNA relaxation assay showed that the ability of topoisomerase I to relax plasmid DNA was inhibited by ethidium bromide control (a well-known DNA intercalator) as demonstrated by downward shift of bands on the gel. On contrary, majority of plasmid DNA remained in relaxed topology in the presence of candesartan cilexetil (Figure 34).

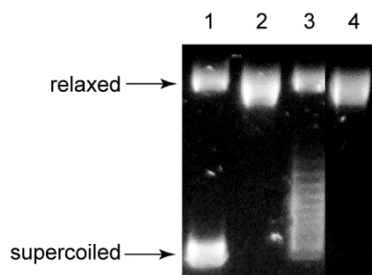


Figure 34. Candesartan cilexetil did not interfere with the activity of topoisomerase I to relax plasmid DNA. Candesartan cilexetil or ethidium bromide was incubated with 0.5 μg of supercoiled plasmid DNA, and the reaction products were run on 1% agarose gel and stained with ethidium bromide. Lane 1: No compound and topoisomerase I. Lane 2: Topoisomerase I only. Lane 3: 2 μM ethidium bromide. Lane 4: 2 μM candesartan cilexetil. Samples in lanes 3 and 4 contained topoisomerase I.

Additionally, as shown in Figure 35, upon mixing of candesartan cilexetil or ethidium bromide, with double-stranded DNA, the bands shifted upwards in the presence of ethidium bromide, while no difference in DNA migration pattern was observed with candesartan cilexetil compared to control. Collectively, these data suggest that candesartan cilexetil may not bind to or intercalate into DNA

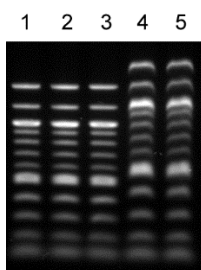


Figure 35. The non-DNA-intercalating property of candesartan cilexetil. Candesartan cilexetil or ethidium bromide was incubated with double-stranded DNA ladder, and the reaction products were run on 1% agarose gel and stained with ethidium bromide. Lane 1: No compound. Lane 2: 0.75 nmol of candesartan cilexetil was incubated with 1.5 nmol DNA. Lane 3: 3 nmol of candesartan cilexetil was incubated with 1.5 nmol DNA. Lane 4: 0.75 nmol of ethidium bromide was incubated with 1.5 nmol DNA. Lane 5: 3 nmol of ethidium bromide was incubated with 1.5 nmol DNA.

The specificity of candesartan cilexetil against Y-family TLS polymerases

In order to further validate the ability of candesartan cilexetil to inhibit pol κ activity, the specificity of this compound toward pol κ was examined by radioactive gel-based primer extension assays with two other human Y-family TLS polymerases, pol η and pol ι on ND template. The results showed that candesartan cilexetil also inhibited the activity of these two enzymes with similar potency (IC_{50} of $11.2 \pm 1.0 \mu\text{M}$ for pol η and $6.2 \pm 0.6 \mu\text{M}$ for pol ι).

5.5. DISCUSSION

Despite the potential significance of targeting pol κ in cancer therapeutics, limited investigations have been reported concerning the discovery of pol κ inhibitors. Although compounds with inhibitory activity against pol κ have been identified, most of these inhibitors were identified as part of screens of natural products against any DNA polymerase and their therapeutic potential may be limited primarily due to either low potency or poor selectivity. For example, a derivative of a natural product kohamaic acid, (1S*,4aS*,8aS*)-17-(1,4,4a,5,6,7,8,8a-octahydro-2,5,5,8a-tetramethylnaphthalen-1-yl)heptadecanoic acid and a derivative of vitamin K₂ and vitamin K₃, MK-2, have been shown to inhibit pol κ activity with IC_{50} s of 7.2 μM and 35.3 μM , respectively (194,299). Pol κ activity is also inhibited by C12:0-Acyl juglone and C18:1-Acyl juglone with an IC_{50} s of 6.8 μM and 8.1 μM , respectively (300). Glycyrrhetic acid is another compound that inhibits pol κ activity (IC_{50} of 15.8 μM) (301). Penicilliois A and B are other natural products that inhibit pol κ ; however, the activities of these compounds are higher against mouse pol ι than pol κ with an IC_{50} against pol ι of 19.8 μM and 32.5 μM for penicilliois

A and B, respectively (195). Collectively, these compounds have low potency as well as poor selectivity against pol κ , since they inhibit many other DNA polymerases with similar potency as they inhibit pol κ . Additionally, although penta-1,2,3,4,6-*O*-galloyl-beta-D-glucose exhibits nanomolar potency against pol κ (IC₅₀ of 30 nM), it is more potent against pol α (IC₅₀ of 13 nM) (302). Thus, the value of this compound as a pol κ inhibitor is lowered by poor selectivity. In contrast to these compounds, 3-*O*-methylfunicone has been determined to exhibit high selectivity against pol κ . However, its low potency (IC₅₀ of 12.5 μ M) limits its utilization as a pharmaceutical or as a tool compound to probe pol κ biology (193). Collectively, these studies emphasize the importance of the identification of pol κ inhibitors with improved potency.

Here we reported the discovery of small molecule inhibitors of pol κ by qHTS utilizing TAMRA/BHQ-2 fluorescence system. The top 60 hits were selected and validated in traditional radioactive primer extension assays with electrophoretic separation. All these hits except 3 compounds inhibited pol κ activity at the top concentration tested (80 μ M), demonstrating the insensitivity of the HTS assay to false positives elicited by interference intrinsic to fluorescence-based assays.

After elimination of weak inhibitors, compounds with potentially reactive functionalities or other undesirable chemical features, as well as compounds which there were no convenient commercial sources, further validation of the remaining three lead compounds, candesartan cilexetil, manoalide, and MK-886, by radioactive gel-based primer extension assays revealed that these compounds were capable of inhibiting the ability of pol κ to copy DNA template unadducted or adducted with acrolein-derived ring-opened reduced

form of γ -HOPdG in a dose-dependent manner with similar potency. Since the predominant role of pol κ is in DNA lesion bypass, these results demonstrated the ability of these compounds to inhibit the biologically relevant activity of pol κ .

It is interesting to note that the slope of dose-response curve of candesartan cilexetil is very steep. This could be due to an inhibitor binding to multiple sites of pol κ , an inhibitor phase transition, such as inhibitor precipitation or colloid formation, and stoichiometric inhibition caused by high pol κ concentration relative to the K_d value of the inhibitor (303). Further investigations are required to determine which of these three mechanisms result in this steep slope.

In order to assess the ability of lead compounds to target intracellular pol κ , cell survival assays were carried out by exposing cells to the combination of pol κ inhibitors and UV. The results showed that candesartan cilexetil could potentiate cellular toxicity induced by UV in XP-V cells. It cannot be ruled out that the cellular effect of candesartan cilexetil may be partly due to its effect on other proteins in addition to pol κ , including pol η and pol ι , since the compound also inhibited the activities of these polymerases *in vitro*; however, our *in vitro* results clearly show that pol κ is inhibited by this compound. Additionally, it has been shown that the depletion of either pol η or pol ι in XP-V cells did not enhance UV cytotoxicity (68). Moreover, candesartan cilexetil is known to function as an effective angiotensin II receptor blocker and is indicated for the treatment of hypertension (304). To the best of our knowledge, the candesartan cilexetil-mediated inhibition of angiotensin II receptor has not been shown to result in increased UV

sensitivity of XP-V cells. Collectively, these observations suggest that pol κ is one of, if not the only, the proteins in the cells that are inhibited by this compound.

Although manoalide and MK-886 could inhibit pol κ activity *in vitro*, they were unable to enhance UV-induced toxicity in XP-V cells under the conditions tested. Both manoalide and MK-886 have anti-inflammatory activity; manoalide is well-known as a non-specific phospholipase A₂ antagonist (305-307), and MK-886 inhibits leukotriene synthesis by blocking 5-lipoxygenase-activating protein (308). The reason for the inability of these compounds to potentiate UV cytotoxicity could be due to their significantly lower binding affinity to intracellular pol κ relative to other cellular targets. Alternatively, these compounds may take a long time to enter the cells and bind to pol κ . Moreover, it is possible that only a small fraction of intracellular pol κ is inhibited by these compounds and the remaining pol κ may be sufficient to process UV-induced DNA lesions, resulting in unaltered cellular sensitivity to UV. Given the presence of multiple back-up TLS polymerases, nearly-complete inhibition of the activity of all intracellular pol κ may be essential for cells to present an apparent phenotype. Further understanding of the inability of these compounds to target intracellular pol κ could involve structure-activity relationship analyses. In fact, several structural analogues of these compounds exist such as secomanoalide and luffariellolide for manoalide (305) and L538,916 for MK-886 (309), thus enabling such analyses.

In summary, we presented herein the discovery of small molecules that could inhibit pol κ activity *in vitro* and the identification of candesartan cilexetil as a compound that could

enhance cell toxicity induced by UV in XP-V cells, likely not by interfering with DNA. Although the current study has not resulted in the identification of compounds exhibiting a large improvement in potency compared to 3-*O*-methylfunicone, the identification of novel chemotypes with established drug properties targeting pol κ validates our HTS platform and sets the stage for exploration of significantly larger diverse compound collections. Thus, these studies would move the research effort one step closer to the development of pol κ -targeted novel combination cancer therapeutics.

6. SUMMARY AND CONCLUSION

The literature review in the first Chapter of this dissertation highlights the significance of understanding the function of each TLS polymerase, particularly, their potential roles in tumorigenesis and chemotherapeutic resistance. The importance of the development of inhibitors targeting TLS polymerases for new cancer therapy is also emphasized.

Since pol ν is a newly discovered DNA polymerase that has unknown biological function, especially in regard to whether it has a role in TLS, in the second Chapter, an investigation of the substrate specificity of pol ν in TLS was discussed. Here, it was shown that pol ν can bypass exceptionally large acrolein-induced major groove N^6 -dA DNA-peptide- and DNA-DNA cross-links. Another interesting finding was that pol ν was blocked by chemically identical minor groove N^2 -dG DNA-peptide- and DNA-DNA cross-links. These studies are the first report showing that pol ν could be involved in TLS when genomic replication is blocked by extremely large major groove DNA lesions.

Reaction of bifunctional electrophiles with DNA in the presence of peptides can result in DNA-peptide cross-links. Specifically, the linkage can be formed in the major groove or minor groove of DNA via N^6 -dA or N^2 -dG, respectively. In order to gain insight into how humans process these DNA lesions, in Chapter 3 and Chapter 4, studies examining the identity of DNA polymerases involved in the replication bypass of these lesions using *E. coli* as a model organism are discussed. In this investigation, we discovered that both *in vitro* and *in vivo*, pol I or pol IV functions to catalyze DNA synthesis past N^6 -dA- or N^2 -

dG-linked peptide cross-links, respectively. As described in Chapter 2, biochemical studies showed that in human, pol ν , a polymerase belonging to the same A family as pol I, can bypass N^6 -dA-linked peptide cross-links. Additionally, pol κ , a human orthologue of pol IV, was shown to carry out replication bypass of N^2 -dG-linked peptide cross-links *in vitro* (Chapter 4). Although no *in vivo* evidence is currently available showing that these human enzymes are responsible for the bypass of these cross-links, findings from our *E. coli* studies strongly suggest that in human cells, pol ν or pol κ could be the major polymerase responsible for the replication bypass of N^6 -dA or N^2 -dG peptide cross-links.

In the last Chapter, the discovery of small molecule inhibitors of pol κ by high throughput, fluorescence-based DNA strand displacement assay using ND DNA was described. The initial screen identified 60 compounds that were subsequently validated by radioactive gel-based primer extension assays. Of the initial hits, candesartan cilexetil, manoalide, and MK-886 were selected as lead compounds and were further characterized for their specificity toward pol κ in radioactive gel-based primer extension assays using DNAs containing site-specific acrolein-derived ring-opened reduced form of γ -HOPdG adduct. The results showed that these compounds could inhibit the ability of pol κ to copy both ND and damage-containing DNAs. Furthermore, candesartan cilexetil was shown to enhance cellular toxicity of UV irradiation in XP-V cells, suggesting an intracellular activity of this compound against pol κ . Collectively, these studies represent an initial step toward the development of pol κ inhibitors for improved combination chemotherapy, as well as the discovery of compounds that could serve as prototypes for future pol κ inhibitor design.

In conclusion, the data presented herein provide us insight into how cancer and chemotherapy resistance may arise as a result of the functions of TLS polymerases. Additionally, ultimately, these studies could lead to the discovery of novel TLS polymerase inhibitors that could be used in combination chemotherapy to combat cancers.

7. FUTURE DIRECTIONS

Candesartan cilexetil was found to exhibit cellular effects against pol κ . However, the mechanism of inhibition is unknown. In order to dissect the mechanism of action of candesartan cilexetil in inhibiting pol κ activity, I proposed to carry out X-ray structural analyses in collaboration with Dr. Robert L. Eoff at University of Arkansas for Medical Sciences. Since it remains challenging to crystalize pol κ , DPO4, a polymerase from *Sulfolobus solfataricus*, will be used instead, as this polymerase shares similarity with pol κ in overall structure, as well as substrate specificity. In this study, structures of DPO4 in complex with DNA and candesartan cilexetil (binary complex) and with DNA, candesartan cilexetil, and dNTP (ternary complex) will be solved.

Since compounds with high potency and selectivity against pol κ were not identified from the screen of ~16,000 compounds, I proposed to expand the screen to ~400,000 compounds. To accomplish this, I purified pol κ (residues 19-526) and together with Dr. Anton Simeonov's group at NCGC recently completed this large screen using the fluorescence-based strand displacement assay as described in Chapter 5 except for the utilization of 5 concentrations of each compound. The data analyses are currently in progress. Selected hits will then be cherry-picked and retested in the same primary assay. Additionally, these cherry-picked compounds will be used for counterscreen for promiscuous DNA binders by using the Thiazole Orange dye displacement assay and KF exo^- . The selected hits will be tested in the radioactive gel-based primer extension assays, and analogues of the top hits will then be synthesized to explore structure-activity relationship and retested in primary and secondary assays if needed. The lead compounds

will be nominated and validated in several tertiary assays, including the determination of the aqueous solubility, cell permeability, plasma and metabolic stability of the compounds, determination of the activity of compounds against pol β and effects on cell survival in response to DNA-damaging agents, and the investigations of whether the compounds are susceptible to efflux and are affected by drug transporters such as P-glycoprotein.

Despite an ongoing investigation, the cellular functions of pol κ remain to be elucidated. For instance, examination of the existence of synthetic lethal partner gene of pol κ has received little attention. In order to further probe the biological roles of pol κ , the identification of synthetic lethal partner gene of pol κ is thus essential. Therefore, I proposed to conduct the screening of library composed of 318 diverse siRNAs in collaboration with Dr. Raymond Monnat at University of Washington.

As the first step toward this screen, I have generated U2OS cell lines stably depleted of pol κ (~80% depletion of pol κ mRNA confirmed by qPCR) using shRNA against pol κ (5'-CAGTTAATCAACCCAAAGAAA-3') provided by Dr. Robert Sobol at University of Pittsburgh. These cells will be used for siRNA screen which will take place in a few months.

In addition to probing pol κ functions, if the synthetic lethal partner gene of pol κ has been identified, a cell-based tertiary assay can be designed to be used for triaging compounds identified through a big compound library screen. I proposed to design an assay in which cell lines stably depleted of pol κ synthetic lethal partner will be generated and used for cell survival assays with mitomycin C in combination with pol κ inhibitors.

Alternatively, these cells can be transiently transfected with siRNA against pol η and treated with UV and pol κ inhibitors. Compounds that could enhance cytotoxicity induced by these DNA-damaging agents will be selected for further studies.

REFERENCES

1. Stone, M.P., Cho, Y.J., Huang, H., Kim, H.Y., Kozekov, I.D., Kozekova, A., Wang, H., Minko, I.G., Lloyd, R.S., Harris, T.M. *et al.* (2008) Interstrand DNA cross-links induced by α,β -unsaturated aldehydes derived from lipid peroxidation and environmental sources. *Acc. Chem. Res.*, **41**, 793-804.
2. Minko, I.G., Kozekov, I.D., Harris, T.M., Rizzo, C.J., Lloyd, R.S. and Stone, M.P. (2009) Chemistry and biology of DNA containing 1,*N*²-deoxyguanosine adducts of the α,β -unsaturated aldehydes acrolein, crotonaldehyde, and 4-hydroxynonenal. *Chem. Res. Toxicol.*, **22**, 759-778.
3. Guo, C., Kosarek-Stancel, J.N., Tang, T.S. and Friedberg, E.C. (2009) Y-family DNA polymerases in mammalian cells. *Cell Mol. Life Sci.*, **66**, 2363-2381.
4. Waters, L.S., Minesinger, B.K., Wiltrout, M.E., D'Souza, S., Woodruff, R.V. and Walker, G.C. (2009) Eukaryotic translesion polymerases and their roles and regulation in DNA damage tolerance. *Microbiol. Mol. Biol. Rev.*, **73**, 134-154.
5. Lange, S.S., Takata, K. and Wood, R.D. (2011) DNA polymerases and cancer. *Nat. Rev. Cancer*, **11**, 96-110.
6. Goodman, M.F. (2002) Error-prone repair DNA polymerases in prokaryotes and eukaryotes. *Annu. Rev. Biochem.*, **71**, 17-50.
7. Suhasini, A.N. and Brosh, R.M., Jr. (2010) Mechanistic and biological aspects of helicase action on damaged DNA. *Cell Cycle*, **9**, 2317-2329.
8. Kusumoto, R., Masutani, C., Shimmyo, S., Iwai, S. and Hanaoka, F. (2004) DNA binding properties of human DNA polymerase η : implications for fidelity and polymerase switching of translesion synthesis. *Genes Cells*, **9**, 1139-1150.

9. Kannouche, P.L., Wing, J. and Lehmann, A.R. (2004) Interaction of human DNA polymerase η with monoubiquitinated PCNA: a possible mechanism for the polymerase switch in response to DNA damage. *Mol. Cell*, **14**, 491-500.
10. Plosky, B.S. and Woodgate, R. (2004) Switching from high-fidelity replicases to low-fidelity lesion-bypass polymerases. *Curr. Opin. Genet. Dev.*, **14**, 113-119.
11. Kannouche, P., Broughton, B.C., Volker, M., Hanaoka, F., Mullenders, L.H. and Lehmann, A.R. (2001) Domain structure, localization, and function of DNA polymerase η , defective in xeroderma pigmentosum variant cells. *Genes Dev.*, **15**, 158-172.
12. Bergoglio, V., Bavoux, C., Verbiest, V., Hoffmann, J.S. and Cazaux, C. (2002) Localisation of human DNA polymerase κ to replication foci. *J. Cell Sci.*, **115**, 4413-4418.
13. Jansen, J.G., Tsaalbi-Shtylik, A., Hendriks, G., Gali, H., Hendel, A., Johansson, F., Erixon, K., Livneh, Z., Mullenders, L.H., Haracska, L. *et al.* (2009) Separate domains of Rev1 mediate two modes of DNA damage bypass in mammalian cells. *Mol. Cell Biol.*, **29**, 3113-3123.
14. Waters, L.S. and Walker, G.C. (2006) The critical mutagenic translesion DNA polymerase Rev1 is highly expressed during G₂/M phase rather than S phase. *Proc. Natl. Acad. Sci.*, **103**, 8971-8976.
15. Heller, R.C. and Marians, K.J. (2006) Replication fork reactivation downstream of a blocked nascent leading strand. *Nature*, **439**, 557-562.
16. Lehmann, A.R. and Fuchs, R.P. (2006) Gaps and forks in DNA replication: Rediscovering old models. *DNA Repair (Amst.)*, **5**, 1495-1498.

17. Huang, T.T., Nijman, S.M., Mirchandani, K.D., Galardy, P.J., Cohn, M.A., Haas, W., Gygi, S.P., Ploegh, H.L., Bernards, R. and D'Andrea, A.D. (2006) Regulation of monoubiquitinated PCNA by DUB autocleavage. *Nat. Cell Biol.*, **8**, 339-347.
18. Arana, M.E. and Kunkel, T.A. (2010) Mutator phenotypes due to DNA replication infidelity. *Semin. Cancer Biol.*, **20**, 304-311.
19. Khare, V. and Eckert, K.A. (2002) The proofreading 3'→5' exonuclease activity of DNA polymerases: a kinetic barrier to translesion DNA synthesis. *Mutat. Res.*, **510**, 45-54.
20. Berdis, A.J. (2008) DNA polymerases as therapeutic targets. *Biochemistry*, **47**, 8253-8260.
21. Glick, E., Vigna, K.L. and Loeb, L.A. (2001) Mutations in human DNA polymerase η motif II alter bypass of DNA lesions. *EMBO J.*, **20**, 7303-7312.
22. Sweasy, J.B., Lauper, J.M. and Eckert, K.A. (2006) DNA polymerases and human diseases. *Radiat. Res.*, **166**, 693-714.
23. Matsuda, T., Bebenek, K., Masutani, C., Hanaoka, F. and Kunkel, T.A. (2000) Low fidelity DNA synthesis by human DNA polymerase- η . *Nature*, **404**, 1011-1013.
24. McCulloch, S.D., Kokoska, R.J., Masutani, C., Iwai, S., Hanaoka, F. and Kunkel, T.A. (2004) Preferential *cis-syn* thymine dimer bypass by DNA polymerase η occurs with biased fidelity. *Nature*, **428**, 97-100.
25. Masutani, C., Kusumoto, R., Iwai, S. and Hanaoka, F. (2000) Mechanisms of accurate translesion synthesis by human DNA polymerase η . *EMBO J.*, **19**, 3100-3109.

26. Johnson, R.E., Washington, M.T., Prakash, S. and Prakash, L. (2000) Fidelity of human DNA polymerase η . *J. Biol. Chem.*, **275**, 7447-7450.
27. Fortune, J.M., Pavlov, Y.I., Welch, C.M., Johansson, E., Burgers, P.M. and Kunkel, T.A. (2005) *Saccharomyces cerevisiae* DNA polymerase δ : high fidelity for base substitutions but lower fidelity for single- and multi-base deletions. *J. Biol. Chem.*, **280**, 29980-29987.
28. Shcherbakova, P.V., Pavlov, Y.I., Chilkova, O., Rogozin, I.B., Johansson, E. and Kunkel, T.A. (2003) Unique error signature of the four-subunit yeast DNA polymerase ϵ . *J. Biol. Chem.*, **278**, 43770-43780.
29. Zhang, Y., Yuan, F., Xin, H., Wu, X., Rajpal, D.K., Yang, D. and Wang, Z. (2000) Human DNA polymerase κ synthesizes DNA with extraordinarily low fidelity. *Nucleic Acids Res.*, **28**, 4147-4156.
30. Masutani, C., Kusumoto, R., Yamada, A., Dohmae, N., Yokoi, M., Yuasa, M., Araki, M., Iwai, S., Takio, K. and Hanaoka, F. (1999) The *XPV* (xeroderma pigmentosum variant) gene encodes human DNA polymerase η . *Nature*, **399**, 700-704.
31. Zhang, Y., Yuan, F., Wu, X., Rechkoblit, O., Taylor, J.S., Geacintov, N.E. and Wang, Z. (2000) Error-prone lesion bypass by human DNA polymerase η . *Nucleic Acids Res.*, **28**, 4717-4724.
32. Vaisman, A., Masutani, C., Hanaoka, F. and Chaney, S.G. (2000) Efficient translesion replication past oxaliplatin and cisplatin GpG adducts by human DNA polymerase η . *Biochemistry*, **39**, 4575-4580.

33. Minko, I.G., Washington, M.T., Kanuri, M., Prakash, L., Prakash, S. and Lloyd, R.S. (2003) Translesion synthesis past acrolein-derived DNA adduct, γ -hydroxypropanodeoxyguanosine, by yeast and human DNA polymerase η . *J. Biol. Chem.*, **278**, 784-790.
34. McCulloch, S.D., Kokoska, R.J., Garg, P., Burgers, P.M. and Kunkel, T.A. (2009) The efficiency and fidelity of 8-oxo-guanine bypass by DNA polymerases δ and η . *Nucleic Acids Res.*, **37**, 2830-2840.
35. Haracska, L., Yu, S.L., Johnson, R.E., Prakash, L. and Prakash, S. (2000) Efficient and accurate replication in the presence of 7,8-dihydro-8-oxoguanine by DNA polymerase η . *Nat. Genet.*, **25**, 458-461.
36. Maga, G., Villani, G., Crespan, E., Wimmer, U., Ferrari, E., Bertocci, B. and Hubscher, U. (2007) 8-oxo-guanine bypass by human DNA polymerases in the presence of auxiliary proteins. *Nature*, **447**, 606-608.
37. Kusumoto, R., Masutani, C., Iwai, S. and Hanaoka, F. (2002) Translesion synthesis by human DNA polymerase η across thymine glycol lesions. *Biochemistry*, **41**, 6090-6099.
38. Haracska, L., Prakash, S. and Prakash, L. (2000) Replication past O^6 -methylguanine by yeast and human DNA polymerase η . *Mol. Cell Biol.*, **20**, 8001-8007.
39. Seki, M., Masutani, C., Yang, L.W., Schuffert, A., Iwai, S., Bahar, I. and Wood, R.D. (2004) High-efficiency bypass of DNA damage by human DNA polymerase η . *EMBO J.*, **23**, 4484-4494.

40. Johnson, R.E., Yu, S.L., Prakash, S. and Prakash, L. (2003) Yeast DNA polymerase zeta (ζ) is essential for error-free replication past thymine glycol. *Genes Dev.*, **17**, 77-87.
41. Nair, J., Barbin, A., Velic, I. and Bartsch, H. (1999) Etheno DNA-base adducts from endogenous reactive species. *Mutat. Res.*, **424**, 59-69.
42. Zhou, Y., Wang, J., Zhang, Y. and Wang, Z. (2010) The catalytic function of the Rev1 dCMP transferase is required in a lesion-specific manner for translesion synthesis and base damage-induced mutagenesis. *Nucleic Acids Res.*, **38**, 5036-5046.
43. Levine, R.L., Miller, H., Grollman, A., Ohashi, E., Ohmori, H., Masutani, C., Hanaoka, F. and Moriya, M. (2001) Translesion DNA synthesis catalyzed by human pol η and pol κ across 1, N^6 -ethenodeoxyadenosine. *J. Biol. Chem.*, **276**, 18717-18721.
44. Rechkoblit, O., Zhang, Y., Guo, D., Wang, Z., Amin, S., Krzeminsky, J., Louneva, N. and Geacintov, N.E. (2002) trans-Lesion synthesis past bulky benzo[*a*]pyrene diol epoxide N^2 -dG and N^6 -dA lesions catalyzed by DNA bypass polymerases. *J. Biol. Chem.*, **277**, 30488-30494.
45. Zhang, Y., Wu, X., Guo, D., Rechkoblit, O., Geacintov, N.E. and Wang, Z. (2002) Two-step error-prone bypass of the (+)- and (-)-*trans-anti*-BPDE- N^2 -dG adducts by human DNA polymerases η and κ . *Mutat. Res.*, **510**, 23-35.
46. Colditz, G.A., Hankinson, S.E., Hunter, D.J., Willett, W.C., Manson, J.E., Stampfer, M.J., Hennekens, C., Rosner, B. and Speizer, F.E. (1995) The use of

- estrogens and progestins and the risk of breast cancer in postmenopausal women. *N. Engl. J. Med.*, **332**, 1589-1593.
47. Grady, D., Gebretsadik, T., Kerlikowske, K., Ernster, V. and Petitti, D. (1995) Hormone replacement therapy and endometrial cancer risk: a meta-analysis. *Obstet. Gynecol.*, **85**, 304-313.
48. Terashima, I., Suzuki, N. and Shibutani, S. (2002) ³²P-Postlabeling/polyacrylamide gel electrophoresis analysis: application to the detection of DNA adducts. *Chem. Res. Toxicol.*, **15**, 305-311.
49. Shen, L., Qiu, S., Chen, Y., Zhang, F., van Breemen, R.B., Nikolic, D. and Bolton, J.L. (1998) Alkylation of 2'-deoxynucleosides and DNA by the Premarin metabolite 4-hydroxyequilenin semiquinone radical. *Chem. Res. Toxicol.*, **11**, 94-101.
50. Zhang, F., Swanson, S.M., van Breemen, R.B., Liu, X., Yang, Y., Gu, C. and Bolton, J.L. (2001) Equine estrogen metabolite 4-hydroxyequilenin induces DNA damage in the rat mammary tissues: formation of single-strand breaks, apurinic sites, stable adducts, and oxidized bases. *Chem. Res. Toxicol.*, **14**, 1654-1659.
51. Bolton, J.L., Pisha, E., Zhang, F. and Qiu, S. (1998) Role of quinoids in estrogen carcinogenesis. *Chem. Res. Toxicol.*, **11**, 1113-1127.
52. Yasui, M., Matsui, S., Laxmi, Y.R., Suzuki, N., Kim, S.Y., Shibutani, S. and Matsuda, T. (2003) Mutagenic events induced by 4-hydroxyequilin in *supF* shuttle vector plasmid propagated in human cells. *Carcinogenesis*, **24**, 911-917.

53. Yasui, M., Laxmi, Y.R., Ananthoju, S.R., Suzuki, N., Kim, S.Y. and Shibutani, S. (2006) Translesion synthesis past equine estrogen-derived 2'-deoxyadenosine DNA adducts by human DNA polymerases η and κ . *Biochemistry*, **45**, 6187-6194.
54. Chen, Y.W., Cleaver, J.E., Hanaoka, F., Chang, C.F. and Chou, K.M. (2006) A novel role of DNA polymerase η in modulating cellular sensitivity to chemotherapeutic agents. *Mol. Cancer Res.*, **4**, 257-265.
55. Zietlow, L., Smith, L.A., Bessho, M. and Bessho, T. (2009) Evidence for the involvement of human DNA polymerase N in the repair of DNA interstrand cross-links. *Biochemistry*, **48**, 11817-11824.
56. Wolfle, W.T., Johnson, R.E., Minko, I.G., Lloyd, R.S., Prakash, S. and Prakash, L. (2006) Replication past a *trans*-4-hydroxynonenal minor-groove adduct by the sequential action of human DNA polymerases ι and κ . *Mol. Cell Biol.*, **26**, 381-386.
57. Betous, R., Rey, L., Wang, G., Pillaire, M.J., Puget, N., Selves, J., Biard, D.S., Shin-ya, K., Vasquez, K.M., Cazaux, C. *et al.* (2009) Role of TLS DNA polymerases eta and kappa in processing naturally occurring structured DNA in human cells. *Mol. Carcinog.*, **48**, 369-378.
58. Lehmann, A.R., Kirk-Bell, S., Arlett, C.F., Paterson, M.C., Lohman, P.H., de Weerd-Kastelein, E.A. and Bootsma, D. (1975) Xeroderma pigmentosum cells with normal levels of excision repair have a defect in DNA synthesis after UV-irradiation. *Proc. Natl. Acad. Sci.*, **72**, 219-223.
59. Cleaver, J.E. (1972) Xeroderma pigmentosum: variants with normal DNA repair and normal sensitivity to ultraviolet light. *J. Invest. Dermatol.*, **58**, 124-128.

60. Tamura, D., DiGiovanna, J.J. and Kraemer, K.H. (2010) Founder mutations in xeroderma pigmentosum. *J. Invest. Dermatol.*, **130**, 1491-1493.
61. Broughton, B.C., Cordonnier, A., Kleijer, W.J., Jaspers, N.G., Fawcett, H., Raams, A., Garritsen, V.H., Sary, A., Avril, M.F., Boudsocq, F. *et al.* (2002) Molecular analysis of mutations in DNA polymerase η in xeroderma pigmentosum-variant patients. *Proc. Natl. Acad. Sci.*, **99**, 815-820.
62. Johnson, R.E., Kondratyck, C.M., Prakash, S. and Prakash, L. (1999) hRAD30 mutations in the variant form of xeroderma pigmentosum. *Science*, **285**, 263-265.
63. Bassett, E., King, N.M., Bryant, M.F., Hector, S., Pendyala, L., Chaney, S.G. and Cordeiro-Stone, M. (2004) The role of DNA polymerase η in translesion synthesis past platinum-DNA adducts in human fibroblasts. *Cancer Res.*, **64**, 6469-6475.
64. Sary, A., Kannouche, P., Lehmann, A.R. and Sarasin, A. (2003) Role of DNA polymerase η in the UV mutation spectrum in human cells. *J. Biol. Chem.*, **278**, 18767-18775.
65. Hendel, A., Ziv, O., Gueranger, Q., Geacintov, N. and Livneh, Z. (2008) Reduced efficiency and increased mutagenicity of translesion DNA synthesis across a TT cyclobutane pyrimidine dimer, but not a TT 6-4 photoproduct, in human cells lacking DNA polymerase η . *DNA Repair (Amst.)*, **7**, 1636-1646.
66. Gueranger, Q., Sary, A., Aoufouchi, S., Faili, A., Sarasin, A., Reynaud, C.A. and Weill, J.C. (2008) Role of DNA polymerases η , ι and ζ in UV resistance and UV-induced mutagenesis in a human cell line. *DNA Repair (Amst.)*, **7**, 1551-1562.

67. Dumstorf, C.A., Clark, A.B., Lin, Q., Kissling, G.E., Yuan, T., Kucherlapati, R., McGregor, W.G. and Kunkel, T.A. (2006) Participation of mouse DNA polymerase ι in strand-biased mutagenic bypass of UV photoproducts and suppression of skin cancer. *Proc. Natl. Acad. Sci.*, **103**, 18083-18088.
68. Ziv, O., Geacintov, N., Nakajima, S., Yasui, A. and Livneh, Z. (2009) DNA polymerase ζ cooperates with polymerases κ and ι in translesion DNA synthesis across pyrimidine photodimers in cells from XPV patients. *Proc. Natl. Acad. Sci.*, **106**, 11552-11557.
69. Albertella, M.R., Green, C.M., Lehmann, A.R. and O'Connor, M.J. (2005) A role for polymerase η in the cellular tolerance to cisplatin-induced damage. *Cancer Res.*, **65**, 9799-9806.
70. Zheng, H., Wang, X., Warren, A.J., Legerski, R.J., Nairn, R.S., Hamilton, J.W. and Li, L. (2003) Nucleotide excision repair- and polymerase η -mediated error-prone removal of mitomycin C interstrand cross-links. *Mol. Cell Biol.*, **23**, 754-761.
71. Ceppi, P., Novello, S., Cambieri, A., Longo, M., Monica, V., Lo Iacono, M., Giaj-Levra, M., Saviozzi, S., Volante, M., Papotti, M. *et al.* (2009) Polymerase η mRNA expression predicts survival of non-small cell lung cancer patients treated with platinum-based chemotherapy. *Clin. Cancer Res.*, **15**, 1039-1045.
72. Teng, K.Y., Qiu, M.Z., Li, Z.H., Luo, H.Y., Zeng, Z.L., Luo, R.Z., Zhang, H.Z., Wang, Z.Q., Li, Y.H. and Xu, R.H. (2010) DNA polymerase η protein expression predicts treatment response and survival of metastatic gastric adenocarcinoma patients treated with oxaliplatin-based chemotherapy. *J. Transl. Med.*, **8**, 126.

73. Pan, Q., Fang, Y., Xu, Y., Zhang, K. and Hu, X. (2005) Down-regulation of DNA polymerases κ , η , ι , and ζ in human lung, stomach, and colorectal cancers. *Cancer Lett.*, **217**, 139-147.
74. Cordonnier, A.M., Lehmann, A.R. and Fuchs, R.P. (1999) Impaired translesion synthesis in xeroderma pigmentosum variant extracts. *Mol. Cell Biol.*, **19**, 2206-2211.
75. Lee, D.H. and Pfeifer, G.P. (2008) Translesion synthesis of 7,8-dihydro-8-oxo-2'-deoxyguanosine by DNA polymerase eta in vivo. *Mutat. Res.*, **641**, 19-26.
76. Delbos, F., De Smet, A., Faili, A., Aoufouchi, S., Weill, J.C. and Reynaud, C.A. (2005) Contribution of DNA polymerase η to immunoglobulin gene hypermutation in the mouse. *J. Exp. Med.*, **201**, 1191-1196.
77. Ohkumo, T., Kondo, Y., Yokoi, M., Tsukamoto, T., Yamada, A., Sugimoto, T., Kanao, R., Higashi, Y., Kondoh, H., Tatematsu, M. *et al.* (2006) UV-B radiation induces epithelial tumors in mice lacking DNA polymerase η and mesenchymal tumors in mice deficient for DNA polymerase ι . *Mol. Cell Biol.*, **26**, 7696-7706.
78. Masuda, K., Ouchida, R., Hikida, M., Kurosaki, T., Yokoi, M., Masutani, C., Seki, M., Wood, R.D., Hanaoka, F. and J, O.W. (2007) DNA polymerases η and θ function in the same genetic pathway to generate mutations at A/T during somatic hypermutation of Ig genes. *J. Biol. Chem.*, **282**, 17387-17394.
79. Delbos, F., Aoufouchi, S., Faili, A., Weill, J.C. and Reynaud, C.A. (2007) DNA polymerase η is the sole contributor of A/T modifications during immunoglobulin gene hypermutation in the mouse. *J. Exp. Med.*, **204**, 17-23.

80. Gerlach, V.L., Aravind, L., Gotway, G., Schultz, R.A., Koonin, E.V. and Friedberg, E.C. (1999) Human and mouse homologs of *Escherichia coli* DinB (DNA polymerase IV), members of the UmuC/DinB superfamily. *Proc. Natl. Acad. Sci.*, **96**, 11922-11927.
81. Bavoux, C., Hoffmann, J.S. and Cazaux, C. (2005) Adaptation to DNA damage and stimulation of genetic instability: the double-edged sword mammalian DNA polymerase κ . *Biochimie*, **87**, 637-646.
82. Gerlach, V.L., Feaver, W.J., Fischhaber, P.L. and Friedberg, E.C. (2001) Purification and characterization of pol κ , a DNA polymerase encoded by the human *DINB1* gene. *J. Biol. Chem.*, **276**, 92-98.
83. Ohashi, E., Bebenek, K., Matsuda, T., Feaver, W.J., Gerlach, V.L., Friedberg, E.C., Ohmori, H. and Kunkel, T.A. (2000) Fidelity and processivity of DNA synthesis by DNA polymerase κ , the product of the human *DINB1* gene. *J. Biol. Chem.*, **275**, 39678-39684.
84. Haracska, L., Unk, I., Johnson, R.E., Phillips, B.B., Hurwitz, J., Prakash, L. and Prakash, S. (2002) Stimulation of DNA synthesis activity of human DNA polymerase κ by PCNA. *Mol. Cell Biol.*, **22**, 784-791.
85. Johnson, R.E., Prakash, S. and Prakash, L. (2000) The human *DINB1* gene encodes the DNA polymerase Pol θ . *Proc. Natl. Acad. Sci.*, **97**, 3838-3843.
86. Ohashi, E., Ogi, T., Kusumoto, R., Iwai, S., Masutani, C., Hanaoka, F. and Ohmori, H. (2000) Error-prone bypass of certain DNA lesions by the human DNA polymerase κ . *Genes Dev.*, **14**, 1589-1594.

87. Zhang, Y., Yuan, F., Wu, X., Wang, M., Rechkoblit, O., Taylor, J.S., Geacintov, N.E. and Wang, Z. (2000) Error-free and error-prone lesion bypass by human DNA polymerase κ *in vitro*. *Nucleic Acids Res.*, **28**, 4138-4146.
88. Suzuki, N., Ohashi, E., Hayashi, K., Ohmori, H., Grollman, A.P. and Shibutani, S. (2001) Translesional synthesis past acetylaminofluorene-derived DNA adducts catalyzed by human DNA polymerase κ and *Escherichia coli* DNA polymerase IV. *Biochemistry*, **40**, 15176-15183.
89. Sassa, A., Niimi, N., Fujimoto, H., Katafuchi, A., Gruz, P., Yasui, M., Gupta, R.C., Johnson, F., Ohta, T. and Nohmi, T. (2011) Phenylalanine 171 is a molecular brake for translesion synthesis across benzo[*a*]pyrene-guanine adducts by human DNA polymerase kappa. *Mutat. Res.*, **718**, 10-17.
90. Minko, I.G., Yamanaka, K., Kozekov, I.D., Kozekova, A., Indiani, C., O'Donnell, M.E., Jiang, Q., Goodman, M.F., Rizzo, C.J. and Lloyd, R.S. (2008) Replication bypass of the acrolein-mediated deoxyguanine DNA-peptide cross-links by DNA polymerases of the DinB family. *Chem. Res. Toxicol.*, **21**, 1983-1990.
91. Yamanaka, K., Minko, I.G., Finkel, S.E., Goodman, M.F. and Lloyd, R.S. (2011) Role of High-Fidelity *Escherichia coli* DNA Polymerase I in Replication Bypass of a Deoxyadenosine DNA-Peptide Cross-Link. *J. Bacteriol.*, **193**, 3815-3821.
92. Minko, I.G., Harbut, M.B., Kozekov, I.D., Kozekova, A., Jakobs, P.M., Olson, S.B., Moses, R.E., Harris, T.M., Rizzo, C.J. and Lloyd, R.S. (2008) Role for DNA polymerase κ in the processing of N^2 - N^2 -guanine interstrand cross-links. *J. Biol. Chem.*, **283**, 17075-17082.

93. Wolfle, W.T., Johnson, R.E., Minko, I.G., Lloyd, R.S., Prakash, S. and Prakash, L. (2005) Human DNA polymerase ι promotes replication through a ring-closed minor-groove adduct that adopts a *syn* conformation in DNA. *Mol. Cell Biol.*, **25**, 8748-8754.
94. Washington, M.T., Minko, I.G., Johnson, R.E., Wolfle, W.T., Harris, T.M., Lloyd, R.S., Prakash, S. and Prakash, L. (2004) Efficient and error-free replication past a minor-groove DNA adduct by the sequential action of human DNA polymerases ι and κ . *Mol. Cell Biol.*, **24**, 5687-5693.
95. Choi, J.Y., Angel, K.C. and Guengerich, F.P. (2006) Translesion synthesis across bulky N^2 -alkyl guanine DNA adducts by human DNA polymerase κ . *J. Biol. Chem.*, **281**, 21062-21072.
96. Irimia, A., Eoff, R.L., Guengerich, F.P. and Egli, M. (2009) Structural and functional elucidation of the mechanism promoting error-prone synthesis by human DNA polymerase κ opposite the 7,8-dihydro-8-oxo-2'-deoxyguanosine adduct. *J. Biol. Chem.*, **284**, 22467-22480.
97. Washington, M.T., Johnson, R.E., Prakash, L. and Prakash, S. (2002) Human *DINB1*-encoded DNA polymerase κ is a promiscuous extender of mispaired primer termini. *Proc. Natl. Acad. Sci.*, **99**, 1910-1914.
98. Yoon, J.H., Bhatia, G., Prakash, S. and Prakash, L. (2010) Error-free replicative bypass of thymine glycol by the combined action of DNA polymerases κ and ζ in human cells. *Proc. Natl. Acad. Sci.*, **107**, 14116-14121.
99. Shachar, S., Ziv, O., Avkin, S., Adar, S., Wittschieben, J., Reissner, T., Chaney, S., Friedberg, E.C., Wang, Z., Carell, T. *et al.* (2009) Two-polymerase

- mechanisms dictate error-free and error-prone translesion DNA synthesis in mammals. *EMBO J.*, **28**, 383-393.
100. Avkin, S., Goldsmith, M., Velasco-Miguel, S., Geacintov, N., Friedberg, E.C. and Livneh, Z. (2004) Quantitative analysis of translesion DNA synthesis across a benzo[*a*]pyrene-guanine adduct in mammalian cells: the role of DNA polymerase κ . *J. Biol. Chem.*, **279**, 53298-53305.
 101. Ogi, T., Shinkai, Y., Tanaka, K. and Ohmori, H. (2002) Pol κ protects mammalian cells against the lethal and mutagenic effects of benzo[*a*]pyrene. *Proc. Natl. Acad. Sci.*, **99**, 15548-15553.
 102. Bi, X., Slater, D.M., Ohmori, H. and Vaziri, C. (2005) DNA polymerase κ is specifically required for recovery from the benzo[*a*]pyrene-dihydrodiol epoxide (BPDE)-induced S-phase checkpoint. *J. Biol. Chem.*, **280**, 22343-22355.
 103. Ogi, T., Mimura, J., Hikida, M., Fujimoto, H., Fujii-Kuriyama, Y. and Ohmori, H. (2001) Expression of human and mouse genes encoding pol κ : testis-specific developmental regulation and AhR-dependent inducible transcription. *Genes Cells*, **6**, 943-953.
 104. Schenten, D., Gerlach, V.L., Guo, C., Velasco-Miguel, S., Hladik, C.L., White, C.L., Friedberg, E.C., Rajewsky, K. and Esposito, G. (2002) DNA polymerase κ deficiency does not affect somatic hypermutation in mice. *Eur. J. Immunol.*, **32**, 3152-3160.
 105. Velasco-Miguel, S., Richardson, J.A., Gerlach, V.L., Lai, W.C., Gao, T., Russell, L.D., Hladik, C.L., White, C.L. and Friedberg, E.C. (2003) Constitutive and

- regulated expression of the mouse *Dinb* (*Polk*) gene encoding DNA polymerase kappa. *DNA Repair (Amst.)*, **2**, 91-106.
106. Ogi, T. and Lehmann, A.R. (2006) The Y-family DNA polymerase κ (pol κ) functions in mammalian nucleotide-excision repair. *Nat. Cell Biol.*, **8**, 640-642.
107. Wang, H., Wu, W., Wang, H.W., Wang, S., Chen, Y., Zhang, X., Yang, J., Zhao, S., Ding, H.F. and Lu, D. (2010) Analysis of specialized DNA polymerases expression in human gliomas: association with prognostic significance. *Neuro. Oncol.* **12**: 679-686
108. J, O.W., Kawamura, K., Tada, Y., Ohmori, H., Kimura, H., Sakiyama, S. and Tagawa, M. (2001) DNA polymerase κ , implicated in spontaneous and DNA damage-induced mutagenesis, is overexpressed in lung cancer. *Cancer Res.*, **61**, 5366-5369.
109. Stancel, J.N., McDaniel, L.D., Velasco, S., Richardson, J., Guo, C. and Friedberg, E.C. (2009) *Polk* mutant mice have a spontaneous mutator phenotype. *DNA Repair (Amst.)*, **8**, 1355-1362.
110. McDonald, J.P., Rasic-Otrin, V., Epstein, J.A., Broughton, B.C., Wang, X., Lehmann, A.R., Wolgemuth, D.J. and Woodgate, R. (1999) Novel human and mouse homologs of *Saccharomyces cerevisiae* DNA polymerase η . *Genomics*, **60**, 20-30.
111. Johnson, R.E., Washington, M.T., Prakash, S. and Prakash, L. (1999) Bridging the gap: a family of novel DNA polymerases that replicate faulty DNA. *Proc. Natl. Acad. Sci.*, **96**, 12224-12226.

112. Tissier, A., McDonald, J.P., Frank, E.G. and Woodgate, R. (2000) ρ 1, a remarkably error-prone human DNA polymerase. *Genes Dev.*, **14**, 1642-1650.
113. Washington, M.T., Johnson, R.E., Prakash, L. and Prakash, S. (2004) Human DNA polymerase ρ utilizes different nucleotide incorporation mechanisms dependent upon the template base. *Mol. Cell Biol.*, **24**, 936-943.
114. Johnson, R.E., Washington, M.T., Haracska, L., Prakash, S. and Prakash, L. (2000) Eukaryotic polymerases ρ and ζ act sequentially to bypass DNA lesions. *Nature*, **406**, 1015-1019.
115. Haracska, L., Johnson, R.E., Unk, I., Phillips, B.B., Hurwitz, J., Prakash, L. and Prakash, S. (2001) Targeting of human DNA polymerase ρ to the replication machinery via interaction with PCNA. *Proc. Natl. Acad. Sci.*, **98**, 14256-14261.
116. Bebenek, K., Tissier, A., Frank, E.G., McDonald, J.P., Prasad, R., Wilson, S.H., Woodgate, R. and Kunkel, T.A. (2001) 5'-Deoxyribose phosphate lyase activity of human DNA polymerase ρ in vitro. *Science*, **291**, 2156-2159.
117. Zhang, Y., Yuan, F., Wu, X., Taylor, J.S. and Wang, Z. (2001) Response of human DNA polymerase ρ to DNA lesions. *Nucleic Acids Res.*, **29**, 928-935.
118. Tissier, A., Frank, E.G., McDonald, J.P., Iwai, S., Hanaoka, F. and Woodgate, R. (2000) Misinsertion and bypass of thymine-thymine dimers by human DNA polymerase ρ . *EMBO J.*, **19**, 5259-5266.
119. Johnson, R.E., Haracska, L., Prakash, L. and Prakash, S. (2006) Role of Hoogsteen edge hydrogen bonding at template purines in nucleotide incorporation by human DNA polymerase ρ . *Mol. Cell Biol.*, **26**, 6435-6441.

120. Choi, J.Y. and Guengerich, F.P. (2006) Kinetic evidence for inefficient and error-prone bypass across bulky N^2 -guanine DNA adducts by human DNA polymerase ι . *J. Biol. Chem.*, **281**, 12315-12324.
121. Petta, T.B., Nakajima, S., Zlatanou, A., Despras, E., Couve-Privat, S., Ishchenko, A., Sarasin, A., Yasui, A. and Kannouche, P. (2008) Human DNA polymerase ι protects cells against oxidative stress. *EMBO J.*, **27**, 2883-2895.
122. Choi, J.H., Besaratinia, A., Lee, D.H., Lee, C.S. and Pfeifer, G.P. (2006) The role of DNA polymerase ι in UV mutational spectra. *Mutat. Res.*, **599**, 58-65.
123. Yang, J., Chen, Z., Liu, Y., Hickey, R.J. and Malkas, L.H. (2004) Altered DNA polymerase ι expression in breast cancer cells leads to a reduction in DNA replication fidelity and a higher rate of mutagenesis. *Cancer Res.*, **64**, 5597-5607.
124. Lee, G.H. and Matsushita, H. (2005) Genetic linkage between Pol ι deficiency and increased susceptibility to lung tumors in mice. *Cancer Sci.*, **96**, 256-259.
125. Lin, W., Xin, H., Zhang, Y., Wu, X., Yuan, F. and Wang, Z. (1999) The human REV1 gene codes for a DNA template-dependent dCMP transferase. *Nucleic Acids Res.*, **27**, 4468-4475.
126. Zhang, Y., Wu, X., Rechkoblit, O., Geacintov, N.E., Taylor, J.S. and Wang, Z. (2002) Response of human REV1 to different DNA damage: preferential dCMP insertion opposite the lesion. *Nucleic Acids Res.*, **30**, 1630-1638.
127. Brown, J.A., Fowler, J.D. and Suo, Z. (2010) Kinetic basis of nucleotide selection employed by a protein template-dependent DNA polymerase. *Biochemistry*, **49**, 5504-5510.

128. Washington, M.T., Minko, I.G., Johnson, R.E., Haracska, L., Harris, T.M., Lloyd, R.S., Prakash, S. and Prakash, L. (2004) Efficient and error-free replication past a minor-groove N^2 -guanine adduct by the sequential action of yeast Rev1 and DNA polymerase ζ . *Mol. Cell Biol.*, **24**, 6900-6906.
129. Haracska, L., Unk, I., Johnson, R.E., Johansson, E., Burgers, P.M., Prakash, S. and Prakash, L. (2001) Roles of yeast DNA polymerases δ and ζ and of Rev1 in the bypass of abasic sites. *Genes Dev.*, **15**, 945-954.
130. Choi, J.Y. and Guengerich, F.P. (2008) Kinetic analysis of translesion synthesis opposite bulky N^2 - and O^6 -alkylguanine DNA adducts by human DNA polymerase REV1. *J. Biol. Chem.*, **283**, 23645-23655.
131. Yang, I.Y., Hashimoto, K., de Wind, N., Blair, I.A. and Moriya, M. (2009) Two distinct translesion synthesis pathways across a lipid peroxidation-derived DNA adduct in mammalian cells. *J. Biol. Chem.*, **284**, 191-198.
132. Xie, K., Doles, J., Hemann, M.T. and Walker, G.C. (2010) Error-prone translesion synthesis mediates acquired chemoresistance. *Proc. Natl. Acad. Sci.*, **107**, 20792-20797.
133. Okuda, T., Lin, X., Trang, J. and Howell, S.B. (2005) Suppression of hREV1 expression reduces the rate at which human ovarian carcinoma cells acquire resistance to cisplatin. *Mol. Pharmacol.*, **67**, 1852-1860.
134. Dumstorf, C.A., Mukhopadhyay, S., Krishnan, E., Haribabu, B. and McGregor, W.G. (2009) REV1 is implicated in the development of carcinogen-induced lung cancer. *Mol. Cancer Res.*, **7**, 247-254.

135. Lin, X., Okuda, T., Trang, J. and Howell, S.B. (2006) Human REV1 modulates the cytotoxicity and mutagenicity of cisplatin in human ovarian carcinoma cells. *Mol. Pharmacol.*, **69**, 1748-1754.
136. Jansen, J.G., Langerak, P., Tsaalbi-Shtylik, A., van den Berk, P., Jacobs, H. and de Wind, N. (2006) Strand-biased defect in C/G transversions in hypermutating immunoglobulin genes in Rev1-deficient mice. *J. Exp. Med.*, **203**, 319-323.
137. Gan, G.N., Wittschieben, J.P., Wittschieben, B.O. and Wood, R.D. (2008) DNA polymerase zeta (pol ζ) in higher eukaryotes. *Cell Res.*, **18**, 174-183.
138. Nelson, J.R., Lawrence, C.W. and Hinkle, D.C. (1996) Thymine-thymine dimer bypass by yeast DNA polymerase ζ . *Science*, **272**, 1646-1649.
139. Lawrence, C.W. and Maher, V.M. (2001) Mutagenesis in eukaryotes dependent on DNA polymerase zeta and Rev1p. *Philos. Trans. R. Soc. Lond. B Biol. Sci.*, **356**, 41-46.
140. Haracska, L., Prakash, S. and Prakash, L. (2003) Yeast DNA polymerase ζ is an efficient extender of primer ends opposite from 7,8-dihydro-8-Oxoguanine and O^6 -methylguanine. *Mol. Cell Biol.*, **23**, 1453-1459.
141. Zhong, X., Garg, P., Stith, C.M., Nick McElhinny, S.A., Kissling, G.E., Burgers, P.M. and Kunkel, T.A. (2006) The fidelity of DNA synthesis by yeast DNA polymerase zeta alone and with accessory proteins. *Nucleic Acids Res.*, **34**, 4731-4742.
142. Ho, T.V., Guainazzi, A., Derkunt, S.B., Enoiu, M. and Scharer, O.D. (2011) Structure-dependent bypass of DNA interstrand crosslinks by translesion synthesis polymerases. *Nucleic Acids Res.*, **39**, 7455-7464.

143. Wu, F., Lin, X., Okuda, T. and Howell, S.B. (2004) DNA polymerase ζ regulates cisplatin cytotoxicity, mutagenicity, and the rate of development of cisplatin resistance. *Cancer Res.*, **64**, 8029-8035.
144. Roos, W.P., Tsaalbi-Shtylik, A., Tsaryk, R., Guvercin, F., de Wind, N. and Kaina, B. (2009) The translesion polymerase Rev3L in the tolerance of alkylating anticancer drugs. *Mol. Pharmacol.*, **76**, 927-934.
145. Wittschieben, J.P., Reshmi, S.C., Gollin, S.M. and Wood, R.D. (2006) Loss of DNA polymerase ζ causes chromosomal instability in mammalian cells. *Cancer Res.*, **66**, 134-142.
146. Hicks, J.K., Chute, C.L., Paulsen, M.T., Ragland, R.L., Howlett, N.G., Gueranger, Q., Glover, T.W. and Canman, C.E. (2010) Differential roles for DNA polymerases eta, zeta, and REV1 in lesion bypass of intrastrand versus interstrand DNA cross-links. *Mol. Cell Biol.*, **30**, 1217-1230.
147. Doles, J., Oliver, T.G., Cameron, E.R., Hsu, G., Jacks, T., Walker, G.C. and Hemann, M.T. (2010) Suppression of Rev3, the catalytic subunit of Pol ζ , sensitizes drug-resistant lung tumors to chemotherapy. *Proc. Natl. Acad. Sci.*, **107**, 20786-20791.
148. Wang, H., Zhang, S.Y., Wang, S., Lu, J., Wu, W., Weng, L., Chen, D., Zhang, Y., Lu, Z., Yang, J. *et al.* (2009) *REV3L* confers chemoresistance to cisplatin in human gliomas: the potential of its RNAi for synergistic therapy. *Neuro. Oncol.*, **11**, 790-802.
149. Lin, X., Trang, J., Okuda, T. and Howell, S.B. (2006) DNA polymerase ζ accounts for the reduced cytotoxicity and enhanced mutagenicity of cisplatin in

- human colon carcinoma cells that have lost DNA mismatch repair. *Clin. Cancer Res.*, **12**, 563-568.
150. Starostik, P., Greiner, A., Schultz, A., Zettl, A., Peters, K., Rosenwald, A., Kolve, M. and Muller-Hermelink, H.K. (2000) Genetic aberrations common in gastric high-grade large B-cell lymphoma. *Blood*, **95**, 1180-1187.
151. Schlegelberger, B., Himmler, A., Bartles, H., Kuse, R., Sterry, W. and Grote, W. (1994) Recurrent chromosome abnormalities in peripheral T-cell lymphomas. *Cancer Genet. Cytogenet.*, **78**, 15-22.
152. Takeuchi, S., Koike, M., Seriu, T., Bartram, C.R., Schrappe, M., Reiter, A., Park, S., Taub, H.E., Kubonishi, I., Miyoshi, I. *et al.* (1998) Frequent loss of heterozygosity on the long arm of chromosome 6: identification of two distinct regions of deletion in childhood acute lymphoblastic leukemia. *Cancer Res.*, **58**, 2618-2623.
153. Morelli, C., Karayianni, E., Magnanini, C., Mungall, A.J., Thorland, E., Negrini, M., Smith, D.I. and Barbanti-Brodano, G. (2002) Cloning and characterization of the common fragile site FRA6F harboring a replicative senescence gene and frequently deleted in human tumors. *Oncogene*, **21**, 7266-7276.
154. Bemark, M., Khamlichi, A.A., Davies, S.L. and Neuberger, M.S. (2000) Disruption of mouse polymerase ζ (*Rev3*) leads to embryonic lethality and impairs blastocyst development *in vitro*. *Curr. Biol.*, **10**, 1213-1216.
155. Esposito, G., Godindagger, I., Klein, U., Yaspo, M.L., Cumano, A. and Rajewsky, K. (2000) Disruption of the *Rev3l*-encoded catalytic subunit of polymerase ζ in mice results in early embryonic lethality. *Curr. Biol.*, **10**, 1221-1224.

156. Wittschieben, J., Shivji, M.K., Lalani, E., Jacobs, M.A., Marini, F., Gearhart, P.J., Rosewell, I., Stamp, G. and Wood, R.D. (2000) Disruption of the developmentally regulated *Rev3l* gene causes embryonic lethality. *Curr. Biol.*, **10**, 1217-1220.
157. Wittschieben, J.P., Patil, V., Glushets, V., Robinson, L.J., Kusewitt, D.F. and Wood, R.D. (2010) Loss of DNA polymerase ζ enhances spontaneous tumorigenesis. *Cancer Res.*, **70**, 2770-2778.
158. Takata, K., Shimizu, T., Iwai, S. and Wood, R.D. (2006) Human DNA polymerase N (POLN) is a low fidelity enzyme capable of error-free bypass of 5S-thymine glycol. *J. Biol. Chem.*, **281**, 23445-23455.
159. Arana, M.E., Takata, K., Garcia-Diaz, M., Wood, R.D. and Kunkel, T.A. (2007) A unique error signature for human DNA polymerase ν . *DNA Repair (Amst.)*, **6**, 213-223.
160. Marini, F., Kim, N., Schuffert, A. and Wood, R.D. (2003) POLN, a nuclear PolA family DNA polymerase homologous to the DNA cross-link sensitivity protein Mus308. *J. Biol. Chem.*, **278**, 32014-32019.
161. Arana, M.E., Seki, M., Wood, R.D., Rogozin, I.B. and Kunkel, T.A. (2008) Low-fidelity DNA synthesis by human DNA polymerase theta. *Nucleic Acids Res.*, **36**, 3847-3856.
162. Yamanaka, K., Minko, I.G., Takata, K., Kolbanovskiy, A., Kozekov, I.D., Wood, R.D., Rizzo, C.J. and Lloyd, R.S. (2010) Novel enzymatic function of DNA polymerase ν in translesion DNA synthesis past major groove DNA-peptide and DNA-DNA cross-links. *Chem. Res. Toxicol.*, **23**, 689-695.

163. Moldovan, G.L., Madhavan, M.V., Mirchandani, K.D., McCaffrey, R.M., Vinciguerra, P. and D'Andrea, A.D. (2010) DNA polymerase POLN participates in cross-link repair and homologous recombination. *Mol. Cell Biol.*, **30**, 1088-1096.
164. Kohzaki, M., Nishihara, K., Hirota, K., Sonoda, E., Yoshimura, M., Ekino, S., Butler, J.E., Watanabe, M., Halazonetis, T.D. and Takeda, S. (2010) DNA polymerases ν and θ are required for efficient immunoglobulin V gene diversification in chicken. *J. Cell Biol.*, **189**, 1117-1127.
165. Lemee, F., Bergoglio, V., Fernandez-Vidal, A., Machado-Silva, A., Pillaire, M.J., Bieth, A., Gentil, C., Baker, L., Martin, A.L., Leduc, C. *et al.* (2010) DNA polymerase θ up-regulation is associated with poor survival in breast cancer, perturbs DNA replication, and promotes genetic instability. *Proc. Natl. Acad. Sci.*, **107**, 13390-13395.
166. Shivapurkar, N., Sood, S., Wistuba, II, Virmani, A.K., Maitra, A., Milchgrub, S., Minna, J.D. and Gazdar, A.F. (1999) Multiple regions of chromosome 4 demonstrating allelic losses in breast carcinomas. *Cancer Res.*, **59**, 3576-3580.
167. Seki, M., Marini, F. and Wood, R.D. (2003) POLQ (Pol θ), a DNA polymerase and DNA-dependent ATPase in human cells. *Nucleic Acids Res.*, **31**, 6117-6126.
168. Prasad, R., Longley, M.J., Sharief, F.S., Hou, E.W., Copeland, W.C. and Wilson, S.H. (2009) Human DNA polymerase θ possesses 5'-dRP lyase activity and functions in single-nucleotide base excision repair *in vitro*. *Nucleic Acids Res.*, **37**, 1868-1877.

169. Seki, M. and Wood, R.D. (2008) DNA polymerase θ (POLQ) can extend from mismatches and from bases opposite a (6-4) photoproduct. *DNA Repair (Amst.)*, **7**, 119-127.
170. Yoshimura, M., Kohzaki, M., Nakamura, J., Asagoshi, K., Sonoda, E., Hou, E., Prasad, R., Wilson, S.H., Tano, K., Yasui, A. *et al.* (2006) Vertebrate POLQ and POL β cooperate in base excision repair of oxidative DNA damage. *Mol. Cell*, **24**, 115-125.
171. Goff, J.P., Shields, D.S., Seki, M., Choi, S., Epperly, M.W., Dixon, T., Wang, H., Bakkenist, C.J., Dertinger, S.D., Torous, D.K. *et al.* (2009) Lack of DNA polymerase θ (POLQ) radiosensitizes bone marrow stromal cells *in vitro* and increases reticulocyte micronuclei after total-body irradiation. *Radiat. Res.*, **172**, 165-174.
172. Higgins, G.S., Prevo, R., Lee, Y.F., Helleday, T., Muschel, R.J., Taylor, S., Yoshimura, M., Hickson, I.D., Bernhard, E.J. and McKenna, W.G. (2010) A small interfering RNA screen of genes involved in DNA repair identifies tumor-specific radiosensitization by POLQ knockdown. *Cancer Res.*, **70**, 2984-2993.
173. Kawamura, K., Bahar, R., Seimiya, M., Chiyo, M., Wada, A., Okada, S., Hatano, M., Tokuhisa, T., Kimura, H., Watanabe, S. *et al.* (2004) DNA polymerase θ is preferentially expressed in lymphoid tissues and upregulated in human cancers. *Int. J. Cancer*, **109**, 9-16.
174. Shima, N., Munroe, R.J. and Schimenti, J.C. (2004) The mouse genomic instability mutation *chaos1* is an allele of *Polq* that exhibits genetic interaction with *Atm*. *Mol. Cell Biol.*, **24**, 10381-10389.

175. Masuda, K., Ouchida, R., Takeuchi, A., Saito, T., Koseki, H., Kawamura, K., Tagawa, M., Tokuhisa, T., Azuma, T. and J, O.W. (2005) DNA polymerase θ contributes to the generation of C/G mutations during somatic hypermutation of Ig genes. *Proc. Natl. Acad. Sci.*, **102**, 13986-13991.
176. Masuda, K., Ouchida, R., Hikida, M., Nakayama, M., Ohara, O., Kurosaki, T. and J, O.W. (2006) Absence of DNA polymerase θ results in decreased somatic hypermutation frequency and altered mutation patterns in Ig genes. *DNA Repair (Amst.)*, **5**, 1384-1391.
177. Martomo, S.A., Saribasak, H., Yokoi, M., Hanaoka, F. and Gearhart, P.J. (2008) Reevaluation of the role of DNA polymerase θ in somatic hypermutation of immunoglobulin genes. *DNA Repair (Amst.)*, **7**, 1603-1608.
178. Yoon, J.H., Prakash, L. and Prakash, S. (2010) Error-free replicative bypass of (6-4) photoproducts by DNA polymerase ζ in mouse and human cells. *Genes Dev.*, **24**, 123-128.
179. Yoon, J.H., Prakash, L. and Prakash, S. (2009) Highly error-free role of DNA polymerase η in the replicative bypass of UV-induced pyrimidine dimers in mouse and human cells. *Proc. Natl. Acad. Sci.*, **106**, 18219-18224.
180. Wang, Y., Woodgate, R., McManus, T.P., Mead, S., McCormick, J.J. and Maher, V.M. (2007) Evidence that in xeroderma pigmentosum variant cells, which lack DNA polymerase η , DNA polymerase ι causes the very high frequency and unique spectrum of UV-induced mutations. *Cancer Res.*, **67**, 3018-3026.
181. Fox, E.J. and Loeb, L.A. (2010) Lethal mutagenesis: targeting the mutator phenotype in cancer. *Semin. Cancer Biol.*, **20**, 353-359.

182. Salk, J.J., Fox, E.J. and Loeb, L.A. (2010) Mutational heterogeneity in human cancers: origin and consequences. *Annu. Rev. Pathol.*, **5**, 51-75.
183. Loeb, L.A., Springgate, C.F. and Battula, N. (1974) Errors in DNA replication as a basis of malignant changes. *Cancer Res.*, **34**, 2311-2321.
184. Loeb, L.A. (1991) Mutator phenotype may be required for multistage carcinogenesis. *Cancer Res.*, **51**, 3075-3079.
185. Jackson, A.L. and Loeb, L.A. (1998) The mutation rate and cancer. *Genetics*, **148**, 1483-1490.
186. Drake, J.W. (1999) The distribution of rates of spontaneous mutation over viruses, prokaryotes, and eukaryotes. *Ann. N Y Acad. Sci.*, **870**, 100-107.
187. Bielas, J.H., Loeb, K.R., Rubin, B.P., True, L.D. and Loeb, L.A. (2006) Human cancers express a mutator phenotype. *Proc. Natl. Acad. Sci.*, **103**, 18238-18242.
188. Pleasance, E.D., Stephens, P.J., O'Meara, S., McBride, D.J., Meynert, A., Jones, D., Lin, M.L., Beare, D., Lau, K.W., Greenman, C. *et al.* (2010) A small-cell lung cancer genome with complex signatures of tobacco exposure. *Nature*, **463**, 184-190.
189. Pleasance, E.D., Cheetham, R.K., Stephens, P.J., McBride, D.J., Humphray, S.J., Greenman, C.D., Varela, I., Lin, M.L., Ordonez, G.R., Bignell, G.R. *et al.* (2010) A comprehensive catalogue of somatic mutations from a human cancer genome. *Nature*, **463**, 191-196.
190. Lee, W., Jiang, Z., Liu, J., Haverty, P.M., Guan, Y., Stinson, J., Yue, P., Zhang, Y., Pant, K.P., Bhatt, D. *et al.* (2010) The mutation spectrum revealed by paired genome sequences from a lung cancer patient. *Nature*, **465**, 473-477.

191. Gottesman, M.M. (2002) Mechanisms of cancer drug resistance. *Annu. Rev. Med.*, **53**, 615-627.
192. Mamenta, E.L., Poma, E.E., Kaufmann, W.K., Delmastro, D.A., Grady, H.L. and Chaney, S.G. (1994) Enhanced replicative bypass of platinum-DNA adducts in cisplatin-resistant human ovarian carcinoma cell lines. *Cancer Res.*, **54**, 3500-3505.
193. Mizushina, Y., Motoshima, H., Yamaguchi, Y., Takeuchi, T., Hirano, K., Sugawara, F. and Yoshida, H. (2009) 3-*O*-methylfunicone, a selective inhibitor of mammalian Y-family DNA polymerases from an Australian sea salt fungal strain. *Mar. Drugs*, **7**, 624-639.
194. Mizushina, Y., Manita, D., Takeuchi, T., Sugawara, F., Kumamoto-Yonezawa, Y., Matsui, Y., Takemura, M., Sasaki, M., Yoshida, H. and Takikawa, H. (2009) The inhibitory action of kohamaic acid A derivatives on mammalian DNA polymerase β . *Molecules*, **14**, 102-121.
195. Kimura, T., Takeuchi, T., Kumamoto-Yonezawa, Y., Ohashi, E., Ohmori, H., Masutani, C., Hanaoka, F., Sugawara, F., Yoshida, H. and Mizushina, Y. (2009) Penicillioles A and B, novel inhibitors specific to mammalian Y-family DNA polymerases. *Bioorg. Med. Chem.*, **17**, 1811-1816.
196. Dorjsuren, D., Wilson, D.M., 3rd, Beard, W.A., McDonald, J.P., Austin, C.P., Woodgate, R., Wilson, S.H. and Simeonov, A. (2009) A real-time fluorescence method for enzymatic characterization of specialized human DNA polymerases. *Nucleic Acids Res.*, **37**, e128.

197. Gening, L.V., Klincheva, S.A., Reshetnjak, A., Grollman, A.P. and Miller, H. (2006) RNA aptamers selected against DNA polymerase β inhibit the polymerase activities of DNA polymerases β and κ . *Nucleic Acids Res.*, **34**, 2579-2586.
198. Malmquist, N.A., Anzinger, J.J., Hirzel, D. and Buxton, I.L. (2001) Ellagic acid inhibits nucleoside diphosphate kinase-B activity. *Proc. West. Pharmacol. Soc.*, **44**, 57-59.
199. Whitley, A.C., Sweet, D.H. and Walle, T. (2005) The dietary polyphenol ellagic acid is a potent inhibitor of hOAT1. *Drug Metab. Dispos.*, **33**, 1097-1100.
200. Cozza, G., Bonvini, P., Zorzi, E., Poletto, G., Pagano, M.A., Sarno, S., Donella-Deana, A., Zagotto, G., Rosolen, A., Pinna, L.A. *et al.* (2006) Identification of ellagic acid as potent inhibitor of protein kinase CK2: a successful example of a virtual screening application. *J. Med. Chem.*, **49**, 2363-2366.
201. Blumenthal, T. and Landers, T.A. (1973) The inhibition of nucleic acid-binding proteins by aurintricarboxylic acid. *Biochem. Biophys. Res. Commun.*, **55**, 680-688.
202. Benchokroun, Y., Couprie, J. and Larsen, A.K. (1995) Aurintricarboxylic acid, a putative inhibitor of apoptosis, is a potent inhibitor of DNA topoisomerase II *in vitro* and in Chinese hamster fibrosarcoma cells. *Biochem. Pharmacol.*, **49**, 305-313.
203. Bina-Stein, M. and Tritton, T.R. (1976) Aurintricarboxylic acid is a nonspecific enzyme inhibitor. *Mol. Pharmacol.*, **12**, 191-193.
204. Simeonov, A., Kulkarni, A., Dorjsuren, D., Jadhav, A., Shen, M., McNeill, D.R., Austin, C.P. and Wilson, D.M., 3rd. (2009) Identification and characterization of

- inhibitors of human apurinic/aprimidinic endonuclease APE1. *PLoS One*, **4**, e5740.
205. Pardridge, W.M. (2007) shRNA and siRNA delivery to the brain. *Adv. Drug Deliv. Rev.*, **59**, 141-152.
206. Medarova, Z., Pham, W., Farrar, C., Petkova, V. and Moore, A. (2007) *In vivo* imaging of siRNA delivery and silencing in tumors. *Nat. Med.*, **13**, 372-377.
207. Grzelinski, M., Urban-Klein, B., Martens, T., Lamszus, K., Bakowsky, U., Hobel, S., Czubayko, F. and Aigner, A. (2006) RNA interference-mediated gene silencing of pleiotrophin through polyethylenimine-complexed small interfering RNAs *in vivo* exerts antitumoral effects in glioblastoma xenografts. *Hum. Gene Ther.*, **17**, 751-766.
208. Wullner, U., Neef, I., Tur, M.K. and Barth, S. (2009) Targeted delivery of short interfering RNAs—strategies for *in vivo* delivery. *Recent Pat. Anticancer Drug Discov.*, **4**, 1-8.
209. Latham, G.J., Harris, C.M., Harris, T.M. and Lloyd, R.S. (1995) The efficiency of translesion synthesis past single styrene oxide DNA adducts *in vitro* is polymerase-specific. *Chem. Res. Toxicol.*, **8**, 422-430.
210. Chary, P. and Lloyd, R.S. (1995) *In vitro* replication by prokaryotic and eukaryotic polymerases on DNA templates containing site-specific and stereospecific benzo[*a*]pyrene-7,8-dihydrodiol-9,10-epoxide adducts. *Nucleic Acids Res.*, **23**, 1398-1405.

211. Yoder, B.L. and Burgers, P.M. (1991) *Saccharomyces cerevisiae* replication factor C. I. Purification and characterization of its ATPase activity. *J. Biol. Chem.*, **266**, 22689-22697.
212. Nechev, L.V., Harris, C.M. and Harris, T.M. (2000) Synthesis of nucleosides and oligonucleotides containing adducts of acrolein and vinyl chloride. *Chem. Res. Toxicol.*, **13**, 421-429.
213. Minko, I.G., Kozekov, I.D., Kozekova, A., Harris, T.M., Rizzo, C.J. and Lloyd, R.S. (2008) Mutagenic potential of DNA-peptide crosslinks mediated by acrolein-derived DNA adducts. *Mutat. Res.*, **637**, 161-172.
214. Micheli, F., Di Fabio, R., Benedetti, R., Capelli, A.M., Cavallini, P., Cavanni, P., Davalli, S., Donati, D., Feriani, A., Gehanne, S. *et al.* (2004) 3-Methyl pyrrole-2,4-dicarboxylic acid 2-propyl ester 4-(1,2,2-trimethyl-propyl) ester: an exploration of the C-2 position. Part I. *Farmaco*, **59**, 175-183.
215. Dooley, P.A., Zhang, M., Korbelt, G.A., Nechev, L.V., Harris, C.M., Stone, M.P. and Harris, T.M. (2003) NMR determination of the conformation of a trimethylene interstrand cross-link in an oligodeoxynucleotide duplex containing a 5'-d(GpC) motif. *J. Am. Chem. Soc.*, **125**, 62-72.
216. Dooley, P.A., Tsarouhtsis, D., Korbelt, G.A., Nechev, L.V., Shearer, J., Zegar, I.S., Harris, C.M., Stone, M.P. and Harris, T.M. (2001) Structural studies of an oligodeoxynucleotide containing a trimethylene interstrand cross-link in a 5'-(CpG) motif: model of a malondialdehyde cross-link. *J. Am. Chem. Soc.*, **123**, 1730-1739.

217. Buterin, T., Hess, M.T., Luneva, N., Geacintov, N.E., Amin, S., Kroth, H., Seidel, A. and Naegeli, H. (2000) Unrepaired fjord region polycyclic aromatic hydrocarbon-DNA adducts in ras codon 61 mutational hot spots. *Cancer Res.*, **60**, 1849-1856.
218. Kumari, A., Minko, I.G., Harbut, M.B., Finkel, S.E., Goodman, M.F. and Lloyd, R.S. (2008) Replication bypass of interstrand cross-link intermediates by *Escherichia coli* DNA polymerase IV. *J. Biol. Chem.*, **283**, 27433-27437.
219. Geacintov, N.E., Cosman, M., Hingerty, B.E., Amin, S., Broyde, S. and Patel, D.J. (1997) NMR solution structures of stereoisometric covalent polycyclic aromatic carcinogen-DNA adduct: principles, patterns, and diversity. *Chem. Res. Toxicol.*, **10**, 111-146.
220. McCulloch, S.D. and Kunkel, T.A. (2008) The fidelity of DNA synthesis by eukaryotic replicative and translesion synthesis polymerases. *Cell Res.*, **18**, 148-161.
221. Nair, D.T., Johnson, R.E., Prakash, L., Prakash, S. and Aggarwal, A.K. (2006) Hoogsteen base pair formation promotes synthesis opposite the 1,*N*⁶-ethenodeoxyadenosine lesion by human DNA polymerase ϵ . *Nat. Struct. Mol. Biol.*, **13**, 619-625.
222. de los Santos, C., Kouchakdjian, M., Yarema, K., Basu, A., Essigmann, J. and Patel, D.J. (1991) NMR studies of the exocyclic 1,*N*⁶-ethenodeoxyadenosine adduct (ϵ dA) opposite deoxyguanosine in a DNA duplex. ϵ dA(*syn*).dG(*anti*) pairing at the lesion site. *Biochemistry*, **30**, 1828-1835.

223. Kouchakdjian, M., Eisenberg, M., Yarema, K., Basu, A., Essigmann, J. and Patel, D.J. (1991) NMR studies of the exocyclic 1,*N*⁶-ethenodeoxyadenosine adduct (ϵ dA) opposite thymidine in a DNA duplex. Nonplanar alignment of epsilon dA(*anti*) and dT(*anti*) at the lesion site. *Biochemistry*, **30**, 1820-1828.
224. Yan, S., Shapiro, R., Geacintov, N.E. and Broyde, S. (2001) Stereochemical, structural, and thermodynamic origins of stability differences between stereoisomeric benzo[*a*]pyrene diol epoxide deoxyadenosine adducts in a DNA mutational hot spot sequence. *J. Am. Chem. Soc.*, **123**, 7054-7066.
225. Yan, S.F., Wu, M., Geacintov, N.E. and Broyde, S. (2004) Altering DNA polymerase incorporation fidelity by distorting the dNTP binding pocket with a bulky carcinogen-damaged template. *Biochemistry*, **43**, 7750-7765.
226. Barker, S., Weinfeld, M. and Murray, D. (2005) DNA-protein crosslinks: their induction, repair, and biological consequences. *Mutat. Res.*, **589**, 111-135.
227. Minko, I.G., Kurtz, A.J., Croteau, D.L., Van Houten, B., Harris, T.M. and Lloyd, R.S. (2005) Initiation of repair of DNA-polypeptide cross-links by the UvrABC nuclease. *Biochemistry*, **44**, 3000-3009.
228. Minko, I.G., Zou, Y. and Lloyd, R.S. (2002) Incision of DNA-protein crosslinks by UvrABC nuclease suggests a potential repair pathway involving nucleotide excision repair. *Proc. Natl. Acad. Sci.*, **99**, 1905-1909.
229. Patel, P.H., Suzuki, M., Adman, E., Shinkai, A. and Loeb, L.A. (2001) Prokaryotic DNA polymerase I: evolution, structure, and "base flipping" mechanism for nucleotide selection. *J. Mol. Biol.*, **308**, 823-837.

230. Cai, H., Yu, H., McEntee, K. and Goodman, M.F. (1995) Purification and properties of DNA polymerase II from *Escherichia coli*. *Methods. Enzymol.*, **262**, 13-21.
231. Kobayashi, S., Valentine, M.R., Pham, P., O'Donnell, M. and Goodman, M.F. (2002) Fidelity of *Escherichia coli* DNA polymerase IV. Preferential generation of small deletion mutations by dNTP-stabilized misalignment. *J. Biol. Chem.*, **277**, 34198-34207.
232. Tang, M., Pham, P., Shen, X., Taylor, J.S., O'Donnell, M., Woodgate, R. and Goodman, M.F. (2000) Roles of *E. coli* DNA polymerases IV and V in lesion-targeted and untargeted SOS mutagenesis. *Nature*, **404**, 1014-1018.
233. Bruck, I., Woodgate, R., McEntee, K. and Goodman, M.F. (1996) Purification of a soluble UmuD'C complex from *Escherichia coli*. Cooperative binding of UmuD'C to single-stranded DNA. *J. Biol. Chem.*, **271**, 10767-10774.
234. Cox, M.M., McEntee, K. and Lehman, I.R. (1981) A simple and rapid procedure for the large scale purification of the recA protein of *Escherichia coli*. *J. Biol. Chem.*, **256**, 4676-4678.
235. Stukenberg, P.T., Studwell-Vaughan, P.S. and O'Donnell, M. (1991) Mechanism of the sliding β -clamp of DNA polymerase III holoenzyme. *J. Biol. Chem.*, **266**, 11328-11334.
236. Pritchard, A.E., Dallmann, H.G., Glover, B.P. and McHenry, C.S. (2000) A novel assembly mechanism for the DNA polymerase III holoenzyme DnaX complex: association of $\delta\delta'$ with DnaX₄ forms DnaX₃ $\delta\delta'$. *EMBO J.*, **19**, 6536-6545.

237. Onrust, R., Finkelstein, J., Naktinis, V., Turner, J., Fang, L. and O'Donnell, M. (1995) Assembly of a chromosomal replication machine: two DNA polymerases, a clamp loader, and sliding clamps in one holoenzyme particle. I. Organization of the clamp loader. *J. Biol. Chem.*, **270**, 13348-13357.
238. Zambrano, M.M., Siegele, D.A., Almiron, M., Tormo, A. and Kolter, R. (1993) Microbial competition: *Escherichia coli* mutants that take over stationary phase cultures. *Science*, **259**, 1757-1760.
239. Yeiser, B., Pepper, E.D., Goodman, M.F. and Finkel, S.E. (2002) SOS-induced DNA polymerases enhance long-term survival and evolutionary fitness. *Proc. Natl. Acad. Sci.*, **99**, 8737-8741.
240. Bonner, C.A., Stukenberg, P.T., Rajagopalan, M., Eritja, R., O'Donnell, M., McEntee, K., Echols, H. and Goodman, M.F. (1992) Processive DNA synthesis by DNA polymerase II mediated by DNA polymerase III accessory proteins. *J. Biol. Chem.*, **267**, 11431-11438.
241. Kogoma, T. and Maldonado, R.R. (1997) DNA polymerase I in constitutive stable DNA replication in *Escherichia coli*. *J. Bacteriol.*, **179**, 2109-2115.
242. del Solar, G., Giraldo, R., Ruiz-Echevarria, M.J., Espinosa, M. and Diaz-Orejas, R. (1998) Replication and control of circular bacterial plasmids. *Microbiol. Mol. Biol. Rev.*, **62**, 434-464.
243. Fernandes, A., Liu, T., Amin, S., Geacintov, N.E., Grollman, A.P. and Moriya, M. (1998) Mutagenic potential of stereoisomeric bay region (+)- and (-)-*cis-anti*-benzo[*a*]pyrene diol epoxide-*N*²-2'-deoxyguanosine adducts in *Escherichia coli* and simian kidney cells. *Biochemistry*, **37**, 10164-10172.

244. Hastings, P.J., Hersh, M.N., Thornton, P.C., Fonville, N.C., Slack, A., Frisch, R.L., Ray, M.P., Harris, R.S., Leal, S.M. and Rosenberg, S.M. (2010) Competition of *Escherichia coli* DNA polymerases I, II and III with DNA Pol IV in stressed cells. *PLoS One*, **5**, e10862.
245. Curti, E., McDonald, J.P., Mead, S. and Woodgate, R. (2009) DNA polymerase switching: effects on spontaneous mutagenesis in *Escherichia coli*. *Mol. Microbiol.*, **71**, 315-331.
246. Hwang, H. and Taylor, J.S. (2005) Evidence for Watson-Crick and not Hoogsteen or wobble base pairing in the selection of nucleotides for insertion opposite pyrimidines and a thymine dimer by yeast DNA pol η . *Biochemistry*, **44**, 4850-4860.
247. Yadav, P.N., Yadav, J.S. and Modak, M.J. (1992) A molecular model of the complete three-dimensional structure of the Klenow fragment of *Escherichia coli* DNA polymerase I: binding of the dNTP substrate and template-primer. *Biochemistry*, **31**, 2879-2886.
248. Huang, H., Kozekov, I.D., Kozekova, A., Rizzo, C.J., McCullough, A.K., Lloyd, R.S. and Stone, M.P. Minor groove orientation of the KWKK peptide tethered via the N-terminal amine to the acrolein-derived 1, N^2 - γ -hydroxypropanodeoxyguanosine lesion with a trimethylene linkage. *Biochemistry*, **49**, 6155-6164.
249. Kurtz, A.J. and Lloyd, R.S. (2003) 1, N^2 -deoxyguanosine adducts of acrolein, crotonaldehyde, and *trans*-4-hydroxynonenal cross-link to peptides via Schiff base linkage. *J. Biol. Chem.*, **278**, 5970-5976.

250. Rothwell, P.J. and Waksman, G. (2005) Structure and mechanism of DNA polymerases. *Adv. Protein Chem.*, **71**, 401-440.
251. Grafstrom, R.C., Dypbukt, J.M., Willey, J.C., Sundqvist, K., Edman, C., Atzori, L. and Harris, C.C. (1988) Pathobiological effects of acrolein in cultured human bronchial epithelial cells. *Cancer Res.*, **48**, 1717-1721.
252. Costa, M., Zhitkovich, A., Harris, M., Paustenbach, D. and Gargas, M. (1997) DNA-protein cross-links produced by various chemicals in cultured human lymphoma cells. *J. Toxicol. Environ. Health*, **50**, 433-449.
253. Kuykendall, J.R. and Bogdanffy, M.S. (1992) Efficiency of DNA-histone crosslinking induced by saturated and unsaturated aldehydes in vitro. *Mutat. Res.*, **283**, 131-136.
254. Curren, R.D., Yang, L.L., Conklin, P.M., Grafstrom, R.C. and Harris, C.C. (1988) Mutagenesis of xeroderma pigmentosum fibroblasts by acrolein. *Mutat. Res.*, **209**, 17-22.
255. Marnett, L.J., Hurd, H.K., Hollstein, M.C., Levin, D.E., Esterbauer, H. and Ames, B.N. (1985) Naturally occurring carbonyl compounds are mutagens in Salmonella tester strain TA104. *Mutat. Res.*, **148**, 25-34.
256. Smith, R.A., Cohen, S.M. and Lawson, T.A. (1990) Acrolein mutagenicity in the V79 assay. *Carcinogenesis*, **11**, 497-498.
257. Cohen, S.M., Garland, E.M., St John, M., Okamura, T. and Smith, R.A. (1992) Acrolein initiates rat urinary bladder carcinogenesis. *Cancer Res.*, **52**, 3577-3581.
258. Uchida, K., Kanematsu, M., Morimitsu, Y., Osawa, T., Noguchi, N. and Niki, E. (1998) Acrolein is a product of lipid peroxidation reaction. Formation of free

- acrolein and its conjugate with lysine residues in oxidized low density lipoproteins. *J. Biol. Chem.*, **273**, 16058-16066.
259. Chung, F.L., Nath, R.G., Nagao, M., Nishikawa, A., Zhou, G.D. and Randerath, K. (1999) Endogenous formation and significance of 1,*N*²-propanodeoxyguanosine adducts. *Mutat. Res.*, **424**, 71-81.
260. Chung, F.L., Pan, J., Choudhury, S., Roy, R., Hu, W. and Tang, M.S. (2003) Formation of *trans*-4-hydroxy-2-nonenal- and other enal-derived cyclic DNA adducts from ω -3 and ω -6 polyunsaturated fatty acids and their roles in DNA repair and human *p53* gene mutation. *Mutat. Res.*, **531**, 25-36.
261. Chung, F.L., Young, R. and Hecht, S.S. (1984) Formation of cyclic 1,*N*²-propanodeoxyguanosine adducts in DNA upon reaction with acrolein or crotonaldehyde. *Cancer Res.*, **44**, 990-995.
262. Pawlowicz, A.J., Munter, T., Zhao, Y. and Kronberg, L. (2006) Formation of acrolein adducts with 2'-deoxyadenosine in calf thymus DNA. *Chem. Res. Toxicol.*, **19**, 571-576.
263. Shapiro, R., Sodum, R.S., Everett, D.W. and Kundu, S.K. (1986) Reactions of nucleosides with glyoxal and acrolein. *IARC Sci. Publ.*, 165-173.
264. Smith, R.A., Williamson, D.S. and Cohen, S.M. (1989) Identification of 3,*N*⁴-propanodeoxycytidine 5'-monophosphate formed by the reaction of acrolein with deoxycytidine 5'-monophosphate. *Chem. Res. Toxicol.*, **2**, 267-271.
265. Smith, R.A., Williamson, D.S., Cerny, R.L. and Cohen, S.M. (1990) Detection of 1,*N*⁶-propanodeoxyadenosine in acrolein-modified polydeoxyadenylic acid and DNA by ³²P postlabeling. *Cancer Res.*, **50**, 3005-3012.

266. Kanuri, M., Minko, I.G., Nechev, L.V., Harris, T.M., Harris, C.M. and Lloyd, R.S. (2002) Error prone translesion synthesis past γ -hydroxypropano deoxyguanosine, the primary acrolein-derived adduct in mammalian cells. *J. Biol. Chem.*, **277**, 18257-18265.
267. Nath, R.G. and Chung, F.L. (1994) Detection of exocyclic 1, N^2 -propanodeoxyguanosine adducts as common DNA lesions in rodents and humans. *Proc. Natl. Acad. Sci.*, **91**, 7491-7495.
268. Nath, R.G., Ocando, J.E. and Chung, F.L. (1996) Detection of 1, N^2 -propanodeoxyguanosine adducts as potential endogenous DNA lesions in rodent and human tissues. *Cancer Res.*, **56**, 452-456.
269. Penn, A., Nath, R., Pan, J., Chen, L., Widmer, K., Henk, W. and Chung, F.L. (2001) 1, N^2 -propanodeoxyguanosine adduct formation in aortic DNA following inhalation of acrolein. *Environ. Health Perspect.*, **109**, 219-224.
270. de los Santos, C., Zaliznyak, T. and Johnson, F. (2001) NMR characterization of a DNA duplex containing the major acrolein-derived deoxyguanosine adduct γ -OH-1, N^2 -propano-2'-deoxyguanosine. *J. Biol. Chem.*, **276**, 9077-9082.
271. Sanchez, A.M., Minko, I.G., Kurtz, A.J., Kanuri, M., Moriya, M. and Lloyd, R.S. (2003) Comparative evaluation of the bioreactivity and mutagenic spectra of acrolein-derived α -HOPdG and γ -HOPdG regioisomeric deoxyguanosine adducts. *Chem. Res. Toxicol.*, **16**, 1019-1028.
272. Reardon, J.T. and Sancar, A. (2006) Repair of DNA–polypeptide crosslinks by human excision nuclease. *Proc. Natl. Acad. Sci.*, **103**, 4056-4061.

273. Reardon, J.T., Cheng, Y. and Sancar, A. (2006) Repair of DNA–protein cross-links in mammalian cells. *Cell Cycle*, **5**, 1366-1370.
274. Baker, D.J., Wuenschell, G., Xia, L., Termini, J., Bates, S.E., Riggs, A.D. and O'Connor, T.R. (2007) Nucleotide excision repair eliminates unique DNA-protein cross-links from mammalian cells. *J. Biol. Chem.*, **282**, 22592-22604.
275. Quievryn, G. and Zhitkovich, A. (2000) Loss of DNA–protein crosslinks from formaldehyde-exposed cells occurs through spontaneous hydrolysis and an active repair process linked to proteasome function. *Carcinogenesis*, **21**, 1573-1580.
276. Jarosz, D.F., Godoy, V.G., Delaney, J.C., Essigmann, J.M. and Walker, G.C. (2006) A single amino acid governs enhanced activity of DinB DNA polymerases on damaged templates. *Nature*, **439**, 225-228.
277. Zhang, Y., Wu, X., Guo, D., Rechkoblit, O. and Wang, Z. (2002) Activities of human DNA polymerase κ in response to the major benzo[*a*]pyrene DNA adduct: error-free lesion bypass and extension synthesis from opposite the lesion. *DNA Repair (Amst.)*, **1**, 559-569.
278. Suzuki, N., Ohashi, E., Kolbanovskiy, A., Geacintov, N.E., Grollman, A.P., Ohmori, H. and Shibutani, S. (2002) Translesion synthesis by human DNA polymerase kappa on a DNA template containing a single stereoisomer of dG-(+)- or dG(-)-*anti-N*²-BPDE (7,8-dihydroxy-*anti*-9,10-epoxy-7,8,9,10-tetrahydrobenzo[*a*]pyrene). *Biochemistry*, **41**, 6100-6106.
279. Huang, X., Kolbanovskiy, A., Wu, X., Zhang, Y., Wang, Z., Zhuang, P., Amin, S. and Geacintov, N.E. (2003) Effects of base sequence context on translesion

- synthesis past a bulky (+)-*trans-anti*-B[a]P- N^2 -dG lesion catalyzed by the Y-family polymerase pol κ . *Biochemistry*, **42**, 2456-2466.
280. Yuan, B., Cao, H., Jiang, Y., Hong, H. and Wang, Y. (2008) Efficient and accurate bypass of N^2 -(1-carboxyethyl)-2'-deoxyguanosine by DinB DNA polymerase *in vitro* and *in vivo*. *Proc. Natl. Acad. Sci.*, **105**, 8679-8684.
281. Moriya, M. (1993) Single-stranded shuttle phagemid for mutagenesis studies in mammalian cells: 8-oxoguanine in DNA induces targeted G.C \rightarrow T.A transversions in simian kidney cells. *Proc. Natl. Acad. Sci.*, **90**, 1122-1126.
282. Kong, X.P., Onrust, R., O'Donnell, M. and Kuriyan, J. (1992) Three-dimensional structure of the β subunit of E. coli DNA polymerase III holoenzyme: a sliding DNA clamp. *Cell*, **69**, 425-437.
283. Dodson, M.L. and Lloyd, R.S. (2002) Mechanistic comparisons among base excision repair glycosylases. *Free Radic. Biol. Med.*, **32**, 678-682.
284. VanderVeen, L.A., Hashim, M.F., Nechev, L.V., Harris, T.M., Harris, C.M. and Marnett, L.J. (2001) Evaluation of the mutagenic potential of the principal DNA adduct of acrolein. *J. Biol. Chem.*, **276**, 9066-9070.
285. Yang, I.Y., Hossain, M., Miller, H., Khullar, S., Johnson, F., Grollman, A. and Moriya, M. (2001) Responses to the major acrolein-derived deoxyguanosine adduct in *Escherichia coli*. *J. Biol. Chem.*, **276**, 9071-9076.
286. Lone, S., Townson, S.A., Uljon, S.N., Johnson, R.E., Brahma, A., Nair, D.T., Prakash, S., Prakash, L. and Aggarwal, A.K. (2007) Human DNA polymerase κ encircles DNA: implications for mismatch extension and lesion bypass. *Mol. Cell*, **25**, 601-614.

287. Forgacs, E., Latham, G., Beard, W.A., Prasad, R., Bebenek, K., Kunkel, T.A., Wilson, S.H. and Lloyd, R.S. (1997) Probing structure/function relationships of HIV-1 reverse transcriptase with styrene oxide N^2 -guanine adducts. *J. Biol. Chem.*, **272**, 8525-8530.
288. Latham, G.J. and Lloyd, R.S. (1994) Deoxynucleotide polymerization by HIV-1 reverse transcriptase is terminated by site-specific styrene oxide adducts after translesion synthesis. *J. Biol. Chem.*, **269**, 28527-28530.
289. Latham, G.J., Forgacs, E., Beard, W.A., Prasad, R., Bebenek, K., Kunkel, T.A., Wilson, S.H. and Lloyd, R.S. (2000) Vertical-scanning mutagenesis of a critical tryptophan in the "minor groove binding track" of HIV-1 reverse transcriptase. Major groove DNA adducts identify specific protein interactions in the minor groove. *J. Biol. Chem.*, **275**, 15025-15033.
290. Yamanaka, C. and Lloyd, R.S. (2012) In Madhusudan, S. and Wilson, D. M., 3rd (eds.), *DNA Repair and Cancer: Bench to Clinic*. Science Publishers, Enfield, NH. *In Press*.
291. Ho, T.V. and Scharer, O.D. (2010) Translesion DNA synthesis polymerases in DNA interstrand crosslink repair. *Environ. Mol. Mutagen.*, **51**, 552-566.
292. Raschle, M., Knipscheer, P., Enoiu, M., Angelov, T., Sun, J., Griffith, J.D., Ellenberger, T.E., Scharer, O.D. and Walter, J.C. (2008) Mechanism of replication-coupled DNA interstrand crosslink repair. *Cell*, **134**, 969-980.
293. Noll, D.M., Mason, T.M. and Miller, P.S. (2006) Formation and repair of interstrand cross-links in DNA. *Chem. Rev.*, **106**, 277-301.

294. Lehoczky, P., McHugh, P.J. and Chovanec, M. (2007) DNA interstrand cross-link repair in *Saccharomyces cerevisiae*. *FEMS Microbiol. Rev.*, **31**, 109-133.
295. Mamelak, A.N. (2005) Locoregional therapies for glioma. *Oncology*, **19**, 1803-1810.
296. Huang, R., Southall, N., Wang, Y., Yasgar, A., Shinn, P., Jadhav, A., Nguyen, D.T. and Austin, C.P. (2011) The NCGC pharmaceutical collection: a comprehensive resource of clinically approved drugs enabling repurposing and chemical genomics. *Sci. Transl. Med.*, **3**, 80ps16.
297. Zhang, J.H., Chung, T.D. and Oldenburg, K.R. (1999) A Simple Statistical Parameter for Use in Evaluation and Validation of High Throughput Screening Assays. *J. Biomol. Screen.*, **4**, 67-73.
298. Inglese, J., Auld, D.S., Jadhav, A., Johnson, R.L., Simeonov, A., Yasgar, A., Zheng, W. and Austin, C.P. (2006) Quantitative high-throughput screening: a titration-based approach that efficiently identifies biological activities in large chemical libraries. *Proc. Natl. Acad. Sci.*, **103**, 11473-11478.
299. Mizushina, Y., Maeda, J., Irino, Y., Nishida, M., Nishiumi, S., Kondo, Y., Nishio, K., Kuramochi, K., Tsubaki, K., Kuriyama, I. *et al.* (2011) Effects of Intermediates between Vitamins K₂ and K₃ on Mammalian DNA Polymerase Inhibition and Anti-Inflammatory Activity. *Int. J. Mol. Sci.*, **12**, 1115-1132.
300. Maruo, S., Kuriyama, I., Kuramochi, K., Tsubaki, K., Yoshida, H. and Mizushina, Y. (2011) Inhibitory effect of novel 5-*O*-acyl juglones on mammalian DNA polymerase activity, cancer cell growth and inflammatory response. *Bioorg. Med. Chem.*, **19**, 5803-5812.

301. Ishida, T., Mizushina, Y., Yagi, S., Irino, Y., Nishiumi, S., Miki, I., Kondo, Y., Mizuno, S., Yoshida, H., Azuma, T. *et al.* (2012) Inhibitory effects of glycyrrhetic Acid on DNA polymerase and inflammatory activities. *Evid. Based Complement. Alternat. Med.*, **2012**, 650514.
302. Mizushina, Y., Zhang, J., Pugliese, A., Kim, S.H. and Lu, J. (2010) Anti-cancer gallotannin penta-*O*-galloyl-beta-D-glucose is a nanomolar inhibitor of select mammalian DNA polymerases. *Biochem. Pharmacol.*, **80**, 1125-1132.
303. Shoichet, B.K. (2006) Interpreting steep dose-response curves in early inhibitor discovery. *J. Med. Chem.*, **49**, 7274-7277.
304. Meredith, P.A. (2007) Candesartan cilexetil—a review of effects on cardiovascular complications in hypertension and chronic heart failure. *Curr. Med. Res. Opin.*, **23**, 1693-1705.
305. Folmer, F., Jaspars, M., Schumacher, M., Dicato, M. and Diederich, M. (2010) Marine natural products targeting phospholipases A₂. *Biochem. Pharmacol.*, **80**, 1793-1800.
306. Ebada, S.S., Lin, W. and Proksch, P. (2010) Bioactive sesterterpenes and triterpenes from marine sponges: occurrence and pharmacological significance. *Mar. Drugs*, **8**, 313-346.
307. Nakao, Y. and Fusetani, N. (2007) Enzyme inhibitors from marine invertebrates. *J. Nat. Prod.*, **70**, 689-710.
308. Evans, J.F., Ferguson, A.D., Mosley, R.T. and Hutchinson, J.H. (2008) What's all the FLAP about?: 5-lipoxygenase-activating protein inhibitors for inflammatory diseases. *Trends Pharmacol. Sci.*, **29**, 72-78.

309. Smirnov, S.V., Knock, G.A. and Aaronson, P.I. (1998) Effects of the 5-lipoxygenase activating protein inhibitor MK886 on voltage-gated and Ca²⁺-activated K⁺ currents in rat arterial myocytes. *Br. J. Pharmacol.*, **124**, 572-578.